ELECTRON TRANSPORT COEFFICIENTS AND COLLISION CROSS SECTIONS IN HYDROGEN

A thesis submitted for the
degree of Doctor of Philosophy
in the Australian National University

A.I. McINTOSH

January, 1967.

STATEMENT

Except where acknowledgements are made in the text all the material contained in this thesis was the work of the candidate.

A.I. McIntosh

A.I. McIntosh

TABLE OF CONTENTS

PART A.

INDEX TO FIGURES

INDEX TO TABLES

SUMMARY

When electrons drift and diffuse through a gas under the influence of an electric field, the energy received from the field by the electrons is transferred to the gas through the elastic and inelastic collisions which occur. The cross sections for these processes can be deduced from accurate values of the electron drift velocity, W, and of the ratio of diffusion coefficient to mobility, D/μ.

In this thesis the experimental techniques necessary for accurate measurement of W and D/μ are described. These techniques have been applied to hydrogen and deuterium at $293^{o}K$ and $77^{o}K$ to yield data for W and D/μ when $2 \times 10^{-20} \leq E/N \leq 1 \times 10^{-16}$ V cm^{2}.

An important part of the investigation was the development of a method for preparing pure para-hydrogen and the subsequent measurement of W and D/μ in this gas at $77^{o}K$. There have been no previous measurements of electron transport coefficients in para-hydrogen. The differences in the values of W and D/μ in hydrogen and para-hydrogen clearly demonstrate the influence of the difference in the statistical weights of the rotational levels in the two gases.

The numerical techniques used to deduce the relevant cross sections from the experimental data are described. When elastic and inelastic collisions occur the electron energy distribution must be calculated from a numerical solution of the Boltzmann equation. Details are given of a solution of the Boltzmann equation when collisions of the second kind between electrons and excited gas molecules are neglected. The restrictions placed on the present analysis by the neglect of collisions of the second kind are discussed.

In the inert gases at energies well below the first excitation threshold it is possible to infer the momentum transfer cross section directly from the experimental data. In such cases the derived cross sections are unique and their accuracy depends ultimately only on the precision of the experiments.

In molecular gases at all energies there are difficulties in obtaining a unique set of elastic and inelastic cross sections which are consistent with the experimental data. Although it does not appear possible to infer the inelastic cross sections directly from the values of W and D/μ, it is possible to proceed in the forward direction by testing an assumed inelastic cross section for consistency with the experimental data. The accuracy of the present results allows such tests for consistency to be made free from any ambiguity due to spread in the experimental data. At the same time the use of para-hydrogen, in which only one rotational level need be considered at $77^{o}K$, provides an opportunity to deduce a unique cross section for rotational excitation.

The theory of Gerjuoy and Stein for rotational excitation of diatomic homonuclear gases is widely accepted, particularly when the polarization correction of Dalgarno and Moffett is taken into account. The analysis presented in chapter 8 shows that this theory is not consistent with the experimental data, although the inclusion of the polarization correction does lead to better agreement between the calculated and experimental values of W and D/μ. The cross sections for vibrational excitation deduced in an earlier analysis by Engelhardt and Phelps are found to be consistent with the present experimental data. The momentum transfer cross section found from the present analysis is the same for all three gases but differs appreciably from that deduced by Engelhardt and Phelps.

Suggestions are made for future analyses to determine more realistic rotational excitation cross sections. The particular importance of the para-hydrogen data in determining a unique cross section for this process is discussed.

In Part B of the thesis a description is given of the extension of the Townsend-Huxley lateral diffusion method of measuring D/μ to electron energies where ionization and the emission of secondary electrons must be taken into account. Results in hydrogen at $293^{o}K$ for $10 \leq E/p \leq 100$ V cm^{-1} $torr^{-1}$ are given and compared with the results of other workers. For gold

electrodes in hydrogen the results show that most of the secondary electrons are produced by the impact of photons on the cathode.

ACKNOWLEDGEMENTS

The author would like to express his deep indebtedness to his supervisor, Dr. R. W. Crompton, for invaluable assistance and constant encouragement throughout this project.

He would like to thank Dr. A. G. Engelhardt (Westinghouse Research Laboratories) for supplying a copy of the basic computer program used to analyse the experimental data.

Thanks are also due to Dr. M. T. Elford for many helpful discussions, for the design of one of the drift chambers and for the construction of the liquid nitrogen level controller, to Mr. J. Gascoigne for technical assistance and to Mr. R. Kemp (C. S. I. R. O., Sydney) for assistance in the design of the para-hydrogen conversion chamber. The author would also like to thank the other members of the Ion Diffusion Unit for their help and co-operation.

The financial assistance of an Australian National University Scholarship is gratefully acknowledged.

PART A.

CHAPTER 1.

INTRODUCTION

Cross sections for the elastic and inelastic collisions between electrons and gas molecules can be determined in a number of ways. The extension of these data to energies less than 1 eV is of particular importance since many interesting processes such as the excitation of rotational levels in molecular gases occur in this energy range.

Measurements of cross sections at energies above 1 or 2 eV have been made since the 1920's and 1930's when beam techniques for studying collisions between particles of closely controlled energy were introduced (e.g. Ramsauer and Kollath, 1932, Tate and Smith, 1932). Experimental difficulties have so far prevented these techniques being extended to energies below 0.3 eV (Bandel and Golden, 1965).

The alternative techniques which are also useful at much lower energies have an even longer history, dating back to the pioneering experiments of Townsend at the beginning of the century. The class of experiments introduced by Townsend are known as swarm experiments since the quantities measured are the average properties of a swarm of particles. Until recently, data from this type of experiment were subject to considerable experimental error and could be interpreted only in terms of various mean quantities. Advances in both experimental techniques and in the analysis of the data have improved swarm techniques to the point where the accuracy of the derived cross sections is often higher than that obtainable in beam experiments. With the use of improved techniques and a better understanding of the factors limiting the accuracy of experiments of this kind, experimental data with an error of less than 1% can be obtained (Crompton and Jory, 1962, Lowke, 1963, Crompton and Elford, 1963). At the same time, modern high speed computers have enabled these data to be used in conjunction with more rigorous formulae to give the true energy dependence of the cross sections.

In very recent times swarm data have been the subject of complex mathematical analysis, as for example in the papers of Phelps and his colleagues at the Westinghouse laboratories (Frost and Phelps, 1962, Engelhardt and Phelps, 1963) and of Crompton and Jory (1965). These papers show that swarm techniques are capable of yielding results of reasonable energy resolution and therefore, in certain circumstances, allow a direct comparison of the results of swarm and beam experiments. Unfortunately the data on which some of these analyses have been based have not warranted the complex mathematical treatment to which they have been subjected and many of the cross sections must be re-determined from accurate swarm data.

In the inert gases at energies well below the first excitation threshold it is possible to infer the momentum transfer cross section directly from the experimental data. In such cases the derived cross sections are unique and their accuracy depends ultimately only on the precision of the experiments. The validity of the results can be checked when data from several types of swarm experiments are available. Crompton and Jory (1965) have achieved considerable success by applying this technique to their own experimental results for helium, but no data of sufficient accuracy are available in the other inert gases.

In the molecular gases, where elastic and inelastic collisions occur at all energies, the results obtained have been less satisfactory, due largely to the inadequacy of the available experimental data but due also to the difficulties in obtaining a unique set of elastic and inelastic cross sections which are consistent with the data. It does not appear possible to infer the inelastic cross sections directly from the experimental results and it is simpler to proceed in the forward direction by testing an assumed form of the inelastic cross section for consistency with the experimental data. However the primary difficulty with previous analyses has been the insufficient accuracy of the experimental data. For example, Engelhardt and Phelps have analysed swarm data in hydrogen and deuterium over a wide range of energies but were unable to find a single form of the rotational cross section which was consistent with the available data in both gases. Moreover, the very large scatter in the experimental data meant that in either gas they were

unable to distinguish between several trial forms of the cross-section.

The present work aims at overcoming some of these difficulties by using experimental techniques of proven accuracy to obtain data in hydrogen, para-hydrogen and deuterium with an accuracy of $\pm$ 2% or better. These data are then used to test a particular theoretical form of the rotational excitation cross section; the results of this test are free from any ambiguity due to spread in the experimental data. Cross sections for momentum transfer and vibrational excitation are obtained from the same analysis.

Hydrogen is the best of the homonuclear diatomic gases to study for at least three reasons. Firstly, the hydrogen molecule is the simplest diatomic molecule and has been the subject of the greatest number of theoretical investigations. Secondly, because of its small mass its rotational cross sections are both small in number and widely spaced in threshold; this makes the interpretation of the experimental data considerably easier. Thirdly, the use of para-hydrogen, which differs from normal hydrogen only in the statistical weights of the rotational levels (see Appendix I), provides a unique opportunity for a stringent test of any theoretical rotational cross sections.

Finally, the experimental techniques for handling deuterium gas are identical to those for hydrogen and it is therefore a simple matter to include it in the experimental program. Since the momentum transfer cross section in deuterium is expected to be very similar to that in hydrogen and since the rotational cross sections in the two gases should have the same form, a further opportunity to test the consistency of any theoretical treatment appropriate to hydrogen is presented.

Before proceeding to discuss the present investigation it is important to understand the complementary nature of the two experimental techniques (i.e. beam and swarm experiments) and the limitations of each. Furthermore, it is essential that what is meant by the various terms used in the discussion be made as precise as possible, and for this reason the following section is devoted to the introduction and definition of the fundamental concepts and quantities.

1.1 Basic Concepts

1.1.1 Types of Collisions.

When two particles, such as an electron and a gas molecule, collide, their total energy can be redistributed in a number of ways, each being typical of a particular type of collision. In an elastic collision there are no internal changes of energy of the colliding particles. When internal changes of energy occur at the expense of the total kinetic energy of the collision partners, the collision is said to be inelastic; the collision may result in an electron of the molecule being excited to a higher energy state or, if the energy exchange is large enough, to its complete separation from the atomic structure i.e. ionization. A collision of the second kind is one in which some of the internal energy of one of the particles is converted to kinetic energy shared by both the collision partners.

1.1.2 Collision Cross Sections.

The cross section is basically a measure of the probability that a given reaction will occur under given conditions. Its value depends on a number of factors for each particular collision considered; these include the nature of the particles, the mutual velocity of approach and the distance of closest approach during the encounter.

Consider a parallel beam of mono-energetic projectiles, the flux being N_p projectiles per cm^2 per second. The beam is directed along the z-axis towards the origin of the co-ordinate system where there are clustered N_t target particles. A finite size is ascribed to the target particles, but the projectiles are considered to be point particles. It is assumed that only elastic scattering occurs and that the number of target particles is small enough for no particle to be shielded by another and for no projectile to be scattered more than once.

Let $d\Omega$ be the element of solid angle whose position is specified by the spherical polar co-ordinates θ and ϕ. Let $N_s(\theta, \phi)\, d\Omega$ be the number of projectiles scattered into $d\Omega$ per second.

Then $N_s(\theta, \phi)\, d\Omega$ is proportional to $N_p N_t\, d\Omega$ and, inserting $I_s(\theta, \phi)$ as the constant of proportionality,

$$N_s(\theta, \phi)\, d\Omega = I_s(\theta, \phi)\, N_p\, N_t\, d\Omega$$

$$= d I_s(\theta, \phi)\, N_p\, N_t \qquad (1.1)$$

The quantity $d I_s(\theta, \phi) = I_s(\theta, \phi)\, d\Omega$ is defined as the differential microscopic elastic scattering cross section.

Since

$$d I_s(\theta, \phi) = \frac{N_s(\theta, \phi)\, d\Omega}{N_p\, N_t} \qquad (1.2)$$

the cross section has units of cm^2 per target particle and is often regarded as the area presented by each particle for scattering of the projectiles into the element of solid angle $d\Omega$.

Intergrating over all differential microscopic cross sections we obtain

$$q_s = \int d I_s(\theta, \phi)$$

$$= \int\int I_s(\theta, \phi)\, d\Omega$$

and therefore,

$$q_s = \int_0^{2\pi}\int_0^{2\pi} I_s(\theta, \phi) \sin\theta\, d\theta\, d\phi \qquad (1.3)$$

q_s is defined as the total microscopic elastic scattering cross section. It represents the area presented by each of the target particles for scattering into the solid angle 4π steradians.

Microscopic cross sections are usually expressed in units of cm^2 or of $\pi a_o^2 = 0.88 \times 10^{-16}\ cm^2$ where $a_o = 0.53 \times 10^{-8}$ cm is the radius of the first Bohr orbit of the hydrogen atom.

A macroscopic cross section may be found if the target particles are now considered to be distributed throughout a volume with a density of N target particles per cm^3. It is still assumed that any elastic collision removes a projectile from the beam. If I, the intensity of the projectile beam at the

point x, is reduced by d I in traversing the distance dx, then

$$d I = - I N q_s dx \tag{1.4}$$

If $I = I_o$ at $x = 0$

$$I = I_o \exp (- N q_s d x) \tag{1.5}$$

$Q_s = N q_s$ is called the macroscopic cross section for elastic scattering.

It is clear that although the above definitions are for elastic scattering, the collision cross section concept can be applied to other types of collision. The term q_i denotes the cross section for scattering of the i th type.

In the experiments to be described later in this thesis, the cross section of importance in elastic scattering is not q_s as defined above, but q_m the diffusion or momentum transfer cross section. Before proceeding to establish the relationship between these two it should be pointed out that in any collision the positions and velocities of the particles must be expressed in a particular frame of reference. It is obviously more convenient to make measurements in the laboratory frame of reference i. e. the frame of reference of a laboratory observer. However in the analysis of collisions it is often convenient to specify the position of the particles with reference to the Centre of Mass system which is one which moves with respect to the laboratory system in such a way that its origin is always coincident with the centre of mass of the colliding particles. General relations between the two systems can be derived (McDaniel, 1964, chapter 1) so that the necessary transformations can be made.

Consider, in the Centre of Mass system of co-ordinates, a collision between an electron of mass m and a gas molecule of mass M. The electron has linear momentum equal to $M_r v_o$ before the collision, where M_r is the reduced mass of m and M (= m M/ (m + M)) and v_o is the relative velocity of approach. If the electron is scattered through an angle θ in the Centre of Mass system, then it suffers a change in its forward momentum of $M_r v_o (1 - \cos \theta)$. The diffusion cross section is defined by the equation

$$q_D = \int (1 - \cos\theta)\, I_s(\theta)\, d\Omega_{C\ of\ M}$$

$$= 2\pi \int_0^{\pi} I_s(\theta)\,(1 - \cos\theta)\sin\theta\, d\theta \qquad (1.6)$$

where $I_s(\theta)\, d\Omega_{C\ of\ M}$ is the differential scattering cross section in the Centre of Mass system.

Since q_D is a measure of the average forward momentum lost by the electron in collisions with the molecules, it is often called the momentum transfer cross section and denoted by q_m ; this is the practice followed in the remainder of this work.

The momentum transfer cross section differs appreciably from the total elastic scattering cross section only when the scattering is distinctly anisotropic. If the differential elastic scattering cross section q_s is independent of θ , i.e. the scattering is isotropic, then $q_m = q_s$. If backward scattering predominates then $q_m > q_s$, whereas the reverse is true if most of the scattering is concentrated in the forward direction.

1.1.3 Transport Coefficients

The collision cross sections described above are for monoenergetic particles. In the swarm experiments of the present investigation the swarm contains electrons with a range of energies, the distribution of these energies depending on the nature of the gas, its temperature and the ratio of electric field to gas pressure.

If a large number of gas molecules is allowed to interact with each other in a confined space without being subject to external forces, the molecules will come to thermal equilibrium and an equilibrium distribution of velocities is established. This distribution is the Maxwell-Boltzmann distribution in which the number of molecules dN with speeds between C and C + dC is

$$dN = (4 N_o / \pi^{\frac{1}{2}})\,(M/2kT)^{3/2} \exp(-MC^2/2kT)\, C^2\, dC \qquad (1.7)$$

N_o being the total number of molecules, T the gas temperature and k Boltzmann's constant.

Considering each velocity $\underline{C}$ as made up of three mutually perpendicular components C_x, C_y and C_z, the distribution function $f(C)$ is defined such that, of the total number N_o of molecules, the number dN whose components of velocity lie between C_x and $C_x + d C_x$, C_y and $C_y + d C_y$, C_z and $C_z + d C_z$ is

$$N_o f(C) d C_x d C_y d C_z .$$

That is, the product $N_o f(C)$ is the density of representative points in velocity space. Since there are no preferred directions of velocity

$$dN = N_o f(C) 4 \pi C^2 d C.$$

If a cloud of free electrons is released into this gas an equilibrium is once more established with $\frac{1}{2} m\overline{c^2} = \frac{1}{2} M\overline{C^2}$, where m and c refer to the electrons and the bar means that the quantities are averaged over all velocities. The velocities are still distributed according to Maxwell's law and since the distribution is symmetrical, the mean velocity $\underline{\bar{c}}$ (or $\underline{\bar{C}}$) is zero.

When an electric field is applied the electrons are acted upon by a force and therefore receive power directly from the field. The molecules remain unaffected by the field and a new equilibrium is established in which $\frac{1}{2} m\overline{c^2} > \frac{1}{2} M\overline{C^2}$, the speeds c are no longer distributed according to Maxwell's law and the mean velocity $\underline{\bar{c}}$ is no longer zero. Thus, in addition to the process of diffusion which takes place with or without the field (but is modified by it), a new phenomenon, that of drift, is introduced. The electron cloud moves as a whole so that its centroid moves with a drift velocity W parallel to the electric field.

Diffusion of the particles arises from their random motion and causes a change in any non-uniform distribution of number density. The diffusion coefficient D is defined such that, if n is the concentration of particles per unit volume, the net transport of particles across a surface of area $\underline{d S}$ is

$$- D \operatorname{grad} n \,.\, \underline{d S}.$$

If the gas is one in which no electrons attach to gas molecules,

and if the energy of the electrons is not high enough to cause ionization, then the two quantities W and D are sufficient to describe the behaviour of the electron cloud. The drift velocity and the diffusion coefficient are known as transport coefficients.

Additional transport coefficients are needed to describe the behaviour of the electron swarm in the presence of a magnetic field and when ionization and attachment occur; these coefficients will be introduced as needed later in this thesis.

1.2 Methods of Studying Electron-Molecule Collisions.

1.2.1 Beam Experiments.

The most direct way to investigate electron-molecule collisions is to allow a beam of mono-energetic electrons to collide with the target gas molecules. The electrons are made mono-energetic by some type of energy filter or analyser and the target gas pressure is sufficiently low that only single collisions are possible in the reaction chamber, i.e. once an electron undergoes a collision it is scattered out of the beam and there is no possibility of a further collision directing it back into the collecting device.

The electron beam enters the chamber with a known intensity and emerges with its intensity reduced by the loss of electrons which have made collisions and whose momentum has therefore been changed. The number of electrons lost by scattering allows a direct measurement of the total scattering cross section for electrons of a given energy and the interpretation of the results is therefore relatively easy. Beams with energy spreads of as little as 10 mV can be obtained and, since this means that electrons have virtually discrete energies, it is possible to examine phenomena for fine structure e.g. resonances in the elastic scattering cross-section.

Several modifications to this technique are used to determine inelastic cross sections. For instance, a homogeneous beam of electrons of known and variable energy is passed through the gas, causing atoms or molecules to be raised to higher energy states. Measurements of the radiation resulting

from de-excitation of these atoms and molecules allow the determination of the excitation cross sections as a function of the electron energy. Another method, applicable to metastable as well as ordinary excited states, is to pass the beam of electrons through the gas and to collect the inelastically scattered electrons. The energy losses are characteristic of the excitation processes, and measurement of the energy spectrum of the scattered electrons provides information on these processes. The technique of "crossed beams" of target molecules and projectiles is useful for examining collisions with unstable atoms or molecules, e.g. for examining electron-atomic hydrogen collisions. A survey of recent experiments using all these techniques is given in chapter 5 of "Collision Phenomena in Ionized Gases" (McDaniel, 1964).

1.2.2 Limitations of Beam Techniques.

There are many difficulties in the application of beam techniques to low energies due to the problems of obtaining adequate beam current and to the presence of stray fields due, for example, to unknown contact potential differences within the chamber. At very low energies contact potential differences may be comparable with the applied voltages and a calibration of the energy scale becomes necessary. The appearance potentials for the positive ions of one of the rare gases which are accurately known are frequently used for this purpose. At lower energies (< 2 eV) there are no processes which can be used to calibrate the energy scale accurately, although there have been some attempts to use the resonance capture cross section of sulphur hexafluoride (see, for example, Compton et al., 1966. These authors finally used a swarm experiment to calibrate both their energy and their cross section scales - see 1.2.4). These limitations restrict beam measurements in general to a little less than 1 eV, although reasonably reliable data have been obtained for electron energies as low as 0.3 eV.

As well as the difficulties in the calibration of the energy scale, there can be quite large (and, until recently, largely unsuspected) errors in the actual magnitudes of the cross sections measured. These errors, which can easily amount to 10 or 20%, are due to the difficulties of absolute pressure

measurement at the very low pressures which must be used to meet the "thin target" conditions described in 1.1.2. The pressures used are usually of the order of 10^{-3} to 10^{-4} torr and are measured with a trapped McLeod gauge. In this pressure range a trapped McLeod gauge can give errors of tens of percent because of the Gaede pumping effect (see, for example, Ishii and Nakayama, 1961); smaller errors can also be caused by the thermal transpiration effect. A useful summary of these errors is given in Keller, Martin and McDaniel (1965).

Thus it can be seen that although beam experiments appear to offer the most straightforward means of measuring cross sections they are subject to experimental difficulties at all energies and have a lower energy limit which is at present about 0.3 eV. However many interesting phenomena occur at energies as low as 0.010 eV and since these energies are inaccessible to beam experiments, an alternative technique must be used.

1.2.3 Swarm Experiments.

The quantities measured in swarm experiments are the transport coefficients for the motion of an assembly of electrons through a high pressure gas under the influence of an electric field. It will be shown later that it is possible to derive expressions for the transport coefficients in terms of the microscopic collision cross sections and it is therefore possible to determine, even though indirectly, these cross sections from the experimental data.

Detailed descriptions of swarm experiments will be given in chapters 2, 3 and 5 but for the purposes of the present comparison it is sufficient to point out that they are carried out at high pressures (2 to 500 torr) in static systems and that the electric field strengths used are high enough to overcome the difficulties inherent in beam experiments. The distribution of the electron energies, as well as the mean energy, is controlled by the electric field strength and the nature, pressure and temperature of the gas. The magnitude of the field determines how much energy the electrons gain between collisions, the nature of the gas determines how much energy they lose in each collision, and, for a given gas, the pressure determines the frequency of the collisions. If the ratio of electric field to gas pressure is high, then the mean electron energy is well above the

mean energy of the gas molecules. On the other hand, if the field is weak and the gas pressure high, the energy gained between collisions will be small and the collisions in which this energy is transferred to the gas will be very frequent. In this case the mean electron energy may exceed the mean energy of the gas molecules by only a few percent and the electron energy can be controlled by varying the gas temperature. Since the mean energies corresponding to $293^{o}K$ and $77^{o}K$ (the gas temperatures used in the present experiments) are 0.04 eV and 0.01 eV respectively, the lower energy limits of swarm experiments are much lower than those obtainable in beam experiments.

1.2.4 Limitations of Swarm Experiments.

The distributed range of electron energies which is an inherent property of swarm experiments is primarily responsible for the limitations of these techniques. The interpretation of the experimental data is not straightforward because the transport properties of the electron swarm are in general controlled by a number of collision processes each with an energy dependent cross section. Thus, for a given set of experimental conditions, the quantities measured experimentally are determined by the cross sections over a limited range of energies rather than by the cross sections at a discrete energy as in a beam experiment. The process of unfolding the energy dependence of the cross sections from a set of data obtained by varying the mean electron energy is therefore complex. Nevertheless, these difficulties have been largely overcome by the application of high speed computing techniques to more rigorous analyses of the dependence of the transport coefficients on the collision cross sections.

The low resolution of swarm techniques is a more fundamental limitation. By comparison with an electron beam of reasonably high resolution which is to be found in most beam experiments, the electron swarm is a relatively blunt probe unsuitable for examining fine scale structure in the cross sections. In general, swarm experiments are therefore unable to detect narrow resonances but it is possible in some instances to determine whether such phenomena are present. For instance, Crompton, Elford and Jory (1966) have used highly

accurate drift velocity data in helium at 293^{o}K to place an upper limit on any resonances in the $q_m - \epsilon$ curve between 0.1 and 5 eV.

It is important to realize that swarm and beam techniques are complementary. Where the cross sections do not exhibit pronounced structure swarm techniques can lead to the most accurate results at all energies less than 3 - 4 eV and are the only techniques available below about 0.5 eV. Beam experiments, on the other hand, have excellent energy resolution but relatively poor absolute accuracy. They are generally useful only for energies greater than 1 eV. In recent years some attempts to correlate the two sets of data have been made and for this reason the extension of swarm techniques to higher energies, as in Part B of this thesis, can be of considerable value.

CHAPTER 2.

SWARM TECHNIQUES

There have been many advances in swarm techniques since the early experiments of Townsend in 1899. Among the most significant advances were the development by Huxley of the improved method of measuring the ratio of drift velocity to diffusion coefficient, the development by Tyndall and by Bradbury and Nielsen of time-of-flight techniques for measuring the drift velocity and the derivation by Huxley and others of more rigorous formulae describing the electronic motion and relating the transport coefficients to the collision cross sections.

The Townsend-Huxley lateral diffusion method of measuring the ratio of drift speed to diffusion coefficient and the Bradbury-Nielsen shutter method of measuring the drift speed are used in the present investigation. The accuracy and reliability of these techniques have been improved in recent years by careful experimentation and critical analyses.

Until the advent of electronic computers, swarm data could only be analysed by assuming a particular form of the distribution function to calculate mean microscopic quantities such as the mean free path between collisions. These quantities are still useful for rapid reduction of the experimental data. However, it is now possible to use computing techniques in conjunction with rigorous formulae describing the electronic motion to calculate the true distribution function and to deduce the variation with energy of the elastic and inelastic cross sections.

In this chapter the principles of both the experimental techniques and of the analysis of the data are discussed. The details of the present investigation are given in chapters 3, 5 and 7.

2.1 Measurement of W/D by the Townsend-Huxley Lateral Diffusion Method.

2.1.1 Townsend's Original Method.

In a series of experiments starting in 1899, Townsend established swarm techniques for the measurement of the ratio of drift velocity to diffusion coefficient and of the magnetic drift velocity. Some of the results of his experi-

ments can be found in Townsend, 1899, Townsend, 1908, Townsend and Tizard, 1913, and Townsend and Bailey, 1921. Summaries of the early results are given in "Motions of Electrons in Gases", Townsend, 1925, "The Motion of Slow Electrons in Gases", Healey and Reed, 1941 and "Electrons in Gases", Townsend, 1948.

Townsend's first direct measurement of W/D in a single apparatus was made in 1908. A schematic diagram of this apparatus is shown in Figure 2.1.

Secondary X-rays from the brass surface S generated electrons or ions in the region above the grid G. The ions were drawn by an electric field to the plate A. Some of them passed through the 1 cm aperture in this plate and travelled through the region of uniform electric field to the collecting electrode C which consisted of an insulated central disc and a surrounding annulus. Townsend was able to relate W/D to the ratio

$$R = \frac{i_1}{i_1 + i_2}$$

where i_1 and i_2 are the currents received by the disc and annulus respectively, and thus by measuring this ratio he was able to find W/D from a single experiment.

In his later experiments the entrance aperture was a slit 2 mm wide and 15 mm long and the collecting electrode consisted of a central strip and two outer segments. Once again W/D could be related to the ratio of the currents received by the various segments. When values of W/D smaller than those predicted were found (Townsend and Tizard, 1913) Townsend attributed this to the breakdown of the theory of equipartition, a possibility which exists when a stream of light charged particles drifts through a gas of much heavier particles under the influence of an electric field. He wrote

$$\tfrac{1}{2} m\overline{c^2} = k_T \tfrac{1}{2} M\overline{C^2}$$

thus introducing the energy factor k_T which will be discussed later.

These two methods of Townsend suffered from several disadvantages. The derivation of the expression relating W/D to the current ratio required the postulation of constant electron density over the source aperture. Since the

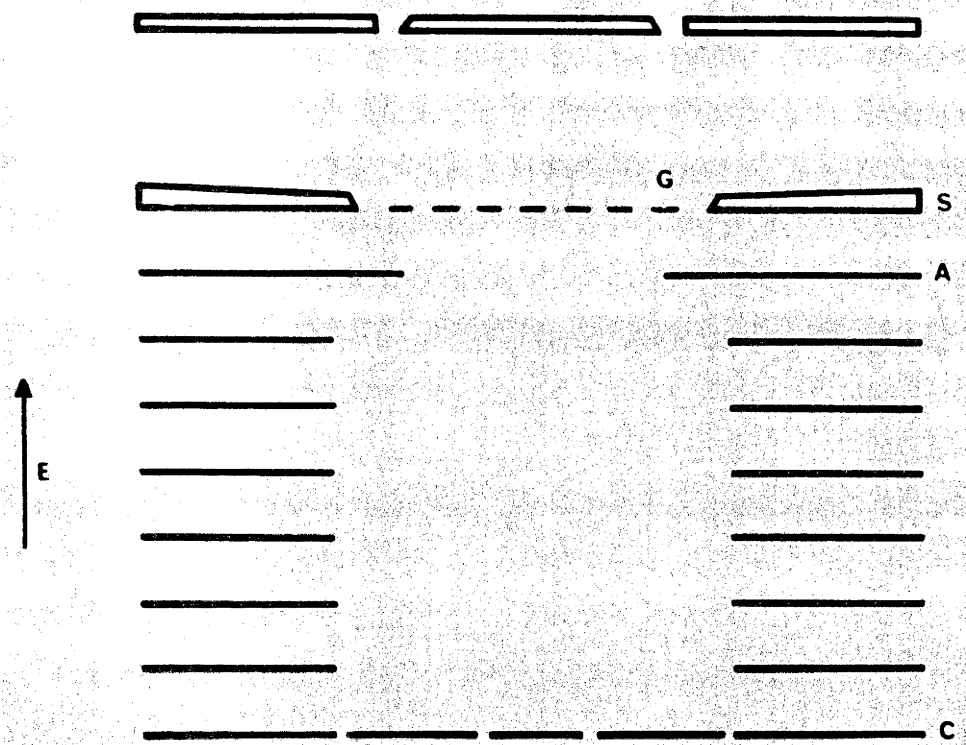

Figure 2.1.

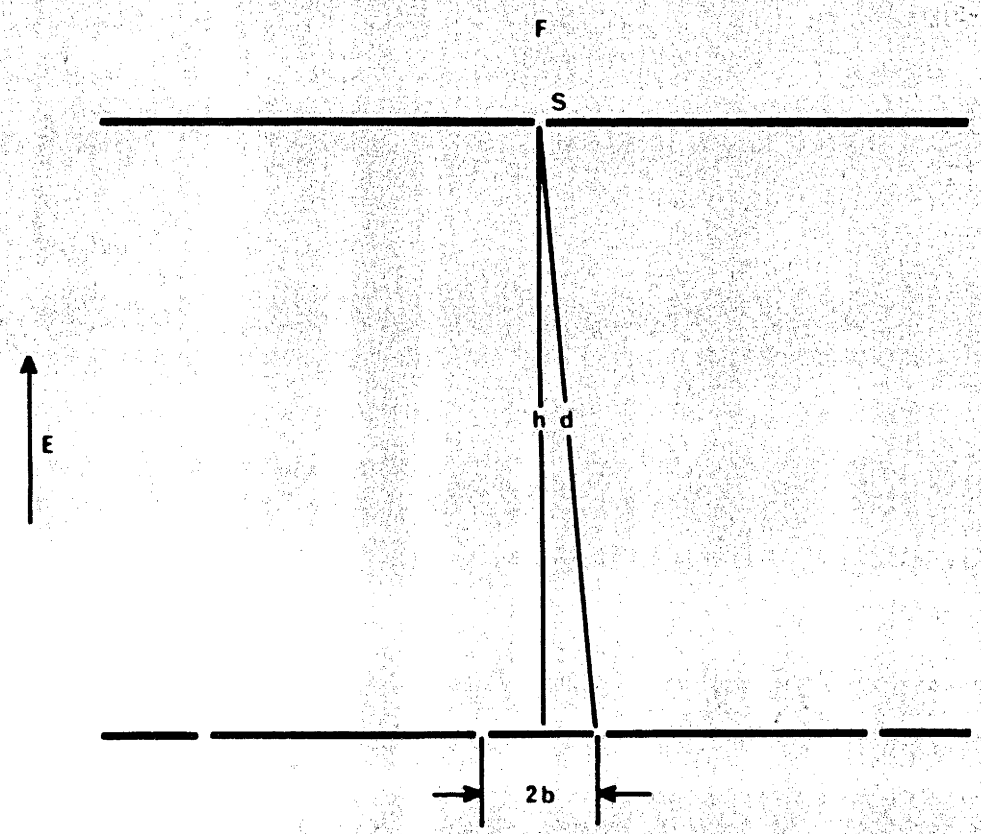

Figure 2.2.

entrance slits were so large this would have been difficult to realize and undoubtedly led to inaccuracies in results. In addition, the formula derived by Townsend for this type of geometry was a series solution and therefore involved a large amount of preliminary calculation to obtain the desired accuracy. Since these calculations had to be repeated for each apparatus of different dimensions there was little tendency to check the results over a wide range of the experimental parameters.

2.1.2 Huxley's Modification of Townsend's Method.

In 1940 Huxley solved the differential equation appropriate to the case of electrons entering the chamber through a small circular hole and travelling to a collecting electrode consisting of an insulated central disc and surrounding annulus. This solution was first applied by Huxley and Zazou in 1949.

The modification allowed a major improvement in the flexibility and the accuracy of the method. It was largely free from both the objections raised to Townsend's method. Firstly, the small circular hole was effectively a point source of electrons and therefore the error incurred by postulating uniform electron density over the source was greatly reduced. Secondly, the expression relating W/D to the current ratio was much simpler and capable of exact determination. As a result, the task of calculating tables of values of the ratio of currents and the corresponding values of W/D for apparatuses of different dimensions was no longer arduous and it was possible to test the method over a wide range of the experimental parameters.

A schematic diagram of the apparatus suggested by Huxley (and used in the present investigation) is shown in Figure 2.2. Electrons generated at F enter the diffusion chamber through the small hole S in the cathode, and from there drift and diffuse to the anode under the influence of a uniform electric field of strength E. The electric field and gas pressures are the same between F and the cathode as they are in the diffusion chamber. This ensures that the electrons have reached a steady state energy distribution before they enter the main section of the apparatus. The anode, or collecting electrode, is at a

distance h from the cathode and consists of a central disc of radius b and an insulated outer annulus. The ratio of the current received by the central disc to that received by the whole electrode is measured and this, through the formula given below, allows the calculation of the value of W/D appropriate to the experimental conditions.

The experiments are designed to ensure that the electron concentration at the outer edge of the diffusion chamber is negligible and that a negligible fraction of the total current falls outside the annulus of the collecting electrode, i.e. the annulus is effectively of infinite radius. In this way the concentration of electrons at the "walls" of the chamber is zero and no modification of the theory need be made to include the effects of the containing walls of the electrode system, as was suggested by Warren and Parker (1962).

As mentioned above, this modification of Townsend's original method was first used by Huxley and Zazou in 1949. In their apparatus the chamber length was 1 cm and electrons entered through a 1 mm hole in the cathode. More accurate measurements were made later by Crompton and Sutton (1952) who used a similar apparatus.

The method forms the basis of most of the more recent studies in this field including those of Cochran and Forrester (1962), Crompton and Jory (1962), Warren and Parker (1962), and Crompton and Elford (1963). Reference to these papers will be made in later chapters. The only recent diffusion measurements known to the author which have not used this method are those of Hurst and his colleagues, and those of Skullerud (1966).

2.1.3 Derivation of the Differential Equation Describing the Electron Concentration.

From the definitions of drift velocity and diffusion coefficient given in 1.1.3 the net transport of electrons across a surface of area $d\underline{S}$ in the diffusion chamber is $n\underline{W} \cdot d\underline{S}$ due to drift and $-D \operatorname{grad} n \cdot d\underline{S}$ due to diffusion (n is the electron number density). The total transfer across $d\underline{S}$ due to drift and diffusion is then

$$(n\underline{W} - D \operatorname{grad} n) \cdot d\underline{S}$$

In an arbitrary volume element $d\tau$ which contains N_1 electrons but no sources or sinks of electrons, the rate of change of N_1 must equal the net flow of electrons across the surface area of the element.

Thus,

$$\frac{dN_1}{dt} = \frac{d}{dt}\left(\int\int\int n\, d\tau\right)$$

$$= -\int\int (n\underline{W} - D \operatorname{grad} n) \cdot d\underline{S}.$$

Transforming the right hand side by using Gauss' theorem we have:

$$\int\int\int \frac{dn}{dt} = -\int\int\int \operatorname{div}(n\underline{W} - D \operatorname{grad} n)\, d$$

and hence

$$\frac{dn}{dt} = -\nabla \cdot (n\underline{W} - D \operatorname{grad} n)$$

$$= D\nabla^2 n - \nabla \cdot (n\underline{W})$$

For steady state conditions the concentration of electrons at any point is constant, i.e. $dn/dt = 0$.

Therefore

$$D\nabla^2 n - \nabla \cdot (n\underline{W}) = 0$$

or

$$D\nabla^2 n - \underline{W} \cdot \nabla n = 0 \qquad (2.1)$$

For a uniform electric field parallel to the z-axis, $\underline{W}$ is constant and $\underline{W} = W_z = W$. In this case equation (2.1) becomes

$$\nabla^2 n = (W/D)\frac{\partial n}{\partial z}$$

$$\nabla^2 n = 2\lambda \frac{\partial n}{\partial z} \qquad (2.2)$$

where

$$2\lambda = W/D.$$

The assumption that W is constant and equal to W_z will be used throughout. Equation (2.2) shows that the concentration of electrons in steady state motion under the influence of an electric field is governed by the ratio of their drift velocity to diffusion coefficient.

2.1.4 Solution of the Differential Equation.

The differential equation (2.2) was solved by Huxley (1940) for the apparatus geometry of Figure 2.2.

He found that

$$n = \frac{e^{\lambda z}}{(\lambda r)^{\frac{1}{2}}} \sum_{s=0} A_s K_{s+\frac{1}{2}} (\lambda r) P_s (\cos \theta) \qquad (2.3)$$

where $K_{s+\frac{1}{2}} (\lambda r)$ is the modified Bessel function of half integral order,

$P_s (\cos \theta)$ is the associated Legendre function,

A_s is a constant

and r is the radial distance from the origin.

An isolated pole source of electrons at the origin corresponds to the case s = 0 in equation (2.3). The electron concentration is then given by

$$n = A \frac{e^{-\lambda (r-z)}}{r} \qquad (2.4)$$

When the boundary condition n = 0 at z = h is used in conjunction with the solution given by equation (2.4) it has been shown (e.g. Huxley and Crompton, 1955) that the expression for the current ratio R is

$$R = 1 - (h/d) \exp (- \lambda (d - h)) \qquad (2.5)$$

where

$$d^2 = h^2 + b^2$$

Other solutions have been investigated. For example, s = 1 in equation (2.3), corresponding to a dipole source of electrons at the origin (that is, n = 0 at z = 0 except at the origin) with the boundary condition n = 0 at z = h, leads to (Huxley

and Crompton, 1955):

$$R = 1 - [\, h/d - 1 / \lambda\, h\,(1 - (h/d)^2)\,]\; h/d\; \exp(-\lambda\,(d-h)) \qquad (2.6)$$

It was originally thought that equation (2.6) should have been the correct solution since the boundary conditions in this case appeared more realistic than those applied to give equation (2.5). An extensive experimental investigation by Crompton and Jory (1962), some details of which are given below, showed conclusively that equation (2.5) is the solution which is consistent with the experimental results over a wide range of the experimental parameters. It should be pointed out that under most experimental conditions, and certainly those to be described in the first half of this thesis, the difference between equations (2.5) and (2.6) is entirely negligible.

A more recent theoretical investigation of the Townsend-Huxley swarm technique by Hurst and Liley (1965) showed that it is impossible to impose a set of physically realistic boundary conditions on equation (2.3). They applied very general boundary conditions to their solution (basically the same as equation 2.5) and found that values of their "reflection coefficients" consistent with equation (2.5) or (2.6) did not correspond to any physically realizable situation. The values of the "reflection coefficients" were therefore found by recourse to experimental results and this meant that the solution consistent with all the experimental results, i.e. equation (2.5), was the one they chose.

The situation is, therefore, that although equation (2.5) is a semi-empirical result, it is known to be completely consistent with observation. This is the solution used throughout this work.

Although measurement of the ratio R leads directly to the value of λ and hence W/D, it is usual to express the results in terms of either k_1, which is closely related to the Townsend energy factor, or in terms of D/μ where μ (= W/E) is the electron mobility. The results are expressed this way because W/D is a pressure dependent quantity, and because, as will be shown below, both k_1 and D/μ are closely related to the physical properties of the swarm.

2.1.5 Analysis of Possible Errors. Experimental Tests.

Crompton and Jory (1962) made an extensive systematic study of the Townsend-Huxley lateral diffusion technique. Using an apparatus of variable geometry they measured W/D in hydrogen over a wide range of the experimental parameters. They also examined a number of possible sources of error. Their results may be summarised as follows:

(a) Over the entire ranges of h and b, h = 2, 5 and 10 cm, b/h = 0.05, 0.10, 0.15, 0.2, and 0.25, they analysed the measured current ratios with both equation (2.5) and equation (2.6). For a given value of E/p (where E is the electric field strength and p the gas pressure) the values of k_1 found using equation (2.5) were always in agreement with one another to within 1%. Poor self consistency was observed when the current ratios were analysed with equation (2.6).

For long chamber lengths, which must be used for maximum accuracy, the differences between the two solutions is less than 0.25% and it is unimportant which is used. However, since equation (2.5) always led to consistent data, Crompton and Jory concluded that this is the solution which should be used to analyse all the results.

(b) They calculated the effect on R of the source hole being off the central axis of the apparatus and the effect of the finite size of the source hole. For axial alignment of the source hole being 0.020 cm in error, the error produced in k_1 was found to rise with R and to be less than 0.5% everywhere for h = 10 cm and b = 0.5 cm. The finite size of the source hole produced a larger error which also increased with R, and which was approximately 1% for R = 0.9 using the same chamber geometry as in the previous example. Crompton and Jory stated that these calculations would probably overestimate the size of these effects and produced experimental results justifying this statement. (This may have been fortuitous - see chapter 4).

(c) They obtained values of k_1 in hydrogen for $0.10 \leq E/p \leq 5.0$ (E in V cm^{-1} and p in torr) which were accurate to within 1% thus firmly establishing

that the Townsend-Huxley technique could be used to produce accurate and reliable data.

Crompton and Elford (1963) reported an extension of these experiments to lower values of E/p in hydrogen and nitrogen. The effect of contact potential differences within the apparatus and the effects of field non-uniformity from other sources were investigated by these authors and by Crompton, Elford and Gascoigne (1965); further discussion of these points will be given in chapter 3.

Parker (1963) has calculated the effect on a lateral diffusion experiment of the spatial distribution of the electron energy. He did this by including in the appropriate form of the Boltzmann transport equation terms involving spatial derivatives of the distribution; such terms are usually assumed small in comparison to the field and collision terms. He found that the values of D/μ should be spatially dependent, particularly when the electron energy is very much greater than the thermal energy of the gas molecules. The approximate error in D/μ expected from Parker's theory is

$$\frac{\delta\,(D/\mu\,)}{D/\mu} = \frac{D}{2\,\mu\,E\,h} - \tfrac{1}{4}\,(b/h)^2$$

and can be as large as 20% for short chamber lengths and large diameter collecting electrodes. There has been no evidence of spatial dependence of D/μ in any lateral diffusion experiments, even when b and h have been varied over wide limits. Parker's theory deals only with elastic collisions between electrons and gas molecules and takes no account of the boundary conditions imposed by the surfaces of the apparatus. Until a more realistic theory is available it is doubtful whether any comparison with experiment could be considered significant.

2.1.6 Skullerud's Variation.

Skullerud (1966) has described a modified apparatus resembling Townsend's 1913 apparatus rather more than it does Huxley's modification. In Skullerud's apparatus the entrance aperture is a narrow slit (5 cm by 0.01 cm)

and the collecting electrode is a centrally divided plane capable of being moved both horizontally and vertically.

The value of D/μ is found by examining the ratio of currents received by the two halves of the plane as the collecting electrode is moved horizontally. The method has the advantage that it is virtually of infinitely variable geometry (c.f. the ratio limitations on a disc apparatus of fixed b/h, section 3.1) and that, to a first order, it is independent of minor asymmetries in the collecting electrode. To date the method has only been used for positive ions at high E/p with an experimental accuracy of about 5%. There is no reason why the method should not be used for electrons as well as ions, or why later mechanical improvements should not make the accuracy comparable with that attained in the present experiments.

2.2 Measurement of W by the Bradbury-Nielsen Time-of-Flight Method.

2.2.1 Principle of the Method.

The essential features of the method are the same as those first reported by Bradbury and Nielsen (1936) and Nielsen (1936). A schematic diagram of the type of apparatus developed by them is shown in Figure 2.3.

Electrons generated at the filament F drift through the region of uniform electric field AB to the collecting electrode at B. Two electrical shutters S_1 and S_2, held at the appropriate d.c. potentials and separated by the accurately known distance h, are placed in the path of the electrons. Each shutter consists of a plane grid of parallel wires with alternate wires being connected to one another, and the two halves so formed being insulated from each other. An a.c. signal of variable frequency but constant voltage is applied to the two halves of each shutter; the voltages applied to each half are exactly 180° out of phase and the signals applied to both shutters are identical in phase and voltage. The current received at B is recorded as the frequency of the a.c. signal is varied. A graph of current against frequency shows a series of maxima as illustrated in Figure 2.4.

The shutter S_1 divides the electron stream into a series of pulses since electrons are transmitted only when the a.c. signal applied to the wires

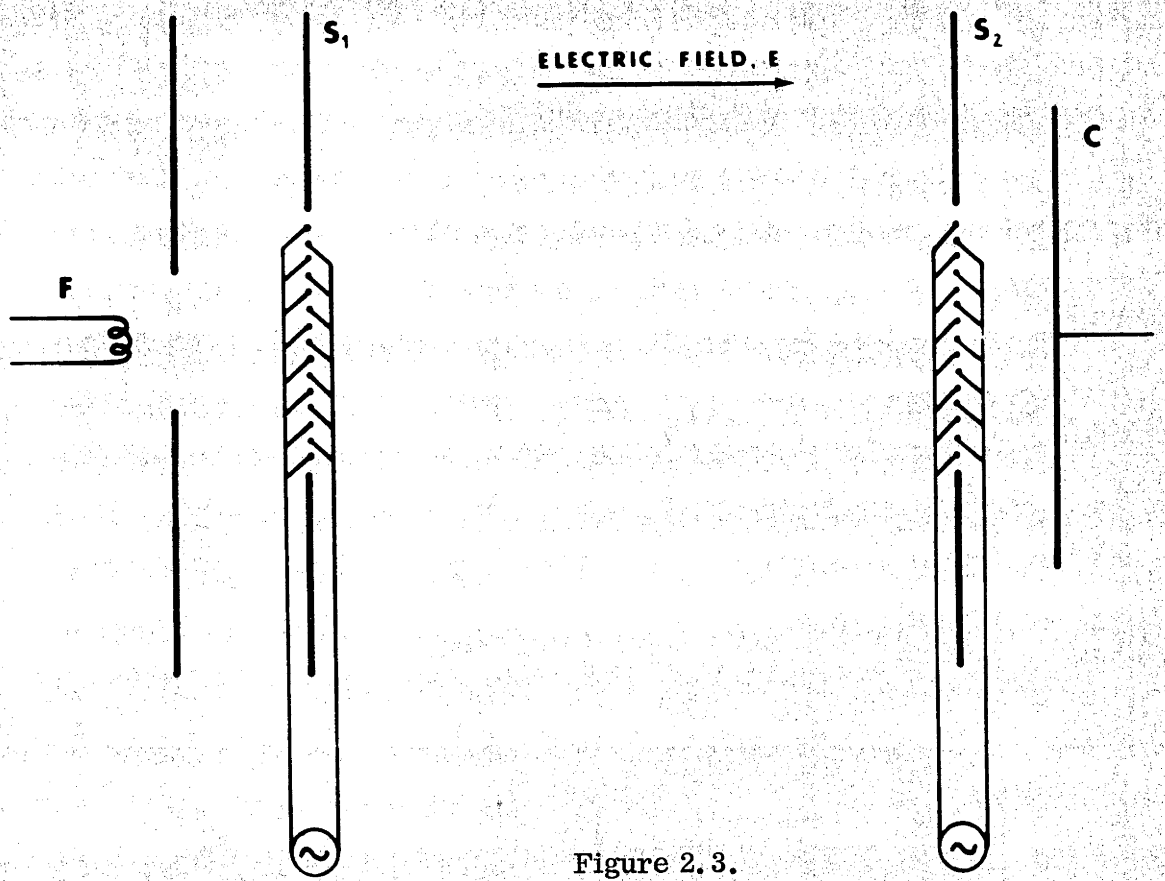

Figure 2.3.

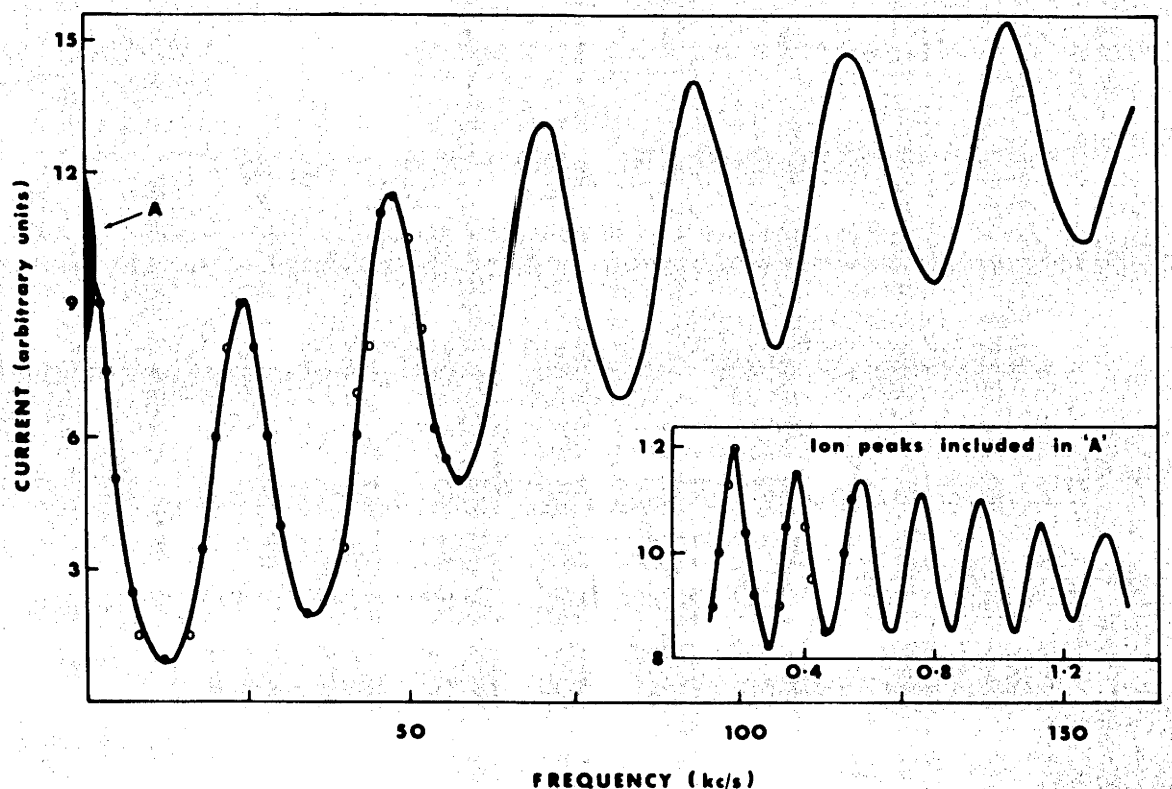

Figure 2.4.

approaches zero. If the frequency applied to the wires is f , then the shutters will open with a frequency 2 f. The second shutter S_2 has the same effect on the electron current as S_1 . The first maximum in the current-frequency curve will correspond to the frequency f_o for which pulses of electrons produced by S_1 arrive at S_2 when the shutters are about to open again; other maxima will occur at integral multiples of f_o . The observed drift velocity is then given by

$$W = 2\,h\,f_o \qquad \text{or} \qquad W = 2\,h\,f_m / m \tag{2.7}$$

where f_m is the frequency of the a. c. signal corresponding to the m th current maximum.

2.2.2 Analysis of Possible Errors. Experimental Tests.

Duncan (1957) made a theoretical investigation of the electron concentration in a drift velocity experiment. Taking into account diffusion of electrons within the pulse he showed that, if W' is the observed drift velocity, then the true value W is given by

$$W' = W\,[\,1 + 2/(hW/D)\,]$$

This relation was useful only when the correction was small, but did show that the effects of diffusion could be reduced by using longer chamber lengths and higher gas pressures.

Qualitative agreement with these predictions was obtained by Crompton, Hall and Macklin (1957) by measuring drift velocities in an apparatus with shutter separations of 3, 6 and 10 cm.

A systematic study of the errors inherent in this type of experiment was made by Lowke (1962, 1963). He investigated possible errors from the following sources:

(a) The position of the maximum electron density in the pulse is altered because, owing to back diffusion, some electrons from each pulse will be absorbed by the first shutter after it has closed.

(b) Similarly, the pulse is disturbed by the absorption of electrons on the unopened second shutter.

(c) Because of the diffusion current, the frequency corresponding to maximum density is not equal to that corresponding to maximum electron current at the second shutter.

(d) The number of electrons in each pulse varies as the frequency is varied.

(e) The peaks in the current frequency curves are not symmetrical because there is a continuous decay of the maximum electron density in the pulse as it passes through the second shutter.

(f) The shutters transmit electrons of high speed more readily than electrons of low speed.

Factors (c), (d) and (e) were included in Duncan's analysis. Lowke was unable to find the effect of factor (f), but showed that the effect of the remaining factors could be taken into account in the following expression relating the observed drift velocity W' to the true drift velocity W :

$$W' = W [1 + 3 / (hW/D)] \qquad (2.8)$$

He was able to obtain quantitative agreement between experimental observations and the predictions of equation (2.8).

In his analysis Lowke included an expression for the resolving power of the method. The resolving power for a given current peak is defined as the frequency corresponding to maximum current divided by the frequency spread at half the maximum current. Thus, if the resolving power is high, the current peak is very sharp and the drift velocity can be determined with high accuracy. Lowke found that the resolving power, RP, was given by

$$RP = \tfrac{1}{4} (h W/D \log_e 2) \qquad (2.9)$$

Lowke also experimentally investigated the effects of a large number of other possible sources of error. These included the non-uniformity of the applied d.c. field, phase errors and distortions in the a.c. voltages, space charge repulsion and the effects of a broken lead to either a guard electrode or a shutter.

Using the results of his analysis to eliminate sources of error and to take into account the effects of diffusion, Lowke obtained highly accurate

values of electron drift velocities in nitrogen and hydrogen at 293°K and 77.6°K. Elford (1966) with an apparatus of improved design and with more accurate pressure measurement has reported electron drift velocities in carbon dioxide with a claimed error limit of 0.5%.

2.3 The Analysis of Data.

Until the introduction of electronic computers, swarm data were analysed by assuming a particular form of the distribution function to calculate mean quantities, such as an effective mean free path or collision cross section. Crompton and Sutton (1952), for example, produced data of this type for hydrogen and nitrogen. Similarly, most of the swarm data in "Basic Processes of Gaseous Electronics" (Loeb, 1955) are average quantities deduced by assuming either a Maxwell or Druyvesteyn distribution.

For a gas in which only elastic scattering occurs it has been found possible to derive an integral expression for the distribution function which can be computed for any given variation of the momentum transfer cross section. The true variation with energy of this cross section can be deduced by calculating the transport coefficients and comparing them with the experimentally measured values.

When inelastic collisions occur the distribution function can be calculated by a numerical solution of the Boltzmann transport equation. The deduction of the momentum transfer and the inelastic cross sections is once again made by comparing the calculated and experimental values of the transport coefficients.

The various formulae used in these calculations are given below.

2.3.1 The Distribution Function for Elastic, Non-isotropic Scattering.

Many derivations of the form of f(c) for the case of elastic, non-isotropic scattering have been given, e.g. Chapman and Cowling (1939), Loeb (1955), Huxley (1960). In all derivations it is found that

$$f(c) = B \exp\left\{ -3m \int_0^c \frac{c \cdot dc}{M\left(\frac{E}{N} \cdot \frac{e}{m} \cdot \frac{1}{c q_m}\right)^2 + 3kT} \right\} \qquad (2.10)$$

$$= B \exp U$$

where

$$U = -3m \int_0^c \frac{c \cdot dc}{M\left(\frac{E}{N} \cdot \frac{e}{m} \cdot \frac{1}{c q_m}\right)^2 + 3kT} \qquad (2.11)$$

To find the value of B use is made of the normalizing integral

$$\int_0^\infty 4\pi c^2 f(c)\, dc = 1$$

from which

$$f(c) = \frac{\exp U}{\int_0^\infty 4\pi c^2 \exp U \cdot dc}$$

Similarly the average of a typical function g(c) is given by

$$\overline{g(c)} = \int_0^\infty 4\pi c^2 g(c) f(c)\, dc$$

$$= \frac{\int_0^\infty \exp U \cdot g(c) \cdot c^2\, dc}{\int_0^\infty \exp U \cdot c^2 \cdot dc}$$

Two special cases, corresponding to $k_1 \sim 1$ (thermal equilibrium) and $k_1 >> 1$, may be distinguished.

(a) When k_1 is >> 1, $\frac{1}{2} mc^2$ is very much greater than $\frac{1}{2} MC^2$ and it is possible to neglect the 3 kT term in the denominator of equation (2.11) i.e.

$$U = -3m \int_0^c \frac{c^3 \cdot q_m^2 \cdot dc}{M(E/N)^2 (e/m)^2} \qquad (2.12)$$

To evaluate this further it is necessary to postulate some form of variation of q_m with c. For generality we take $q_m = A' c^{-r}$.
Substituting this in (2.12) we have,

$$U = -3m \int_0^c \frac{c^3 (A')^2 c^{-2r}}{M(E/N)^2 (e/m)^2} \cdot dc$$

$$= -\frac{c^n}{\alpha^n}$$

with $$\alpha^n = \frac{M n}{3 m} (E/N)^2 (e/m)^2 (A')^2 \qquad (2.13)$$

and $n = 4 - 2r$.

The distribution function can now be written

$$f(c) = \frac{\exp(-c^n/\alpha^n)\, dc}{\int_0^\infty 4\pi c^2 \exp(-c^n/\alpha^n)\, dc}$$

Using the identity $\int_0^\infty \exp(-y^n)\, y^m\, dy = \Gamma\left[\frac{m+1}{n}\right]$, f(c) is given by

$$f(c) = \frac{n \exp(-c^n/\alpha^n)}{4\pi \alpha^3 \Gamma(3/n)} \qquad (2.14)$$

From this it can be seen that the average value of c^s is

$$\overline{c^s} = \alpha^s \Gamma\left[\frac{s+3}{n}\right] \left(\Gamma\left[\frac{3}{n}\right]\right)^{-1} \qquad (2.15)$$

Two special cases of this are of particular interest:

(1) if $q_m \propto 1/c$, then $r = 1$ and $n = 2$

$$f(c) = \frac{\exp(-c^2/\alpha^2)}{\alpha^3 \pi^{3/2}} \qquad (2.16)$$

which is the Maxwell distribution.

(2) if q_m is constant, then r = 0 and n = 4

$$f(c) = \frac{\exp(-c^4/\alpha^4)}{\pi \alpha^3 \Gamma(3/4)} \qquad (2.17)$$

which is the distribution of Druyvesteyn (1930).

(b) In the case of thermal equilibrium $k_1 \sim 1$, and 3 kT becomes the controlling factor in the denominator of equation (2.11). The expression for U then becomes

$$U = -3m\int_0^c \frac{c \cdot dc}{3kT}$$

$$= -\frac{m}{kT}\,\frac{c^2}{2}$$

$$= -c^2/\alpha^2$$

with $\alpha^2 = 2kT/m$.

The distribution function can once more be written in the form

$$f(c) = \frac{\exp(-c^2/\alpha^2)}{\alpha^3 \pi^{3/2}}$$

showing that for thermal equilibrium the distribution is Maxwellian regardless of the form of variation of q_m with c.

An alternative form of the distribution function is often used. The distribution function $f(\epsilon)$ is defined such that the probability of an electron having an energy between ϵ and $\epsilon + d\epsilon$ is $\epsilon^{\frac{1}{2}} f(\epsilon)\, d\epsilon$. The expression for $f(\epsilon)$ is:

$$f(\epsilon) = A \exp\left[-\int_0^{\epsilon} \left[\frac{M}{6m} \left(\frac{E}{Nq_m} \right) \frac{1}{\epsilon} + kT/e \right]^{-1} d\epsilon \right] \qquad (2.18)$$

The value of A is found through the normalization

$$\int_0^\infty \epsilon^{\frac{1}{2}} f(\epsilon)\, d\epsilon = 1$$

2.3.2 Mean Quantities.

The formulae given in this section are included since they can be extremely useful for rapid reduction of experimental data. The following relations can be derived (Huxley and Zazou, 1949, Crompton and Sutton, 1952):

Townsend energy factor $$k_T = 2/3 \left[\overline{c^2}\ \overline{c^{-1}} / \bar{c} \right] k_1 \qquad (2.19)$$

Mean velocity $$\bar{c} = (2kT/m)^{\frac{1}{2}} \left[\bar{c}\ \overline{c^{-1}} \right]^{\frac{1}{2}} k_1^{\frac{1}{2}} \qquad (2.20)$$

Root Mean square velocity $$\left(\overline{c^2} \right)^{\frac{1}{2}} = (2kT/m)^{\frac{1}{2}} \left[\overline{c^2}\ \overline{c^{-1}} / \bar{c} \right]^{\frac{1}{2}} k_1^{\frac{1}{2}} \qquad (2.21)$$

Mean free path at unit pressure

$$L = (3/2)\ (m/e)\ (2kT/m)^{\frac{1}{2}} \left[\bar{c}\ \overline{c^{-1}} \right]^{-\frac{1}{2}} W k_1^{\frac{1}{2}} / E/p \qquad (2.22)$$

Mean fractional energy loss per collision

$$\eta = 3\ (m/2kT) \left[\left(\overline{c^{-1}} \right)^2 \overline{c^2} \right]^{-1} W^2 / k_1 \qquad (2.23)$$

Each of the square bracketted terms is a dimensionless quantity; the bar indicates an average over the velocity distribution. By specifying either a Maxwell or Druyvesteyn distribution the various velocity averages can be evaluated using equation (2.15). The results are

Velocity Average	Maxwell	Druyvesteyn
$\bar{c}$	$2\alpha / \pi^{\frac{1}{2}}$	$0.8161\ \alpha$
$\overline{c^2}$	$3\alpha^2 / 2$	$0.7397\ \alpha^2$
$\overline{c^{-1}}$	$2 / \alpha \pi^{\frac{1}{2}}$	$1.4464 / \alpha$

These values can be substituted in the above relations to give the numerical constants appropriate to each distribution.

2.3.3 Formulae for Drift and Diffusion.

For the case of non-isotropic scattering the following formulae have been derived (Huxley, 1960) :

$$W = \mu E = - \frac{E e}{3 m} \int_0^\infty 4 \pi c^2 \frac{1}{N q_m(c)} \frac{d f}{d c} d c \qquad (2.24)$$

$$D = \frac{1}{3} \int_0^\infty 4 \pi c^2 \frac{c}{N q_m (c)} f (c) d c \qquad (2.25)$$

It should be noted that these equations are applicable only when $M \gg m$ and that, since they are given in terms of the electron speed c, q_m is $q_m(c)$. The normalising integral for f(c) in this case is

$$\int_0^\infty 4 \pi c^2 f(c) d c = 1 \qquad (2.26)$$

Alternative forms in terms of the electron energy ϵ are (Allis, 1956)

$$DN = \frac{(2/m)^{\frac{1}{2}}}{3} \int_0^\infty \frac{\epsilon f (\epsilon) d \epsilon}{q_m (\epsilon)} \qquad (2.27)$$

and

$$\mu N = - \frac{e(2/m)^{\frac{1}{2}}}{3} \int_0^\infty \frac{\epsilon}{q_m (\epsilon)} \frac{d f}{d \epsilon} . d \epsilon \qquad (2.28)$$

in which case the normalizing integral is

$$\int_0^\infty \epsilon^{\frac{1}{2}} f (\epsilon) d \epsilon = 1 \qquad (2.29)$$

Since many of the formulae to be given below were derived by Huxley using equations (2.24) and (2.25) it is simpler to use only these forms of the transport integrals in the present chapter.

2.3.4 Use of the Coefficient D/μ .

As mentioned in 2.2.3 above, although the Townsend-Huxley lateral diffusion technique directly measures W/D, it is customary to report the results of these experiments in terms of the ratio D/μ or the quantity k_1 which will be defined below. The reason for this choice, apart from the obvious one that W/D is pressure dependent but D/μ is not, can be seen from the argument which follows.

If we integrate the expression for W (equation (2.24)) by parts we obtain :

$$W = \frac{E\,e}{3\,m}\left\{ \left[-4\pi c^2 (1/N q_m(c))\ f(c) \right]_0^\infty + \int_0^\infty 4\pi c^2 c^{-2} \frac{d}{dc}\left(\frac{c^2}{N q_m(c)} \right) f(c)\, dc \right\}$$

The square bracketted term vanishes at both limits since $f(c) \to 0$ as $c \to \infty$, but f(c) remains finite for c = 0. Also, since the average of any quantity X(c) is defined to be

$$\overline{X(c)} = \int_0^\infty 4\pi c^2 f(c)\, X(c)\, dc$$

where the bar denotes an average of this type, we have

$$W = \frac{E\,e}{3\,m}\left[\overline{c^{-2} \frac{d}{dc} \frac{c^2}{N q_m(c)}} \right] \qquad (2.30)$$

In a similar way equation (2.25) becomes

$$D = \frac{1}{3}\left[\overline{\frac{c}{N q_m(c)}} \right] \qquad (2.31)$$

Thus

$$D/\mu = \frac{m}{e} \frac{\left[\overline{\frac{c}{q_m(c)}}\right]}{\left[c^{-2}\frac{d}{dc}\overline{\frac{c^2}{q_m(c)}}\right]}$$

$$= \tfrac{1}{2} m\overline{c^2} \cdot \frac{1}{e} \cdot \frac{1}{F} \qquad (2.32)$$

where

$$F = \frac{\left[c^{-2}\frac{d}{dc}\left(\overline{\frac{c^2}{q_m}}\right)\right]\overline{c^2}}{2\left[\overline{\frac{c}{q_m}}\right]}$$

is a dimensionless average. D/μ is thus proportional to the mean electron energy. The alternative parameter k_1 which was used extensively in the older literature is closely related to the ratio of electronic to molecular energy, i.e. it is closely related to k_T, the Townsend energy ratio. From the definition of k_T (section 2.1.1)

$$\tfrac{1}{2} m\overline{c^2} = k_T \tfrac{1}{2} M\overline{C^2}$$

$$= k_T \cdot \frac{3}{2} kT$$

From equation (2.32)

$$W/D = \frac{e E F}{\tfrac{1}{2} m\overline{c^2}}$$

and substituting for $\tfrac{1}{2} m\overline{c^2}$

$$W/D = \frac{e E F}{k_T(3/2) kT}$$

$$= \frac{e}{k_T} \frac{E}{k_1} \qquad (2.33)$$

where k_1 is related to k_T through the simple expression

$$k_1 = \frac{3\,k_T}{2\,F}$$

Although k_1 is not exactly the ratio of electronic to molecular energies, it is a measure of this ratio which, unlike k_T, does not depend on a knowledge of the distribution function for its evaluation.

2.3.5 Special Case of a Gas in which Only Elastic Scattering Occurs.

Equations (2.10), (2.24) and (2.25) show that for a gas in which only elastic collisions occur the transport coefficients are entirely determined by the variation of q_m with c. With computing techniques these integrals can be readily evaluated.

The true variation of q_m with c is found by an iterative procedure; the transport coefficients are evaluated for a trial variation of q_m with c and the calculated values compared with the experimental results. The trial variations are continued until the agreement between calculated and experimental values is considered satisfactory.

In principle it would be possible to deduce the variation of q_m with c from only one measured transport coefficient. In practice it is desirable to have experimental data for more than one transport coefficient to provide a valuable cross-check on the values of q_m selected.

This method has been used in helium (Frost and Phelps, 1964, Crompton and Jory, 1965) and in most of the other inert gases (Frost and Phelps, 1964). Of these analyses only Crompton and Jory's is based on experimental data of adequate precision. They measured three transport coefficients with accuracies of 1%, 1% and 3% respectively and found that their calculated values agreed with these data to within the experimental accuracy.

2.3.6 Analysis Including the Effects of Inelastic Collisions.

A more complex analysis of the data must be used whenever inelastic collisions occur, i.e. in the polyatomic gases at all energies and in the

inert gases for energies above the first inelastic threshold. The techniques are essentially the same as those described above for the case of purely elastic scattering. The important differences are :

(a) The form of f(c) is no longer given by a closed expression such as (2.10) but must be found by numerical methods from the solution of the appropriate Boltzmann transport equation. Details of these solutions will be given in chapters 7 and 8.

(b) Since several cross sections must be determined from the limited amount of experimental data; the results are not necessarily unique but merely represent a set of cross sections consistent with observation (see 1.3).

(c) Due to the approximations involved in setting up the initial equations and to the inaccuracies involved in the numerical techniques available at present, it is unlikely that the cross sections can be deduced with an accuracy of better than 5% even under the most favourable conditions.

2.4 Use of the Parameter E/N.

It has been almost universal practice to report the results of experiments in ionized gases in terms of the parameter E/p. This was satisfactory while all experiments were done at room temperature and while the variation in the constant of proportionality between the gas pressure p and the gas number density N was small compared with the experimental error. Neither of these are true of the present investigation or of most modern experiments in this field. Although the use of the parameter E/N would overcome this objection it is not generally accepted because of the cumbersome powers of ten involved.

Huxley, Crompton and Elford (1966) noted this tendency and suggested the use of a new unit of E/N which they proposed to call the "Townsend". The suggested magnitude was

$$1 \text{ Townsend} = 10^{-17} \text{ V cm}^2 .$$

The choice of this factor creates approximately a one-to-one correspondence between E/N and E/p for experiments at liquid nitrogen temperature and a one-to-three correspondence to within 3% for ambient temperatures in the range

$282^{o}K \leq T \leq 293^{o}K$. More precisely

$$E/N \text{ (Townsend)} = (1.0354 \times 10^{-2} T)\ E/p_T \text{ (V cm}^{-1} \text{ torr}^{-1})$$

Many of the present results are expressed as a function of E/N with units of V cm^2. Some of the data were taken prior to 1966 and are therefore expressed in terms of the older parameter E/p with p being measured at $293^{o}K$. These data have been converted to standard values of E/N by a graphical method. Since some loss of precision was unavoidable such data are given only as subsidiary results in Appendix 2.

CHAPTER 3.

APPARATUS AND EXPERIMENTAL TECHNIQUES IN THE LATERAL DIFFUSION EXPERIMENT.

Only one experimental tube was used for all the measurements of D/μ at both $293^{o}K$ and $77^{o}K$. Many of the details of the design, of the construction and of the methods of eliminating errors in this type of experiment were given in Crompton, Elford and Gascoigne (1965). An earlier report of this experiment together with a brief summary of some experimental results was given in Crompton and Elford (1963). The sections of the present chapter dealing with the design of the apparatus, the production of the uniform field and the instruments for measuring the ratio of the currents are based largely on these papers; the design of the collecting electrode used in the present form of the apparatus was not described in either of them. The collecting electrode which was used throughout this work, and which will be described below, was, however, also the work of these authors.

As well as dealing with these aspects of the experiment, the present chapter contains a description of the vacuum systems and gas handling techniques, details of the associated electrical equipment and the methods of measuring the gas temperature and pressure.

3.1 Design and Construction of the Apparatus.

3.1.1 Choice of the Dimensions of the Diffusion Chamber.

The choice of the critical dimensions of the apparatus, namely the source electrode to collecting electrode separation, h , and the radius of the central disc of the collecting electrode, b , is a compromise between the following conflicting requirements:

(a) the ratio of the currents received by the central disc and the outer annulus must be measured with adequate precision.

(b) the diameter of the diffusion chamber must be such that no electrons come within the vicinity of the walls and that the electric field is held uniform to the required tolerance.

(c) the diameter of the disc must not be so small as to lead to large errors from the finite size of the source hole.

(d) the chamber length h must be kept as small as possible to reduce the length of the vacuum envelope to be refrigerated for the low temperature experiments and the quantity of high purity gas needed.

Of these requirements, the most obvious, and perhaps the most difficult to satisfy, is the need to choose values of b and h which will lead to values of R in the range $0.2 < R < 0.9$, this being the range over which R can be measured with adequate accuracy by the instruments to be described in 3.3. The effect of this restriction on the choice of values for b and h was discussed at length by Crompton, Elford and Gascoigne. Examination by these authors of the solution for R given in the previous chapter (equation 2.5) showed that for $k_1 > 5$ it is fairly easy to choose dimensions which will lead to current ratios in the centre of the prescribed range when field strengths of 10.0 V cm^{-1} or greater are used. The pressure can then be chosen to give the desired value of E/p and cross checks obtained by varying E and p in the same proportion.

The choice of parameters becomes more difficult for near-thermal electrons and even more difficult if the gas temperature is lowered. It is desirable to keep the field strength above 3.0 V cm^{-1} to minimize the errors from contact potential differences within the chamber (see section 3.4) but this in turn implies small values of b and large values of h if the electron stream is to spread enough for a significant fraction of the current to be received on the outer annulus of the receiving electrode. Small values of b are not desirable because of the difficulties in accurately measuring the small diameter, the greater influence of the finite size of the source hole and the fact that as the disc size is decreased the unknown effect of the air gap between the disc and the annulus becomes increasingly important. Large values of h are undesirable, too, for the reasons given in (d) above. The final dimensions selected by Crompton, Elford and Gascoigne were h = 10 cm and b = 0.5 cm. With these values R remains within the prescribed range for near thermal electrons only if field strengths of less than 9.0 V cm^{-1} and of less than 2.5 V cm^{-1} are used at $293^{o}K$ and $77^{o}K$ respectively.

This latter value is less than the 3.0 V cm^{-1} usually chosen as the minimum field strength at which errors from contact potential differences within the chamber are sufficiently small to be compensated for or eliminated by the methods described in section 3.4. A different experimental technique was therefore required at $77^{o}K$ and this is discussed in section 4.1.4.

The choice of these values of b and h removes the possible source of error in the interpretation of the results arising from the pole and dipole forms of the solution (section 2.1.4) and also makes insignificant the uncertainty due to the spatial dependence of W/D as discussed by Parker (1963) (see section 2.1.5).

As stated in (b) above the diameter of the diffusion chamber must be large enough to ensure that the electric field is uniform to the required tolerance and that no electrons reach the walls even when the electron stream is most divergent. An internal diameter of 10 cm satisfies both these requirements. For a 10 cm chamber length virtually no electrons reach a diameter of 8 cm when R lies in the range $0.2 < R < 0.9$. The diameter of the outer annulus of the collecting electrode was 8.5 cm. The spacing between the central disc and the annulus was 0.005 cm.

Crompton, Elford and Gascoigne calculated that the distance required for the electrons to reach their equilibrium energy under typical E/p conditions was of the order of 0.1 cm. In the present apparatus the electrons travelled through a 2 cm region with the same electric field as in the diffusion chamber before they entered the latter through the 0.1 cm diameter source hole.

3.1.2 Production of a Uniform Electric Field.

There are two problems to be overcome in any apparatus requiring a highly uniform electric field for its successful operation. One is the production of a uniform field by the geometric design and construction of the apparatus. The other is the elimination of field distortion due to internal contact potential differences. Crompton, Elford and Gascoigne reported the results of a large number of experiments they performed in investigating the effects of various

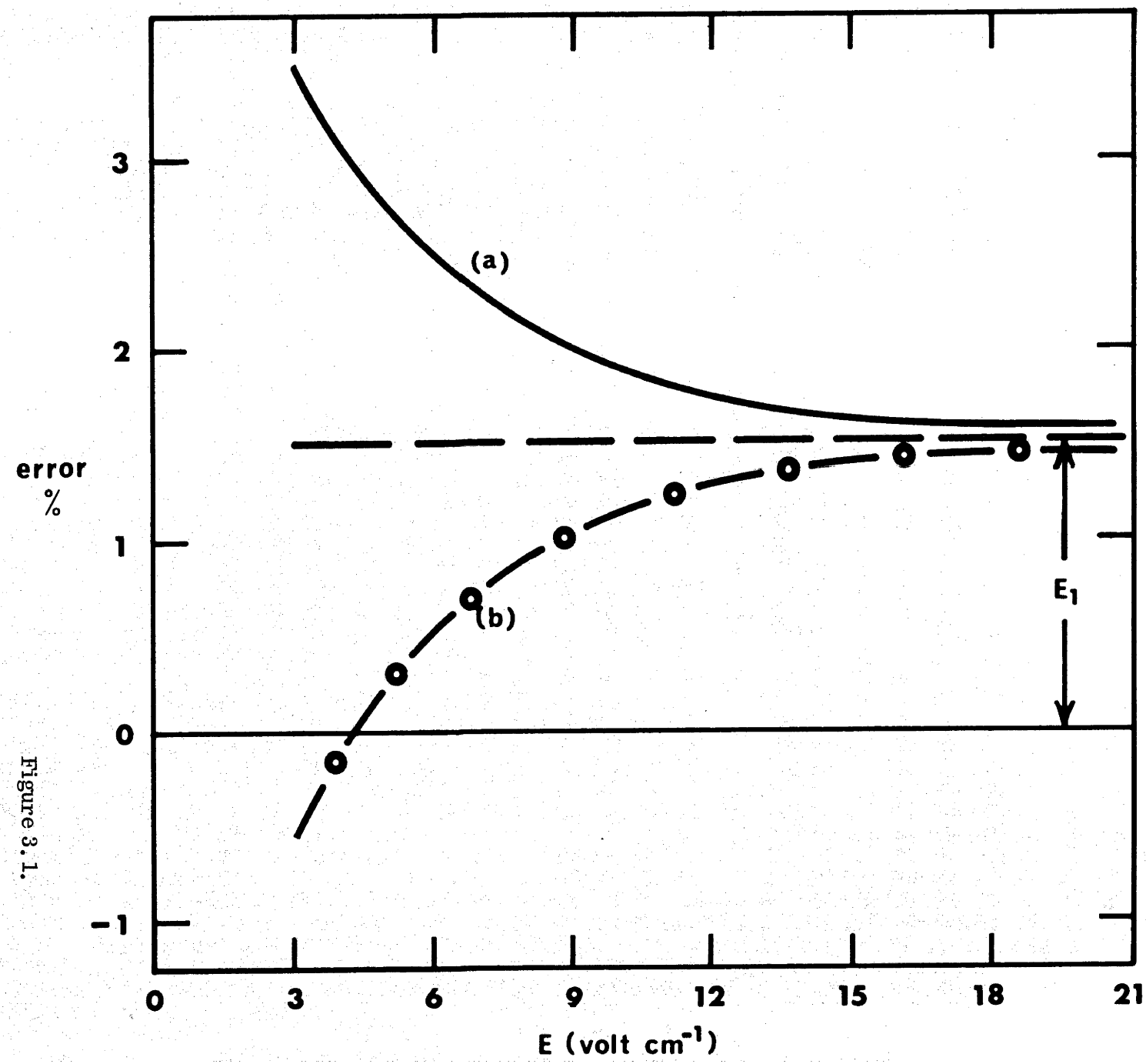

Figure 3.1.

types of field distortion on the lateral diffusion experiment.

From these experiments they concluded that by far the largest source of error was the presence of radial components in the electric field within the chamber, the results being relatively insensitive to quite large amounts of non-uniformity in the longitudinal field. A radial component in the field has its maximum effect if it occurs in the vicinity of the annular gap of the collecting electrode since it will here cause a spurious distribution of current between the central disc and outer annulus. The region around the gap is also the region where field distortion is most likely to occur because of relatively abrupt changes in contour of the receiving electrode; extreme care must be taken to ensure that the whole surface of the electrode is a true geometrical plane.

Crompton, Elford and Gascoigne pointed out that the effects of field distortion due to geometrical inaccuracies or to incorrect potentials applied to the electrodes because of errors in the voltage dividing chain, are almost independent of the electric field strength and are the same for measurements made with either positive ions or electrons. On the other hand errors due to contact potential differences within the chamber change sign as the sign of the particles is changed and decrease as the field strength is increased. The size of the error almost exactly halves as the field strength is doubled.

On the basis of these observations they devised a simple test to distinguish between the two types of field distortion. This can best be understood by reference to Figure 3.1 where it is assumed that both types of error are present. Curve (a) shows the percentage error observed for electrons as E is increased; curve (b) is that obtained for positive ions. At high values of E errors due to contact potential differences become negligible and the residual error (E_1) due to geometrical inaccuracies can be found. This error can be subtracted from the total discrepancy to obtain the error due to contact potential differences at low values of E.

Crompton, Elford and Gascoigne showed that electric fields of adequate uniformity could be obtained by using guard electrodes which are very much thicker than the glass spacers between them (c.f. the thin guard ring

structure described by Crompton and Jory, 1962, in which the electrodes are very much thinner than the glass spacers). The mathematical analysis of Hurst (1960) shows that although the field generated by the thick ring structure is badly distorted near the edge of the electrodes, it is possible with the dimensions chosen to obtain a high degree of uniformity in the important region of the chamber. By contrast with the more conventional form of electrode structure the mechanical stability of the thick rings allows the theoretical result to be achieved in practice. Other advantages of the thick ring construction include the screening of the diffusion chamber from stray electric fields exterior to it and the elimination of dielectric soakage in the glass spacers.

3.1.3 The Apparatus.

The diffusion chamber of the apparatus is shown in Figure 3.2 and the entire experimental tube in Figure 3.3. It should be noted that the collecting electrode is only schematically represented; its actual construction can be seen from Figure 3.4.

The main electrode structure was made of copper, the only other metals used being non-magnetic stainless steel and nichrome. To minimize contact potential differences only gold surfaces were presented to the electron stream. The source and receiving electrodes were gold coated by vacuum deposition under carefully controlled conditions and showed contact potential differences across the surfaces of less than 8 mV, the difference in the central region of the receiving electrode being only 3 mV.

The interior surfaces of the guard ring structure were gold plated as it was not possible to produce sufficiently uniform surfaces by vacuum deposition with the techniques available. A small contact potential difference existed between the gold surfaces of these electrodes and the end electrodes of the chamber, but this was eliminated, or compensated for, by using the techniques to be described in 3.4.

The receiving electrode used to obtain some of the early data presented in chapter 4 consisted essentially of the central disc and outer annulus

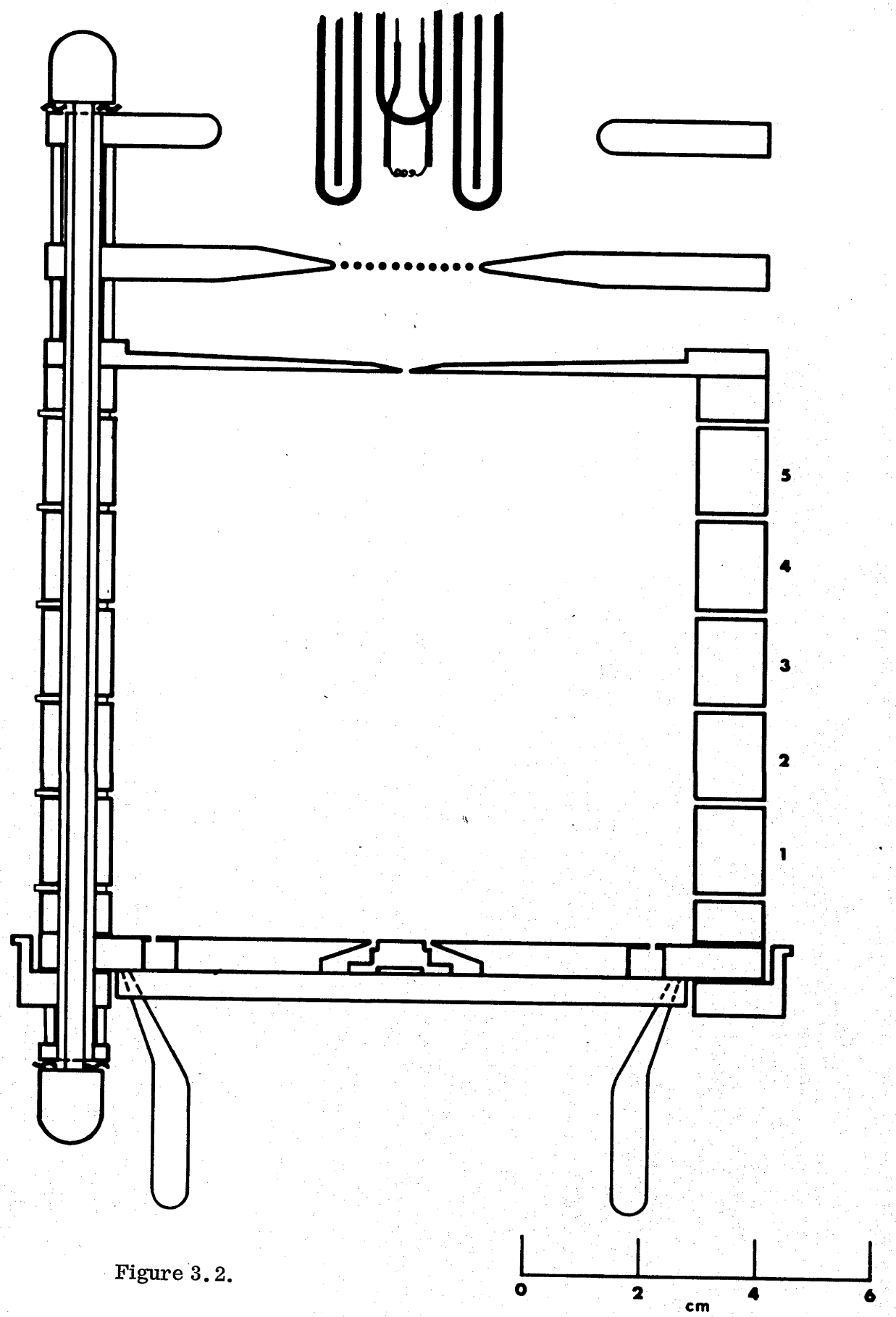

Figure 3.2.

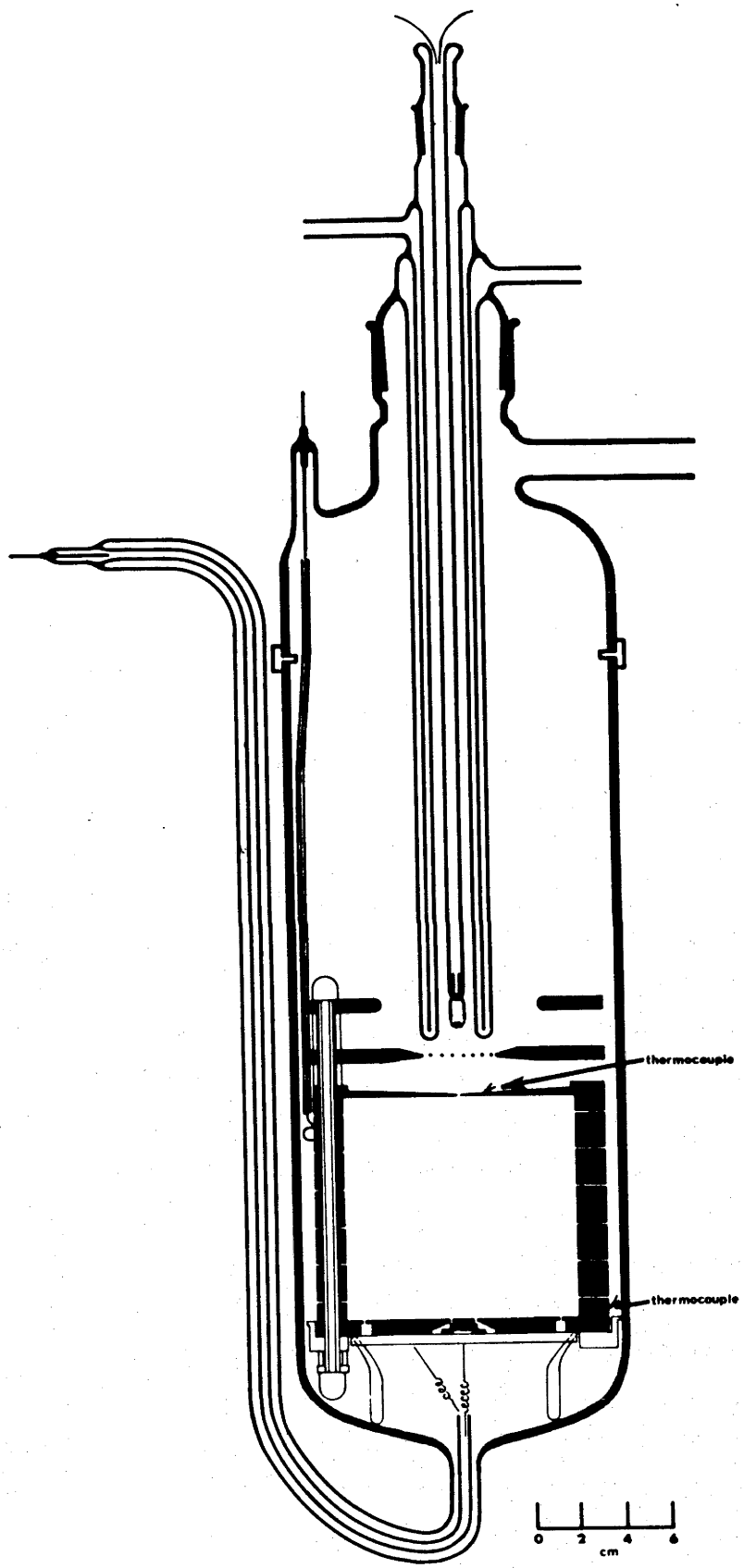

Figure 3.3.

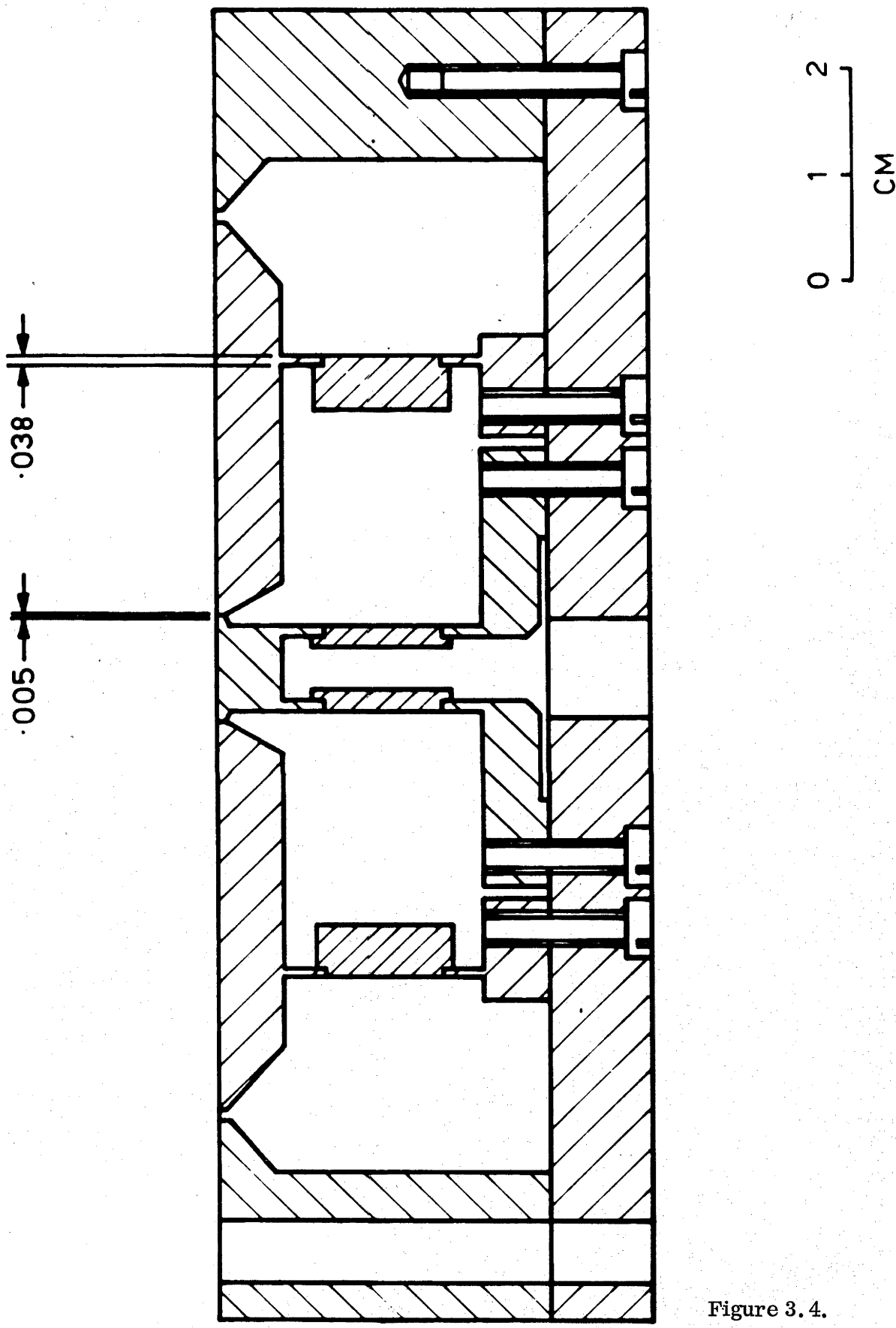

Figure 3.4.

being mounted rigidly on a glass backing plate. This form of construction proved unsatisfactory below $90^{o}K$ when differential contraction of the components caused the disc and annulus to touch.

Figure 3.4 shows the electrode of greatly improved design which was used for most of the present investigation. This electrode was designed by Mr. J. Gascoigne and Dr. R. W. Crompton. Its success is due to the effectiveness of the thin-walled cylindrical section (0.125" long and 0.015" thick) in uniformly absorbing the differential contraction between the copper and ceramic components as the electrode is cooled to $77^{o}K$. The construction of the electrode, with the individual components vacuum brazed to the concentric ceramic cylinders, is clear from the diagram. The entire electrode was optically tested to check that it was flat to within 2 - 3 fringes of sodium light. The resistance to ground of each component was greater than 10^{14} Ω.

For the reasons to be given in 3.5 it was not necessary to thoroughly outgas the tube for the experiments in molecular gases; accordingly no attempt was made to heat the tube in any way. Such a step was undesirable in any case because of the risk of changing the contact potential differences within the chamber. It was thus possible to use Apiezon W 100 vacuum wax and Apiezon N grease for the demountable seals in the apparatus.

Detailed dimensions and the alignment procedures were also given in Crompton, Elford and Gascoigne and so will not be repeated here.

3.2 Electrical Equipment

3.2.1 Power Supplies.

The potentials applied to the electrodes were derived from a voltage divider in which the resistors were matched to better than 0.05%. The voltage divider was supplied by a Keithley model 241, 0 - 1000 V d.c. supply whose output accuracy was 0.05% above 2 V and 1 mV below this figure.

The potentials between the filament and the platinum coating on the water cooler and between the filament and the top plate of the apparatus were variable within the range 0-180 V and were supplied by dry cells.

3.2.2 The Electron and Ion Sources.

For many of the experiments electrons were produced from a platinum filament consisting of approximately 10 turns of 0.0015" diameter platinum wire. The positive ions needed for the tests to be described in 3.4. were generated from a heated potassium alumino-silicate bead mounted on a small coil of fine tungsten wire (Blewett and Jones, 1936). Both of these filaments were mounted on the one support to enable the change from electrons to ions to be made without changing the gas sample thereby avoiding the possibility of changes in the contact potential differences within the apparatus. The power supply for these filaments was a highly stabilized 0 - 6 V d.c. supply whose output was variable through a 10 turn potentiometer.

For the measurements in para-hydrogen the platinum filament could not be used because of reconversion of the gas to the normal 75% ortho-, 25% para- form (see Appendix I) and in this case the currents were generated from a small silver coated foil of Americium 241 (an α emitter). The foil was mounted inside a small copper cylinder on the end of the filament stem. A set of baffles inside this cylinder ensured that no α particle directly entered the diffusion chamber through the 1 mm hole in the cathode.

3.3 Measurement of the Ratio of Currents.

As was pointed out in section 2.1.4 the quantity of interest in determining W/D is not the total current in the chamber but the ratio of the current received by the central disc to the total current reaching the anode. In order to avoid the effects of Coulomb repulsion in the electron swarm it is necessary for the total current in the diffusion chamber to be as low as 10^{-12} A. This means that if the ratio is to be measured to the desired accuracy (0.1%), currents of the order of 10^{-15} to 10^{-16} A must be detected, and leakage currents must be less than 10^{-16} A and stable during the period of measurement. Also, to avoid effects similar to those of contact potential differences on the surfaces, the potential of the disc and annulus must not depart significantly from earth potential during the course of the measurement.

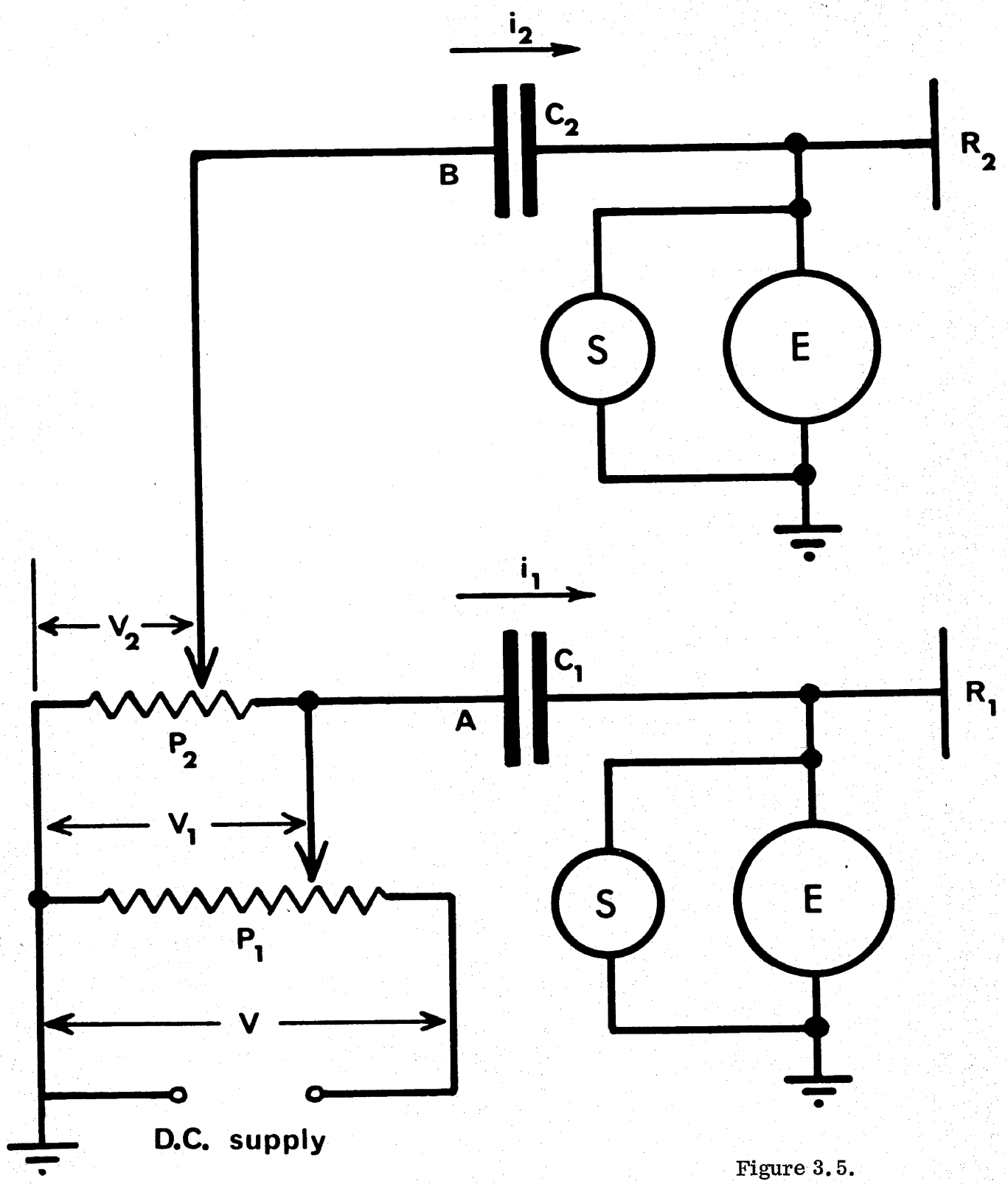

Figure 3.5.

The method adopted to measure the current ratio was a modification devised by Dr. R. W. Crompton of the double induction balance - electrometer unit of Crompton and Sutton (1952). The electrometer and the double induction balance used in the present work were described by Crompton, Elford and Gascoigne.

3.3.1 Double Induction Balance.

A simplified circuit of the integrating induction balance unit is shown in Figure 3.5. The potentiometer P_1 is a 12 kΩ Colvern potentiometer, cam-corrected to give an output within $\pm$ 0.05% of linear when loaded with the 450 kΩ, 10-turn helipot P_2. A voltage V, variable from 1 to 10 V, is applied to P_1 from a highly stabilized d. c. power supply of low impedance. The magnitude of V is adjusted to balance the larger of the two currents received by the segments of the collecting electrode. When P_1 is driven at a constant rate of 1 rev/minute by a synchronous motor, a highly linear sweep voltage is generated at A while a similar signal, the relative amplitude of which is determined by the setting of P_2, appears at B. The two potentials are applied to the matched capacitors C_1 and C_2 which are based on the design of Crompton and Sutton (1952). With this arrangement two constant displacement currents i_1, and i_2 are generated; their ratio is determined by the setting of P_2.

When measuring the ratio of currents received by the segments R_1 and R_2 of the receiving electrode the potential difference between each segment and earth is measured by the electrometers E. Adjustments of the voltage V and the setting of the potentiometer P_2 are made until R_1 and R_2 are maintained at earth potential to within 0.2 mV. The ratio R is then the required ratio of the currents.

Maximum accuracy of the method is obtained by making it an integrating one with the integration commencing when $V_1 = V_2 = 0$ and terminating just before $V_1 = V$ (Crompton and Sutton, 1952, Crompton, 1953). To effect this a correctly phased cam operates a microswitch which in turn operates the electromagnetic earthing switches S.

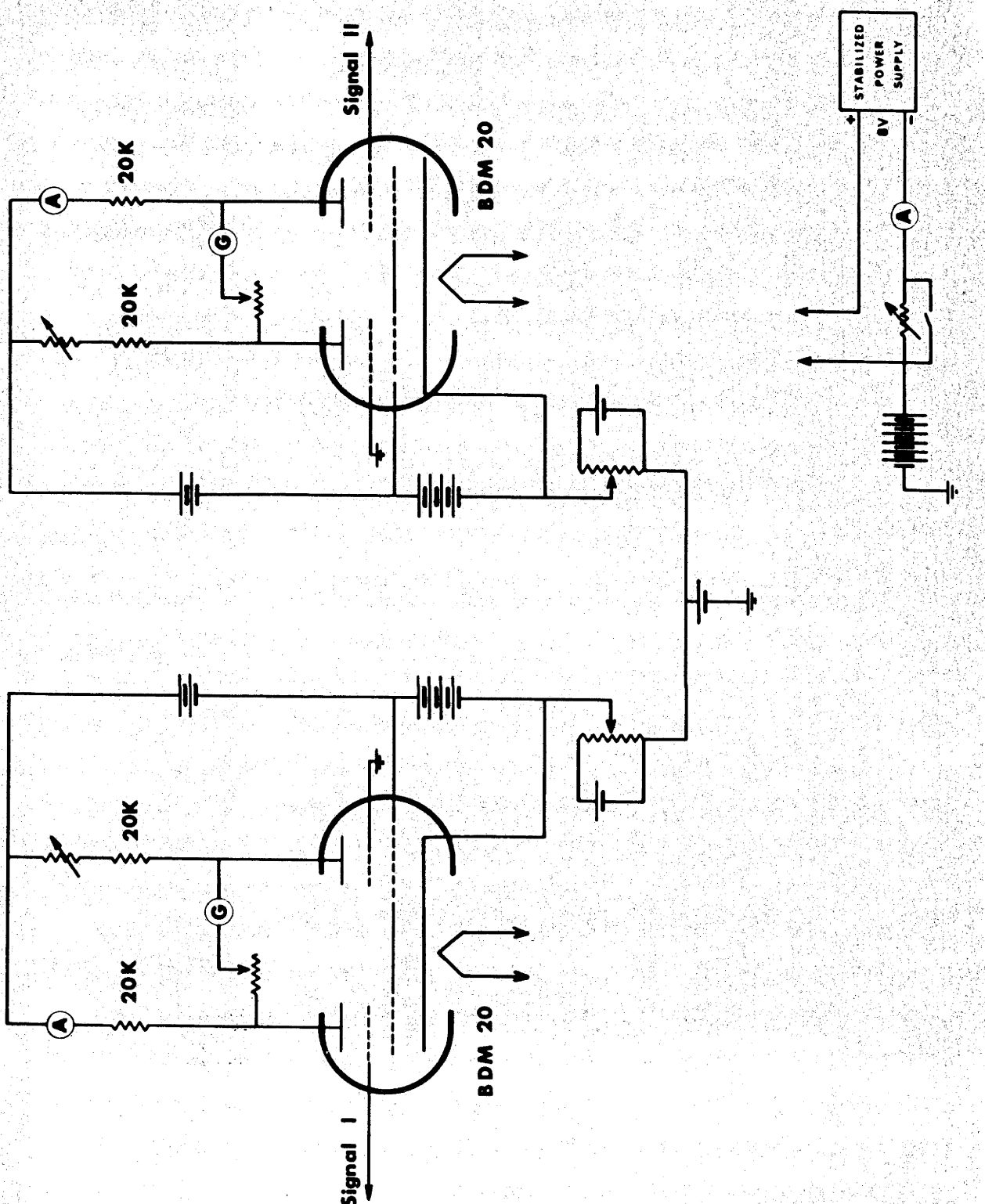
Signal II
BDM 20
20K
20K
G
STABILIZED
POWER
SUPPLY
8V
+
-
A
20K
20K
G
BDM 20
Signal I

Figure 3.6.

3.3.2 Electrometers.

Crompton, Elford and Gascoigne demonstrated the advantages of operating the electrometer valves (Ferranti BDM 20) on the cross over point of the grid current vs grid voltage curve, rather than on the plateau of this curve as is usually done. The major advantage of operating the tubes in this way is that by a suitable adjustment of the grid bias a leakage current of either sign can be introduced. Any small residual leakage current in either electrometer circuit generated either externally or internally, can be annulled. Before each measurement of the ratio R one complete integration was made with no current arriving at the receiving electrode to ensure that leakage currents in each electrometer were negligible.

The circuit of the double electrometer unit is shown in simplified form in Figure 3.6. All the resistors were high precision wire wound types and the voltages were supplied by a bank of 1.5 V dry cells. The filament current is drawn from a highly stabilized "Gossan Constanter" d.c. supply.

3.4 Compensation for Residual Errors due to Contact Potential Differences.

Small contact potential differences remain in the diffusion chamber despite the attention given to this problem; the most likely place for the existence of these potential differences is between the internal surface of the guard electrode structure and the surfaces of the anode and cathode. Smaller contact potential differences can exist across the surface of the collecting electrode. It must be stressed that the errors due to these sources are very small, generally of the order of 1% or less.

Crompton, Elford and Gascoigne (1965) reported a number of tests they carried out to determine the validity of compensating for these small contact potential differences in both places by applying a small potential between the guard electrodes and the cathode and anode. They found that this method of compensating for contact potential differences was a reasonable procedure provided the error in the absence of any compensating potential was not more than 1 - 2%. They suggested that the best way to set the compensating voltage was to adjust

it until k_1 for positive ions was found to be 1.000 at E/p = 0.3 V cm^{-1} $torr^{-1}$. After following this procedure the results obtained during experiments with electrons were found to be virtually free of errors due to contact potential differences.

A further correction to the method suggested by Crompton, Elford and Gascoigne requires taking into account the slight ratio dependence of the results. Results taken with electrons using very high field strengths (so that errors due to contact potential differences are completely negligible) show that the results are very slightly ratio dependent, the values tending to rise as the ratio rises, with a maximum spread over the whole range of R of 0.7% (see 4.1.2). This dependence is a combination of the effect of the finite size of the source hole and of a small error of unknown origin which becomes important when R is small. This error is apparently a solution error of a different type to that mentioned in 2.1.5.

If these effects are taken into account it turns out that when k_1 is actually 1.000 the observed value should, in fact, be 1.003 or 1.004. The compensating potential in all the present experiments was adjusted until k_1 for the K^+ ions was 1.004 at E/p = 0.3. In practice the effect of this additional correction is very small since the ions and electrons are equally ratio dependent. At the very worst the maximum effect would be 0.4% at E = 3.0 V cm^{-1} and negligible at higher field strengths.

3.5 Gas Handling Techniques.

The aim of the present experiments was the measurement of D/μ in the molecular gases H_2, p - H_2 and D_2. Some of the most commonly considered sources of error in electronic and atomic collision processes are those arising from the presence of gaseous impurities. Although these may be a significant source of error in some swarm experiments, for example in argon when the mean energy of the swarm is near that corresponding to the Ramsauer minimum (Bowe, 1960, Uman, 1964), it is generally not so for experiments in molecular gases. Calculations for these gases show that impurity levels of up to

100 ppm have negligible effect on the results (oxygen is a dramatic exception at very low values of E/p - see 4.1). It is thus possible to use fairly conventional vacuum techniques with long pumping periods to reduce the impurity level from outgassing to the required degree. Experience has shown that it is not necessary to bake the apparatus to achieve this level. This step would, in all probability, increase the contact potential differences within the chamber and would lead to greater errors from this source than could be handled with the compensation technique. Baking of the apparatus was therefore avoided.

3.5.1 Vacuum System.

The vacuum system was constructed of Pyrex and used glass taps greased with Apiezon N grease. A conventional Edwards type 2S20 rotary oil backing pump was used to reduce the pressure to the order of 1 micron and second stage pumping to better than 10^{-6} torr was made with an 8 litre/sec Vacion pump. A liquid nitrogen trap was always maintained between the backing pump and the main system. Liquid nitrogen traps were also placed on the gas admittance line and immediately adjacent to the apparatus; these traps were filled with copper foil to increase their trapping efficiency and to minimize the re-evolution of previously trapped vapours. A low closure-torque metal valve (manufactured by Vacuum Generators Ltd.) was used to isolate the Vacion pump, this type of valve being preferred to a greased tap solely on the grounds of convenience of operation.

Isolation tests without using liquid nitrogen traps showed that the rate of rise of pressure was of the order of 5×10^{-6} torr/hour which corresponds to a gas influx rate of 8×10^{-8} torr litre/sec. The rate of rise of impurity level was therefore approximately 1 part in 10^{8}/hour into a 500 torr sample of gas.

3.5.2 Gas Admittance.

The hydrogen and deuterium were obtained by diffusion through a heated palladium osmosis tube using the apparatus and technique described by Crompton and Elford (1962). For the low temperature experiments a greatly

increased admittance rate was achieved by operating a battery of 5 palladium tubes in parallel.

The hydrogen used was obtained from a commercial cylinder of C.I.G. gas. The deuterium was supplied by Liquid Carbonics Division of General Dynamics Corporation in cylinders containing 100 N.T.P. litres and was stated by them to contain not less than 99.9% of the isotope. The small amounts of hydrogen and deuterium hydride admitted would affect D/μ and W by approximately 0.1%.

Diffusion through palladium is known to produce gas with an impurity level less than 0.1 ppm (Young, 1963). During the course of the measurements the oxygen concentration was proved to be less than 0.001 ppm. Discussion of the experiments which showed this is deferred until section 4.1.

3.5.3 Pressure Measurement.

Two types of pressure gauge were available: a pair of capsule gauges (Crompton and Elford, 1957) covering the ranges 0 - 40 torr and 0 - 500 torr, and a fused quartz spiral gauge manufactured by Texas Instruments Ltd. All the gauges were calibrated against a C.E.C. type 6-201 primary pressure standard.

With the capsule gauges the pressure could be measured with an error of less than 1% at 500 torr, and 0.25% at 40 torr. The larger errors at higher pressures are due to hysteresis effects in the capsules. Fortunately the high pressures are needed only for the very low values of E/N where D/μ varies slowly with E/N and hence errors in pressure measurement are relatively unimportant. The 0 - 40 torr capsule gauge was used only for some of the early data (see 4.2) and was later superseded by the quartz manometer which was used to measure all pressures below 250 torr. The accuracy of the calibrated gauge was better than 0.1% over the entire range 5 - 250 torr. The fused quartz construction means that the gauge is virtually free from hysteresis and is therefore not subject to the limitations of the capsule gauge.

3.6 Temperature Control and Measurement.

3.6.1 At 293°K.

The temperature at which the measurements are made can affect the values of D/μ either directly (see equation 2.32) or indirectly through its effect on the gas number density, since the gas pressure rather than N is measured to determine E/N. Since an uncertainty of 1 degree centigrade leads to an error of 0.3% in N at 293°K it is necessary to exercise considerable care in both the control and the measurement of the gas temperature.

Two fine wire copper-constantan thermocouples were used to measure the gas temperature; one was attached to the source electrode and the other to the earthed ring of the collector electrode. To avoid the danger of thermal e.m.f's being produced at conventional tungsten seals, hollow Kovar tube seals were used.

The temperature of the laboratory was controlled to $\pm$ 1 degree C and the experimental tube was surrounded by a 3" thick jacket of "Styrofoam". Heat generated by the filament was removed by means of the water cooler (Figure 3.3); distilled water in a closed system was circulated through the cooler by a small electrically operated pump.

3.6.2 At 77°K.

At 77°K an error of 1 degree in temperature measurement is responsible for an error in N of more than 1%. Accurate measurement of the temperature therefore becomes increasingly important as the gas temperature is lowered. It was necessary to make several modifications to the vacuum envelope, the liquid nitrogen container and the thermocouples before the apparatus could be successfully used at 77°K.

The first two of these arose from the existence of temperature gradients of the order of 1°C between the source and receiving electrodes when the outer jacket was filled with liquid nitrogen. Subsidiary tests made with an identical electrode stack showed that this could be overcome by raising the level of the liquid nitrogen by 3". This necessitated the lengthening of the vacuum

envelope and the construction of a new liquid nitrogen container.

The new container consisted of a copper can surrounded by approximately 3" of solid poly-urethane externally clad with aluminium foil.

Erratic behaviour in the thermocouples was traced to thermal e.m.f's in the soldered joints near the seals. The trouble was eliminated by spot welding the eureka wires and using a special Leeds and Northrup low thermal solder for the joins in the copper wires.

Work hardening of the wires caused changes of the order of 40 - 50 μ V in the thermocouple e.m.f. of approximately 5400 μ V corresponding to 77^{o}K. However, provided fully annealed copper wires and annealed eureka wires were used and both were carefully handled, a calibration figure of $5401 \pm 1\mu$ V was found to correspond to a temperature of 76.8^{o}K. This figure was repeated many times with different couples and was checked for the actual thermocouples used immediately before assembling the apparatus. The e.m.f's were measured with a Leeds and Northrup K3 Potentiometer and Electronic Null Detector. The reference junction was immersed to a depth of 3 - 4" in an ice pot.

The thermocouples were calibrated against the known boiling point of a liquid nitrogen bath. The boiling point of liquid nitrogen depends on the atmospheric pressure and on its purity (1% of oxygen raises the boiling point by approximately 0.1^{o}K). The purity of the liquid nitrogen used was always greater than 99% but, nevertheless, both factors were accurately measured and the appropriate corrections to the boiling point made; care was taken to ensure that the liquid nitrogen was not superheating. The sensitivity of the thermocouples used was 16 μ V /degree at this temperature.

The level of the liquid nitrogen was controlled automatically by a device designed and constructed by Dr. M.T. Elford (1965) who considerably modified the design of Pursar and Richards (1959). Using this device the level of the liquid nitrogen could be held constant to within $\pm \frac{1}{2}$" which corresponds to a pressure variation in the experimental tube of approximately 1 - 2%. (The actual pressures used were, of course, recorded: see section 4.1.6.)

CHAPTER 4.

RESULTS FROM THE LATERAL DIFFUSION EXPERIMENTS.

Measurements of the ratio of diffusion coefficient to mobility were made for electrons in hydrogen and deuterium at 293°K and 77°K and in para-hydrogen at 77°K. These results are presented and discussed in this chapter.

Before proceeding to the results themselves it is convenient to discuss several minor investigations which were made to understand and to overcome some of the experimental difficulties. The investigation of one of these difficulties, namely the current dependence of the results at low E/N, led to the discovery of the extreme sensitivity of the results to oxygen in concentrations several orders of magnitude too small to be detected by any other known method. This effect was shown to be capable of at least semi-quantitative determination of oxygen present in hydrogen or deuterium at concentrations of the order of 1 part in 10^{10}.

4.1 Experimental Difficulties and Minor Investigations.

During the course of the experiments many measurements of D/μ in hydrogen were made. Whenever a new apparatus was to be tested or an existing apparatus checked for suspected faults, hydrogen was used as the test gas. It is particularly suitable for a number of reasons. Firstly, it can be prepared easily in pure form. Secondly, the transport properties of low energy electron swarms in hydrogen are relatively insensitive to the presence of molecular impurities should the gas subsequently become contaminated by outgassing of the apparatus. Thirdly, it is always possible to obtain adequate emission from thermionic sources in the gas. Fourthly, the contact potential differences of the gold surfaces used in the apparatus have been found to remain stable over lengthy periods when hydrogen is used as a test gas.

4.1.1. The Effect of the Finite Size of the Source Hole.

The effect of the finite size of the source hole was frequently observed. Table 4.1 shows the variation of k_1 with pressure at E/p = 0.02. This

variation is typical of that observed at any value of E/p where results can be obtained over a wide range of pressures. It shows that the value of k_1 rises as the pressure rises, i.e. as R increases. This change is of the same form as that calculated by Crompton and Jory (1962) to be due to the finite size of the source hole.

Table 4. 1.

Variation of k_1 with pressure.

Electrons at E/p = 0.02 in hydrogen.

p (torr) =	500	400	300	200	150
k_1 =	1.133	1.132	1.132	1.129	1.127

Their calculations for a chamber geometry identical to that of the present apparatus show that the maximum variation over the range of R used should be 0.8%, a figure which agrees well with the observed variation. The failure of these authors to detect variations of this magnitude in their own experiments was almost certainly due to the masking of the effect by the contact potential differences in their apparatus; no compensation for these contact potential differences was made by them.

Since the majority of the results were taken under conditions for which the ratios were such that Crompton and Jory's calculations show the effect to be negligible and since in any case the total variation over the whole range of R used is so small, values of D/μ at any value of E/p were obtained by simply averaging the results obtained at all pressures. Any errors due to the finite size of the source hole are then much less than the error limit of $\pm$ 1% placed on the final data at 293^{o}K.

4.1.2 Errors Observed with Widely Divergent Electron Streams.

In section 3.1.1 it was stated that the maximum value of field strength which could be used in the present apparatus at 77^{o}K when $D/\mu \sim kT/e$ was 2.5 V cm^{-1}. Before proceeding to 77^{o}K some measurements were made with low field strengths at room temperature to investigate the effect of such low

fields on the reliability of the results.

It was found that errors due to contact potential differences could be kept to a satisfactorily low level. However, if the contact potential compensating voltage was set to give $k_1 = 1.000$ for positive ions at $E = 2.0$ V cm^{-1}, then electron results taken with this field strength and compensating potential were approximately 1½% lower than the accepted values. When this test was repeated with $E = 3.0$ V cm^{-1}, the lowest field strength previously used, results substantially in agreement with the accepted values were obtained.

A further set of results for electrons taken at a constant value of E/p and high field strengths (so that contact potential differences were negligible) showed that the observed value of k_1 increased as the field strength, or the ratio, increased. This is shown in Table 4.2.

Table 4.2.

Change in k_1 as ratio is increased.
$E/p = 1.0$ V cm^{-1} torr^{-1} for electrons in hydrogen.

Field strength (V cm^{-1})	Ratio	k_1
10	.236	9.22
20	.415	9.25
30	.551	9.28
40	.656	9.28
50	.736	9.29
60	.798	9.29

The effect is not due to the finite size of the source hole since

(a) the finite size of the source hole is important only for narrow electron streams, i.e. high ratios.

(b) the calculations of Crompton and Jory (1962) show that if the effect of the source hole is important, the slope of the k_1 v R curve decreases as R decreases whereas the slope of this curve increases at low R in the present observations.

Since all other tests showed that the effect was unlikely to be instrumental in origin, it is suggested that the expression

$$R = 1 - (h/d) \exp (- \lambda (d - h)) \qquad (4.1)$$

may not adequately describe the divergence of the electron stream over the whole range of experimental parameters. This result is not unexpected (Hurst and Liley, 1965).

It is now possible to explain the $1\frac{1}{2}\%$ error observed for electrons in the tests with E = 2.0 V cm^{-1}. The result taken with E = 2.0 for positive ions was taken with a widely divergent stream and was in error by $\sim$ 0.7% because of the effect just described. By setting the compensating voltage to give $k_1 = 1.000$ for the ions, this error was falsely compensated. As a result, the electron values taken at the same field strength were $\sim$0.7% low due to the incorrect compensation and $\sim$ 0.7% low due to the systematic error, i.e. $1\frac{1}{2}\%$ low overall. At field strengths of 3.0 V cm^{-1} or greater, the ratio was higher and the systematic error was reduced to a negligible level.

Table 4.2 shows that the error exceeds 0.5% only when R < 0.4. With the exception of the data to be given in 4.2.2, all the data taken at 293°K were obtained with R > 0.5 so that errors from this effect were entirely negligible. At room temperature the difficulty can generally be avoided by using higher gas pressures and electric field strengths to obtain the same value of E/p. In the case of the data of section 4.2.2, the difficulty could not be avoided because of the limitations imposed by the onset of electrical breakdown in the apparatus. At 77°K the ratios corresponding to the low field strengths are much higher than they are at 293°K and no problems with widely divergent electron streams were encountered.

4.1.3 Effect of an Insulating Layer on the Collecting Electrode.

After the failure of the collecting electrode described by Crompton, Elford and Gascoigne (1965), the apparatus was dismantled to insert the collecting electrode described in 3.1.3.

On re-assembly, tests of the apparatus with both ions and electrons

showed a time dependence of the current ratios during the course of the experiments. For example, the apparent value of k_1 for positive ions rose continually during the measurements, but after switching off the filament and waiting some time the value of k_1 was observed to have fallen considerably. The effects were repetitive and could not be explained as resulting from changes in the gas temperature. Furthermore, the results for both ions and electrons depended on the nature of the previous measurement. Thus if the previous measurement had been made with electrons, the results for ions were found to be low in contrast to the high values which resulted from prolonged use of ions. Similar effects were observed for electrons.

It was concluded that these effects could be due to the presence of an insulator on the surface of the collecting electrode. The presence of charge on the insulator would explain the phenomena described above and the relaxation observed when no measurements were made.

The most likely explanation on this basis was that a chip of glass from one of the electrode spacers had fallen on to the lower electrode. To test this hypothesis a similar apparatus was assembled and a small piece of glass placed on the outer collecting electrode close to the gap between the central disc and surrounding annulus. The behaviour of this apparatus was identical to the main apparatus thereby confirming the validity of the hypothesis. On dismantling the main apparatus no glass chip could be found. However, when the collecting electrode was viewed at oblique incidence a thin layer of white powder could be seen on the surface. The distribution of the powder indicated that it had been deposited at some stage during assembly of the electrode structure. The dust was removed and the electrode system re-assembled. Results for electrons then agreed to within 0.25% of the standard values taken with the previous collecting electrode.

4.1.4 Compensation for Contact Potential Differences at 77°K.

Immediately after cooling the apparatus it was found that the contact potential compensation could be adjusted using positive ions in the same

way as at room temperature. Electron results taken shortly afterwards with the same compensating potential appeared to be quite consistent. However some time after cooling, the use of the positive ion test was found to cause large and increasing errors: with constant compensating potential the departure of D/μ from kT/e was found to increase from approximately 1% to approximately 14% over a period of several hours. Electron results taken during this time showed a similar, but smaller, increase.

It was decided not to use the positive ions at low temperature and to rely on the agreement of electron results taken at different field strengths as the test of the correctness of the contact potential compensation. Any errors from incorrect setting of the compensating voltage were generally less than the experimental scatter arising from the effects to be described in subsequent sections, i.e. they were of the order of 0.5% or less at $E = 1$ V cm^{-1}. When appreciable errors due to incorrect compensation were observed at low field strengths, only data taken at field strengths sufficiently high to reduce these errors to less than 0.25% were included in the final analysis.

4.1.5 Surface Effects at 77^{o}K.

On several occasions when attempting to check results at low E/N, values of D/μ that were higher than the other data by approximately 3% at $E = 1.0$ V cm^{-1} were obtained. The magnitude of this error did not scale with E as would an error due to a contact potential difference in the apparatus. On the other hand, whenever such an error was observed and an attempt was made to investigate it by taking results with field strengths of 10 V cm^{-1} or greater, the values so obtained were always in agreement with the data obtained when no error was observed at low E/N. Once this error was present in the apparatus it did not disappear as long as the apparatus was held at low temperature, even when the apparatus was evacuated for some time prior to a new experimental run. On the other hand, it disappeared as soon as the apparatus was returned to room temperature and usually did not re-appear at low temperature until a considerable amount of data had been obtained.

It became clear that errors of the type just described were only observed after taking results at high values of E/N and that they were enhanced after long periods at low temperature. A possible mechanism to explain this effect is the formation of an insulating layer by the somewhat more energetic electrons bombarding an adsorbed layer on the collector surface. This view is supported by (a) the fact that the errors became worse after long periods at low temperature, and (b) the fact that the effect could always be eliminated simply by warming the tube to room temperature for several days before returning to the low temperature, low E/N experiments.

Fortunately the effect, although inconvenient, could always be eliminated and the data to be given in subsequent sections were not subject to errors from this source. At low E/N, results were included in the final analysis only when the effect was known to be absent during a particular experimental run. At high E/N where high field strengths were used, the values of D/μ were always in agreement whether or not the effect was present. All the data obtained at high E/N and high field strengths were therefore included in the final analysis.

4.1.6 The Determination of Gas Number Density at $77^{o}K$.

Small fluctuations in the level of the liquid nitrogen made it impracticable to work at predetermined values of E/p as had been the practice at $293^{o}K$. Moreover, D/μ, like the other transport coefficients, is fundamentally a function of E/N rather than E/p. Accordingly each experimental observation consisted of the measurement of the current ratio together with the temperature and pressure of the gas. These data and the known value of the electric field strength enabled the value of E/N and the corresponding value of D/μ to be determined.

4.1.7 Current Dependence of Results at Low E/N.

Crompton and Elford (1963) reported a slight dependence of the divergence of the electron stream on the total current received. This phenomenon was frequently observed in the present experiments for $E/p < 0.01$ and sometimes at much higher values of E/p.

When such a dependence was observed it was found that the apparent values of k_1 were linearly dependent on the current. The true values of k_1 were found in such cases by extrapolating to zero current from values recorded at currents of 6×10^{-13} A and 1.2×10^{-12} A. The difference between the extrapolated value of k_1 and the value recorded at the lowest current was nearly always less than 1% at E/p = 0.006, and always decreased with increasing E/p.

The slope of the k_1 v current curve increased progressively with time for a given gas sample and, depending on the "history" of the apparatus, was much steeper at times than at others. These effects indicated that the phenomenon was associated with the outgassing of the tube, even though the level of contamination from this source was known to be less than 0.1 ppm for a 500 torr sample of gas. It was also frequently observed that when a high current dependence was found in a particular sample of gas, a moderately high dependence was found in the next sample used, even though the apparatus was evacuated to better than 10^{-6} torr between experimental runs.

The current dependence of the results was the subject of two series of tests. The first of these isolated the impurity causing the dependence and lead to a hypothesis which could explain it. The second, which arose from the measurements in hydrogen and deuterium at 77°K, showed the order of magnitude of impurity concentration required and lead to semiquantitative measurements of this concentration.

The first series of tests was conducted with the apparatus in a bell-jar as a temporary vacuum envelope. Since the current dependence was often associated with difficulty in obtaining sufficient filament emission all the results in this investigation were made at slightly higher values of E/p, viz. E/p = 0.010. The hypothesis put forward to explain the current dependence was that an unknown fraction of negative ions was present in the electron stream resulting in space charge repulsion of the stream. At very low values of E/p both the ions and the electrons are almost in thermal equilibrium with the gas molecules and so the current distribution at the anode is the same for both species. If space charge were negligible the current ratios would therefore be unaffected by the presence

of a small number of negative ions in the stream. On the other hand, if space charge repulsion does affect the beam, a small number of ions will have an enhanced effect since at low E/p their drift velocity is about one thousand times smaller than the corresponding electron value.

A series of more than twenty experiments was conducted in an attempt to isolate the impurity responsible for the suggested negative ion formation. Since hydrogen produced by diffusion through palladium is known to be of very high purity (see 3.5.2), the most likely source of impurity was outgassing of the apparatus and vacuum envelope. The gases most likely to be present from outgassing are oxygen, carbon dioxide and water vapour. Known proportions of these gases were added to the hydrogen in concentrations of a few ppm. In other tests small amounts of the solvents used during the assembly of the apparatus (hexane, acetone and iso-propyl alcohol) and excessive amounts of the tap grease and the W 40 wax were also added.

With the exception of oxygen the presence of all the impurities added had a negligible effect on the current dependence of the results. In the case of oxygen, the slope of the apparent k_1 v current curve was approximately linearly dependent on the amount of impurity added. These observations are in accordance with the known facts that attachment of thermal electrons to carbon-dioxide and water vapour does not occur and that three body attachment of electrons to oxygen is appreciable.

Investigation of the effect was not pursued at this stage. Conditions could always be arranged to ensure that a difference of 1% or less occurred between the extrapolated value and the value measured at the lowest current. After prolonged periods of pumping this difference was often reduced to as little as 0.25% at E/p = 0.006 and was not measurable at higher values of E/p. All the 293^{o}K data presented in subsequent sections were obtained under these conditions.

The investigation was resumed when preliminary experiments in deuterium at 77^{o}K showed a number of inconsistencies which were not apparent with the experiments in hydrogen. From a somewhat confused picture of results

two observations provided clues to the source of these inconsistencies. The first was that the slope of the D/μ v current curve was greater in deuterium than it was in hydrogen. Since the time of admission of the gas sample was approximately twice as long for deuterium as it was for hydrogen this fact was in agreement with the suggestion made above that the oxygen causing the current dependence derived from outgassing of the apparatus. On the other hand, the outgassing rate of the apparatus was only 0.1 micron per 24 hours at room temperature and at low temperature, with the apparatus and most of the walls of the vacuum envelope held at $77^{o}K$, this rate must have been very much reduced. This made the increased dependence at $77^{o}K$ somewhat surprising. The second and more important observation was that with a 500 torr sample of gas in which the dependence of the apparent values of D/μ on the current was comparatively high, the apparent value corresponding to a given current fell slowly until a transfer of liquid nitrogen to the cooling jacket took place. The apparent value then rose rapidly by several percent and the cycle was repeated.

Since no electrical faults external to the apparatus could be found it was concluded that the effect was due to a genuine change in the divergence of the electron stream caused by a change in either N or the gas temperature T. The change in gas pressure, and hence N, resulting from the change in the level of liquid nitrogen in the cooling jacket was about 2%. When a change in N of the same size was simulated by using the backing pump to reduce the pressure in the system by 2%, it was found that the apparent value of D/μ changed by the same amount as it had in the cyclic variation described above. The effect was thus shown to be dependent on N rather than on the gas temperature. Subsequent tests showed that the variation was caused by a change in the current dependence of the measured ratios rather than a real change in D/μ itself. As expected, all these effects became negligible when the current dependence was sufficiently small.

The explanation put forward to account for these effects is based on the effect of space charge repulsion due to negative ions in the electron stream. As N is altered two effects take place to change the current dependence. Firstly, as the effective E/N is lowered the drift velocities of the electrons and ions decrease, and for a given attachment rate, the effect of space charge on the

stream is increased. Secondly, since the attachment of thermal electrons to oxygen is a three-body process, the rate of attachment depends on the square of the pressure: raising N again leads to a larger current dependence. The mathematical theory of this effect (Liley, 1966) shows that the combination of these two processes makes the current dependence vary as the fourth power of N. Thus the change produced by only a 2% change in N could easily be observed.

Although the current dependence of the results at low E/N and the apparent inconsistencies in the initial measurements in deuterium could both be explained in terms of space charge repulsion enhanced by negative oxygen ions formed by thermal attachment, the number of oxygen molecules was known to be so small that it was difficult to see how they could have such a large effect. To find what concentration of oxygen was needed to produce the observed effects it was decided to make up mixtures of known concentrations of oxygen in hydrogen and to determine the current dependence in these mixtures.

In the first attempt to make such a mixture a pressure of the order of 100 microns of oxygen was inadvertently admitted to the experimental tube. When reducing the pressure it was observed that a large amount of oxygen had been adsorbed on the cold surfaces of the apparatus leading to a high desorption rate when the pressure was reduced. This provided a reasonable explanation for the fact that a high current dependence in a given set of measurements was invariably followed by a dependence greater than normal in subsequent measurements made in fresh samples of gas, even though the system is pumped to less than 10^{-6} torr between gas fillings. This effect could only be avoided by leaving the apparatus evacuated for an extended period. The desorption of oxygen presumably continues for some time thereby slightly contaminating subsequent gas samples.

In the case cited above, the pressure of oxygen was reduced to a stable value of 0.2 - 0.3 micron before a 500 torr sample of hydrogen was admitted. With this concentration of oxygen, of the order of 0.5 ppm, the current ratio was immeasurably small; that is, the space charge repulsion in the stream was so excessive that only a negligible fraction of the electron current fell on the central disc of 1 cm diameter. When this sample of gas was removed

and the system evacuated for several hours, a subsequent filling with clean gas led to a current dependence 6 - 7 times larger than normal; this confirmed the "memory" of the apparatus for oxygen as described above.

Several tests with decreasing oxygen concentrations were made. The mixtures were prepared in the following way:

After isolating the evacuated apparatus from the vacuum system the required pressure of oxygen was admitted. The oxygen pressure was measured on the Pirani gauge and was of the order of 0.1 to 5 microns. High pressure hydrogen was admitted and the oxygen concentration calculated. The pressure of the contaminated hydrogen was reduced to a lower value (2 - 10 torr) before sharing volumes with the apparatus and increasing the pressure to 500 torr by admitting pure hydrogen.

The same final oxygen concentration could be produced in several different ways by selecting the appropriate pressures at each stage. A complete experimental run with zero oxygen concentration was made to check that back diffusion from the backing pump was not a significant factor. The results of the various tests are set out in Table 4.3. The "% slope" refers to the percentage difference in the values of D/μ as measured at currents of 6×10^{-13} A and 1.2×10^{-12} A.

Table 4.3

Effect of oxygen concentration on the current slope at $E/N = 2 \times 10^{-19}$ V cm^2

Oxygen concentration	% Slope
4 in 10^7	Too large to measure
5.8 in 10^8	59%
6.3 in 10^9	49%
5.2 in 10^{10}	21%
2.6 in 10^{10} *	16%
2.6 in 10^{10} *	17%

* prepared in different ways.

From this table and the observed current dependence under normal experimental conditions at 77°K it can be seen that the oxygen concentration must be much less than 2 parts in 10^{10}. The close agreement of the slopes for the mixtures of 2.6 in 10^{10} is gratifying in view of the difficulty in measuring the pressure at each stage of preparation; it shows that the effect could be used for at least semi-quantitative determinations of oxygen in a carrier gas and that the method would be a useful means of detection at least three orders of magnitude more sensitive than any other known method.

Once again, closer examination of the theoretical analysis of Liley (1966) shows that the sensitivity to oxygen depends approximately on the fifth power of the gas temperature. This explains why the effect was more pronounced at 77°K than it was at 293°K and why such small concentrations of oxygen could be detected at low temperature. It furthermore shows that the sensitivity of the oxygen detector could be made variable by altering the gas temperature.

4.2 Results for Hydrogen.

Some of the data in hydrogen were measured at predetermined values of the parameter E/p rather than at predetermined values of E/N. In such cases E/p is used to mean E/p_{293} where the gas pressure is measured at 293°K. Where not specifically stated the units of E/p are V cm^{-1} $torr^{-1}$, and of E/N, V cm^2.

4.2.1 At 293°K. $0.006 \leq E/p \leq 2.0$ V cm^{-1} $torr^{-1}$.

Two sets of results were taken covering the full range $0.006 \leq E/p \leq 2.0$ in hydrogen. One of these was made with an early version of the collecting electrode which proved unsuitable for the low temperature work (see 3.1.3) and the other with the collecting electrode used for the majority of the present investigation. The early set of data were taken before the quartz manometer was available and before the small correction to the method of setting the contact potential compensation described in 3.4 was employed, i.e. in this case the experimental techniques were identical to those of Crompton, Elford and Gascoigne (1965). If no compensating voltage was applied an error in k_1

for both positive ions and electrons of 0.7% occurred at a field strength of 3.0 V cm^{-1}. This error was eliminated, or compensated for, by applying a voltage of 100 mV between the guard rings and end plates of the apparatus. For completeness, tabulated values of k_1 found in this investigation are given in Table 4.4. The entries in this table are the averages of two complete sets of data taken with different gas samples. The maximum discrepancy at any point between these two sets was 0.3%; most of the results agreed to 0.1% or better.

Table 4.5 shows the values of k_1 found in a later investigation using the apparatus rebuilt to incorporate the collecting electrode described in 3.1.3. The data shown in this table were obtained using the various modifications to the techniques of Crompton, Elford and Gascoigne described in the previous chapter. Principally, these were the use of the quartz manometer for $p \leq 200$ torr and the method of adjusting the compensating potential. One further technique was employed to obtain the best values of k_1 at the lowest values of E/p. This involved the taking of results with a field strength of 1.5 V cm^{-1} over a limited range of E/p.

If the field strength is held constant and E/p is varied by changing the pressure p, then the current ratios remain practically constant provided the electron temperature does not rise by more than a few percent. Since the current distribution across the collecting electrode is always similar under these circumstances, errors due to symmetrical or asymmetrical field distortion should remain constant to a first order. The results obtained in this way have a small systematic error which can be removed by normalizing them against a value taken at a field strength sufficiently high to reduce contact potential errors to a negligible level, the highest E/p value being used for this purpose.

Measurements were made with a field strength of 1.5 V cm^{-1} and with pressures of 150, 200, 300, 400 and 500 torr. The k_1 v E/p curve obtained in this way was approximately 0.9% below the curve obtained at higher field strengths. When the points of the E = 1.5 curve were increased by 0.9% they fell exactly on the high field curve except at E/p = 0.006 and 0.008, and the curve obtained in this way extrapolated to $k_1 = 1.000$ at E/p = 0.0. The difference

Table 4.4

k_1 in Hydrogen at 293°K.

p	500	400	300	200	150	100	40	20	10
E/p									
0.006	1.021								
0.008	1.035	1.034							
0.01	1.049	1.047	1.047						
0.015	1.087	1.088	1.087	1.084					
0.02	1.130	1.128	1.129	1.127	1.124				
0.025		1.173	1.173	1.171	1.170				
0.03			1.216	1.216	1.215	1.212			
0.04				1.304	1.304	1.304			
0.05				1.391	1.391	1.392			
0.06					1.477	1.479			
0.07					1.563	1.564			
0.08					1.648	1.648			
0.09						1.732			
0.1						1.816	1.806		
0.12							1.974		
0.15							2.23	2.22	
0.18							2.48	2.46	
0.20							2.65	2.63	
0.25							3.08	3.07	
0.3							3.52	3.50	3.51
0.4							4.41	4.39	4.40
0.5							5.28	5.27	5.28
0.6								6.13	6.15
0.7								6.96	6.98
0.8								7.76	7.77
0.9								8.51	8.51
1.0								9.22	9.22
1.2									10.55
1.5									12.29
1.8									13.84
2.0									14.82

Table 4.5

k_1 in Hydrogen at 293°K

p	500	400	300	200	150	100	40	20
E/p								
0.006	1.022							
0.008	1.037	1.037						
0.010	1.051	1.052	1.051					
0.015	1.091	1.091	1.091	1.087				
0.020	1.135	1.135	1.134	1.131	1.130			
0.025		1.181	1.179	1.177	1.175			
0.03			1.224	1.222	1.221	1.218		
0.04				1.312	1.311	1.311		
0.05				1.399	1.400	1.400		
0.06					1.486	1.487		
0.07					1.573	1.573		
0.08					1.657	1.659		
0.09						1.742		
0.1						1.827	1.817	
0.12							1.985	
0.15							2.23	
0.18							2.50	
0.20							2.66	
0.25							3.10	
0.3							3.54	
0.4							4.42	
0.5							5.31	
0.6								
0.7								
0.8								
0.9								
1.0								
1.2								
1.5								
1.8								
2.0								

between the values of k_1 at E/p = 0.006 and 0.008 obtained in this way and those obtained in the conventional manner was only 0.2%. Since the method produces points which agree well with the rest of the data and since they give a better extrapolation to (0.0, 1.000) it is thought that the values at E/p = 0.006 and 0.008 found in this way would be accurate.

The agreement between the two sets of data in Tables 4.4. and 4.5 can be seen to be extremely good (better than 0.5%) and since there is no reason to prefer one set to the other, the averages of these two sets are presented as the final values in Table 4.6. Since the quantity of interest in the later calculations is D/μ rather than k_1, the data in this table are values of D/μ. To prevent errors due to rounding off, the values of D/μ shown have been recalculated from the original ratio measurements rather than by dividing the average values of k_1 by kT/e. An error limit of $\pm$ 1% is placed on the average values in this table.

A further reduction of these data to the values corresponding to the required values of E/N was made graphically. The values so obtained are given in Table 1 of Appendix 2.

4.2.2. Results for $1.0 \leq E/p \leq 10.0$ V cm^{-1} $torr^{-1}$.

The geometry of the chamber and the limitation of the maximum voltage which could be applied meant that results in this range could only be obtained with current ratios lower than those normally measured. As a result, the data to be given in Table 4.7 may be slightly too low because of the low ratio effect discussed in 4.1.2. Nevertheless, even including an allowance for this error the data are claimed to be in error by less than 2%. Errors from sources other than the use of low current ratios should be very small since the temperature and pressure were accurately measured and the field strengths were so high that contact potential effects were completely negligible. Table 4.7 gives the values of D/μ in hydrogen for $1.0 \leq E/p \leq 10.0$; the values of the parameter k_1 corresponding to the average values in this table are also given.

Table 4.6

Values of D/μ in hydrogen at 293°K.

p	500	400	300	200	150	100	40	20	10	Average
E/p										
0.006	0.0258(1)									0.0258(1)
0.008	0.0261(7)	0.0261(6)								0.0261(7)
0.010	0.0265(3)	0.0265(1)	0.0265(0)							0.0265(1)
0.015	0.0275(1)	0.0275(2)	0.0275(1)	0.0274(2)						0.0274(9)
0.020	0.0286(1)	0.0285(8)	0.0285(9)	0.0285(2)	0.0284(7)					0.0285(5)
0.025		0.0297(3)	0.0297(1)	0.0296(6)	0.0296(2)					0.0296(8)
0.03			0.0308	0.0308	0.0308	0.0307				0.0308
0.04				0.0330	0.0330	0.0330				0.0330
0.05				0.0352	0.0353	0.0353				0.0353
0.06					0.0374	0.0375				0.0375
0.07					0.0396	0.0396				0.0396
0.08					0.0418	0.0418				0.0418
0.09						0.0439				0.0439
0.10						0.0461	0.0458			0.0459
0.12							0.0500			0.0500
0.15							0.0563	0.0561		0.0562
0.18							0.0629	0.0621		0.0625
0.20							0.0671	0.0664		0.0668
0.25							0.0781	0.0776		0.0779
0.3							0.0892	0.0884	0.0887	0.0888
0.4							0.1116	0.1109	0.1111	0.1112
0.5							0.1338	0.1331	0.1334	0.1334
0.6								0.1548	0.1554	0.1551
0.7								0.1758	0.1763	0.1761
0.8								0.1960	0.1963	0.1962
0.9								0.215(0)	0.215(0)	0.215(0)
1.0								0.232(9)	0.232(9)	0.232(9)
1.2									0.266(5)	0.266(5)
1.5									0.310	0.310
1.8									0.350	0.350
2.0									0.374	0.374

Table 4.7

D/μ in Hydrogen at 293^{o} K.

p E/p	10	8	6	4	Average	k_1
1	.2334				.233	9.24
1.2	.2665				.267	10.55
1.5	.3112				.311	12.33
1.8	.3507				.351	13.88
2.0	.3758	.3738			.375	14.84
2.5	.4322	.4307			.432	17.08
3	.4840	.4829	.4825		.483	19.12
4	.5766	.5763	.5769		.577	22.8
5	.6614	.6618	.6614		.662	26.2
6	.7406	.7414	.7411		.741	29.3
7	.8178	.8185	.8191		.819	32.4
8		.8932	.8932	.8980	.896	35.5
9			.9882	.9751	.982	38.9
10				1.060	1.060	42.0

For each value of E/p the temperature and pressure were recorded to enable the corresponding value of E/N to be determined. Small corrections to the measured values of D/μ were then made to convert them to the values corresponding to the values of E/p_{293} shown in the table.

4.2.3 <u>At 77^{o}K. $2.0 \times 10^{-20} \leq E/N \leq 1.2 \times 10^{-16}$ V cm^2.</u>

Other than data excluded for the reasons given in 4.1.4 and 4.1.5 all the results for hydrogen were plotted on a graph with scales sufficiently large to allow the values of D/μ to be read off at the required values of E/N with an error of no more than 0.3%. Almost 250 individual data points fairly evenly distributed over the whole range of E/N were plotted and every point lay within

$\pm$ 1% of the line of best fit drawn through the data.

It was observed that a temperature gradient of approximately 0.3^{o} appeared between the cathode and anode of the diffusion chamber as the pressure was progressively lowered from 500 to 5 torr over a period of some hours. A corresponding change in mean temperature from 77.3^{o}K to 77.4^{o}K was observed. The rise in temperature of the top plate of the apparatus is due almost entirely to radiant heating from that part of the apparatus not immersed in the liquid nitrogen bath. At high pressures conduction and convection through the hydrogen helps to keep the temperature of the top plate close to that of the liquid nitrogen bath; as the pressure is reduced the apparatus becomes less effectively coupled to the heat sink and the temperature gradient across the chamber increases.

This temperature rise has been taken into account in preparing Table 4.8. An error limit of $\pm$ 2% is placed on the data in this table. The actual conversion factors used were :

$2 \times 10^{-20} \leq E/N < 5 \times 10^{-18}$	$T = 77.2(8)^{o}K$	$kT/e = 0.006659$ eV
$5 \times 10^{-18} \leq E/N < 2.5 \times 10^{-17}$	$T = 77.3(4)^{o}K$	$kT/e = 0.006664$ eV
$2.5 \times 10^{-17} \leq E/N \leq 1.2 \times 10^{-16}$	$T = 77.4(0)^{o}K$	$kT/e = 0.006669$ eV

4.2.4 Comparison with Other Data.

Other results for k_1 in hydrogen at 293^{o}K have been reported by Townsend and Bailey (1921), Crompton and Sutton (1952), Crompton and Jory (1962), Cochrane and Forester (1962) and Crompton and Elford (1963). Warren and Parker (1962) have reported values for D/μ in hydrogen at 77^{o}K.

With the exception of Crompton and Elford, whose results were presented only in a graphical form, none of the other workers have obtained accurate values of k_1 in the near thermal region. Figure 4.1 shows the present results expressed as either k_1 or D/μ and plotted as a function of E/p_{293} or E/N. The data of Table 4.7 have been included in this figure.

The agreement of the present results with the unpublished but tabulated data of Crompton and Elford (1963) is of the order of 0.5% over the common range of E/p ($0.006 \leq E/p \leq 0.10$). The agreement with the results

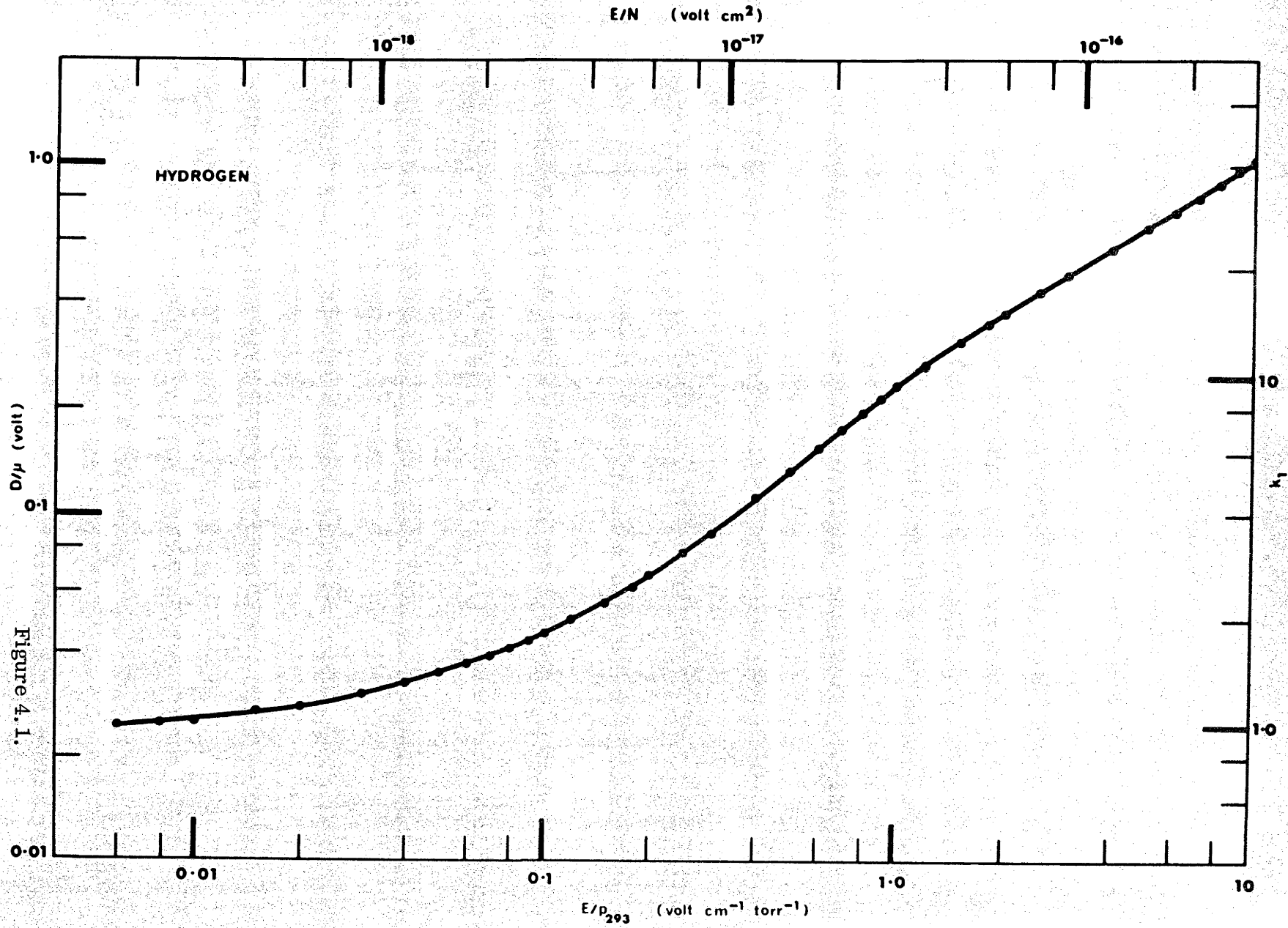
E/N (volt cm²)
10⁻¹⁸
10⁻¹⁷
10⁻¹⁶
HYDROGEN
1·0
0·1
0·01
D/μ (volt)
10
1·0
μ
0·01
0·1
1·0
10
E/p293 (volt cm⁻¹ torr⁻¹)

Figure 4.1.

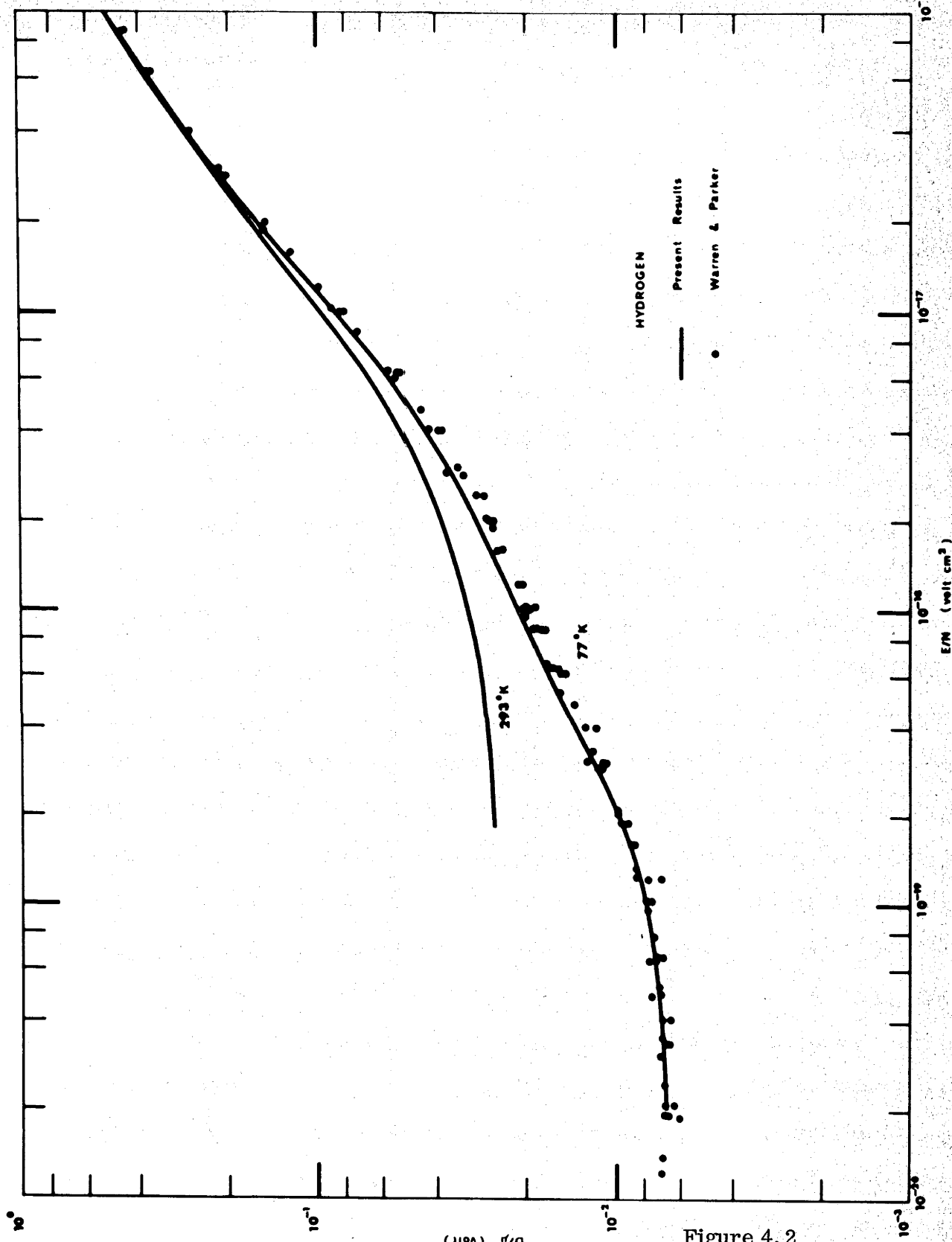
HYDROGEN
Present Results
Warren & Parker
293°K
77°K
D/μ (volt)
E/N (volt cm²)

Figure 4.2

Table 4.8

D/μ and k_1 in hydrogen at 77.3°K.

E/N	D/μ	k_1
2.0×10^{-20}	0.00676	1.01(5)
2.5	0.00681	1.02(2)
3.0	0.00685	1.02(9)
3.5	0.00690	1.03(6)
4.0	0.00696	1.04(5)
4.5	0.00702	1.05(4)
5.0	0.00709	1.06(4)
6.0	0.00723	1.08(5)
7.0	0.00738	1.10(8)
8.0	0.00755	1.13(4)
9.0	0.00772	1.15(9)
1×10^{-19}	0.00790	1.18(6)
1.2	0.00827	1.24(2)
1.4	0.00867	1.30(2)
1.6	0.00907	1.36(2)
1.8	0.00946	1.42(1)
2.0	0.00986	1.48(0)
2.5	0.0108(4)	1.62(8)
3.0	0.0117(9)	1.77(1)
3.5	0.0126(8)	1.90(4)
4.0	0.0135(3)	2.03
4.5	0.0143(2)	2.15
5.0	0.0150(8)	2.26
6.0	0.0164(9)	2.48
7.0	0.0177(7)	2.67
8.0	0.0189(3)	2.84
9.0	0.0200	3.01

E/N	D/μ	k_1
1.0×10^{-18}	0.0210	3.16
1.2	0.0229	3.44
1.4	0.0247	3.71
1.6	0.0263	3.95
1.8	0.0278	4.18
2.0	0.0294	4.42
2.5	0.0329	4.94
3.0	0.0364	5.47
3.5	0.0398	5.98
4.0	0.0433	6.50
4.5	0.0467	7.01
5.0	0.0502	7.54
6.0	0.0572	8.59
7.0	0.0642	9.63
8.0	0.0713	10.7(0)
9.0	0.0786	11.8(0)
1.0×10^{-17}	0.0860	12.9(1)
1.2	0.100(8)	15.1(3)
1.4	0.115(7)	17.3(6)
1.6	0.130(6)	19.6(0)
1.8	0.145(3)	21.8
2.0	0.159(5)	23.9
2.5	0.192(9)	29.0
3.0	0.224	33.6
3.5	0.252	37.8
4.0	0.278	41.7
4.5	0.302	45.3
5.0	0.325	48.8
6.0	0.366	54.9
7.0	0.405	60.7

E/N	D/μ	k_1
8.0	0.440	66.0
9.0	0.474	71.1
1.0×10^{-16}	0.506	75.9
1.2	0.565	84.7

of Crompton and Jory (1962)($0.1 \leq E/p \leq 5.0$) is also well within the combined experimental error provided a small correction is made to the published data of these workers. This correction results from the 0.37% difference between the torr and the 20^{o}C mm of mercury used by them. If a temperature of 15^{o}C is assumed for the work of Townsend and Bailey their results also agree well with the present data. Above $E/p = 1.0$ there is also fair agreement with Crompton and Sutton's values. A discussion of the possible sources of error in Crompton and Sutton's data below $E/p = 1.0$ was given in Crompton and Jory (1962). The discrepancy between the present results and those of Cochrane and Forester is surprisingly large (in excess of 25% in some places) in view of the modern techniques applied in each case. Because of the good agreement with earlier data above $E/p = 1.0$ and the excellent agreement with Crompton and Elford below $E/p = 1.0$, none of the other sets of data have been plotted in Figure 4.1.

In Figure 4.2 the present results at 77^{o}K are compared with those of Warren and Parker (1962), the only other data available. All the present experimental points lie within the thickness of the line plotted. The agreement between these data and those of Warren and Parker is not good since discrepancies of up to 15 - 20% exist between the two sets. These authors made no compensation for contact potential differences within their apparatus and used field strengths which, at times, were as low as 1/10 the smallest used in the present experiments. Errors from contact potential and other surface effects could reasonably be expected to be much larger than in the present results. The self consistency of Warren and Parker's data was so poor that they were forced to use an empirical calibration to obtain meaningful results. Even with this calibration the scatter in the tabulated data supplied by them is still often in excess of 5%; a true comparison with the present results thus becomes difficult.

By using such low electric field strengths Warren and Parker extended their data to values of E/N approximately an order of magnitude lower than the present results. However the doubtful reliability of their data and the fact that the present data extend to within $1\frac{1}{2}$% of thermal energy suggest that such a step is neither justified nor essential.

A comparison between the values of D/μ measured at both $77^{o}K$ and $293^{o}K$ is also given in Figure 4.2 As expected, the curves at both temperatures extrapolate to the thermal value of kT/e. As E/N is increased the energy supplied to the electrons by the electric field increases and the effect of the thermal energy of the gas molecules becomes less important. Thus the D/μ curves at the two temperatures gradually merge and the value of D/μ is virtually independent of the gas temperature from about $E/N = 4 \times 10^{-17}$ upwards.

Closer examination of the data of Tables 4.6 and 4.8 shows that the results at the two temperatures do not exactly agree, the results of the $77^{o}K$ experiment being 1.3% below the $293^{o}K$ values over a considerable range of E/N. Since the results are taken with exactly the same electric field strengths and gas number densities at the two temperatures the measured current ratios are exactly the same in each case. For this reason it is unlikely that the small difference is instrumental and it should therefore be considered significant.

4.3 Results for Deuterium.

4.3.1 At $293^{o}K$. $0.006 \leq E/p \leq 2.0$ V cm^{-1} $torr^{-1}$.

Results in deuterium were taken immediately after establishing the reliability of the apparatus and measuring equipment with hydrogen. The small potential applied to compensate for the effects of contact potential differences in the apparatus was exactly the same in deuterium as it was in hydrogen.

Two complete sets of data for k_1 in deuterium were obtained, the experimental details being exactly the same as those given in 4.2.1. However, the agreement of the two sets of data taken with the different collecting electrodes was slightly worse in deuterium at the intermediate values of E/p than it was in hydrogen. Over most of the E/p range the results agreed to 0.5% or better but for $0.1 \leq E/p \leq 0.6$ the discrepancy was of the order of 0.75%. Since the results were taken under identical conditions to those in hydrogen it was thought that the disagreement might have been due to a real difference in the purity of the gas samples used on the two occasions. A further set of results were taken with gas from a third cylinder of deuterium: these results were in excellent agreement

with the other data taken with the new collecting electrode. The results given in Table 4.9 are, nevertheless, the averages of the two sets, but in the E/p region in question slightly greater weight was given to the later data.

Table 4.9 gives the values of D/μ as a function of E/p_{293} ; an error limit of $\pm$ 1% is placed on the average values in this table. As in hydrogen, the data were obtained directly from the measured current ratios and not by conversion from the calculated values of k_1.

The values of D/μ at various values of E/N were found graphically and are presented in Table 2 of Appendix 2.

4.3.2 <u>At 77°K. $2.0 \times 10^{-20} \leq E/N \leq 1.2 \times 10^{-16}$ V cm^2.</u>

With the exception of those data excluded for the reasons given in 4.1.4 and 4.1.5, all the results for deuterium were plotted on a graph sufficiently large for the values of E/N and D/μ to be read off to better than 0.3%. A slight improvement to the techniques used for hydrogen was made since account was taken of the different sensitivity to temperature of k_1 and D/μ at low and high E/N. Thus for $D/\mu < 10$ kT/e the graphs were plotted in terms of k_1 since in this range k_1 is relatively insensitive to changes in the gas temperature. For $D/\mu \geq 10$ kT/e the graphs were plotted in terms of D/μ since at high E/N, D/μ is relatively independent of the gas temperature.

The small temperature rise described in 4.2.3 was also observed in deuterium and this has been taken into account in analysing the raw data. Interchange between D/μ and k_1 was made by multiplying or dividing by kT/e, the actual factors used being :

$2 \times 10^{-20} \leq E/N < 2 \times 10^{-19}$	kT/e = 0.006651 eV
$2 \times 10^{-19} \leq E/N < 1.2 \times 10^{-18}$	kT/e = 0.006662 eV
$1.2 \times 10^{-18} \leq E/N \leq 1.2 \times 10^{-16}$	kT/e = 0.006665 eV

Almost 300 individual data points were plotted over the whole range of E/N and only 3 of these did not lie within $\pm$ 1% of the line of best fit drawn through the remainder. Tabulated values of D/μ and k_1 are given in Table 4.10; the expected error limit on these data is $\pm$ 2%.

Table 4.9.

D/μ in Deuterium at 293° K

p	D/μ volts									
E/p	500	400	300	200	150	100	40	20	10	Average
0.006	0.0257(2)									0.0257(2)
0.008	0.0260(2)	0.0259(7)								0.0260(0)
0.010	0.0263(5)	0.0263(5)	0.0263(2)							0.0263(4)
0.015	0.0271(6)	0.0271(8)	0.0271(6)	0.0271(0)						0.0271(5)
0.020	0.0281(2)	0.0281(4)	0.0281(2)	0.0280(6)	0.0279(9)					0.0280(9)
0.025		0.0292(0)	0.0291(5)	0.0291(0)	0.0290(8)					0.0291(3)
0.03			0.0303	0.0302	0.0302	0.0301				0.0302
0.04				0.0326	0.0325	0.0325				0.0325
0.05				0.0350	0.0350	0.0349				0.0350
0.06					0.0376	0.0375				0.0376
0.07					0.0402	0.0400				0.0401
0.08					0.0429	0.0428				0.0429
0.09						0.0456	0.0454			0.0455
0.10						0.0483	0.0482			0.0483
0.12							0.0540			0.0540
0.15							0.0629	0.0627		0.0628
0.18							0.0722	0.0720		0.0721
0.20							0.0785	0.0783		0.0784
0.25							0.0943	0.0942		0.0943
0.3							0.1102	0.1101	0.1094	0.1099
0.4							0.1406	0.1402	0.1399	0.1402
0.5							0.1682	0.1679	0.1670	0.1677
0.6								0.1931	0.1920	0.1926
0.7								0.216(2)	0.215(1)	0.215(7)
0.8								0.237(9)	0.236(2)	0.237(1)
0.9								0.258(5)	0.257(2)	0.257(9)
1.0								0.277(7)	0.276(6)	0.277(2)
1.2								-	0.313	0.313
1.5								0.366	0.364	0.365
1.8								-	0.411	0.411
2.0								0.441	0.440	0.441

Table 4.10

D/μ and k_1 in Deuterium at 77.3°K.

E/N	D/μ	k_1
2.0×10^{-20}	0.00680	1.02(3)
2.5	0.00682	1.02(6)
3.0	0.00685	1.03(0)
3.5	0.00688	1.03(5)
4.0	0.00692	1.04(1)
4.5	0.00697	1.04(8)
5.0	0.00702	1.05(5)
6.0	0.00712	1.07(0)
7.0	0.00722	1.08(6)
8.0	0.00733	1.10(2)
9.0	0.00744	1.11(8)
1.0×10^{-19}	0.00756	1.13(6)
1.2	0.00778	1.17(0)
1.4	0.00801	1.20(4)
1.6	0.00824	1.23(9)
1.8	0.00846	1.27(2)
2.0	0.00866	1.30(2)
2.5	0.00916	1.37(5)
3.0	0.00962	1.44(4)
3.5	0.0100(7)	1.51(1)
4.0	0.0104(9)	1.57(5)
4.5	0.0109(0)	1.63(6)
5.0	0.0113(1)	1.69(7)
6.0	0.0121(1)	1.81(8)
7.0	0.0128(9)	1.93(5)
8.0	0.0136(6)	2.05
9.0	0.0144(3)	2.17

E/N	D/μ	k_1
1.0×10^{-18}	0.0152(1)	2.28
1.2	0.0168(1)	2.52
1.4	0.0184(0)	2.76
1.6	0.0200	3.01
1.8	0.0217	3.26
2.0	0.0234	3.51
2.5	0.0278	4.17
3.0	0.0323	4.84
3.5	0.0371	5.57
4.0	0.0421	6.32
4.5	0.0471	7.06
5.0	0.0521	7.81
6.0	0.0627	9.41
7.0	0.0737	11.1(0)
8.0	0.0848	12.7(0)
9.0	0.0957	14.4(0)
1.0×10^{-17}	0.106(6)	15.9(9)
1.2	0.127(9)	19.1(9)
1.4	0.147(6)	22.2
1.6	0.166(2)	24.9
1.8	0.183(6)	27.6
2.0	0.199(7)	30.0
2.5	0.237	35.5
3.0	0.270	40.5
3.5	0.302	45.3
4.0	0.331	49.7
4.5	0.358	53.7
5.0	0.385	57.8
6.0	0.435	65.3

E/N	D/μ	k_1
7.0	0.484	72.6
8.0	0.527	79.1
9.0	0.570	85.5
1.0×10^{-16}	0.612	91.8
1.2	0.694	104. (0)

The raw data showed some evidence of a plateau in the D/μ v E/N curve for both hydrogen and deuterium at about $E/N = 2.5 \times 10^{-20}$ V cm^2. An investigation of the shape of the curve by taking results with a field strength of 0.65 V cm^{-1} confirmed the possibility of such a plateau, particularly in deuterium. However the maximum divergence from the shapes of the curves represented by Tables 4.8 and 4.10 was only 0.5 - 0.8% and since this was within the experimental error no firm conclusion could be drawn.

4.3.3 Comparison with Other Data.

The room temperature data of Table 4.9 are shown plotted as a function of E/p_{293} or E/N in Figure 4.3. Also shown in this figure are the results of Hall (1955) and of Creaser (1966) these being the only other data for deuterium at 293^{o}K. All the 31 average values from the present experiment lie within the thickness of the line plotted.

There is only limited overlap of Hall's results with the present range of E/p. Since she used lower gas pressures and did not correct for the effects of contact potential differences in her apparatus her results are more susceptible to experimental error than are the present ones. Nevertheless, at the highest values of E/p where the effects of contact potential differences are least, the two sets of data agree to within the combined experimental error. Creaser's data cover only the range $2.0 \leq E/p \leq 10$.

A comparison of the present results at 77^{o}K with those at 293^{o}K and with the data of Warren and Parker (1962) for 77^{o}K is shown in Figure 4.4. All the present experimental points lie within the thickness of the lines plotted.

All the remarks of section 4.2.4 are equally relevant here. Thus, the scatter in Warren and Parker's data is often in excess of 5% and the estimated real difference between their results and the present data is about 15%. Similarly, a comparison of the data of Tables 4.9 and 4.10 shows that, as in hydrogen, the 77^{o}K data do not merge completely with the 293^{o}K values but remain approximately 1.3% below them from $E/N = 4 \times 10^{-17}$ upwards.

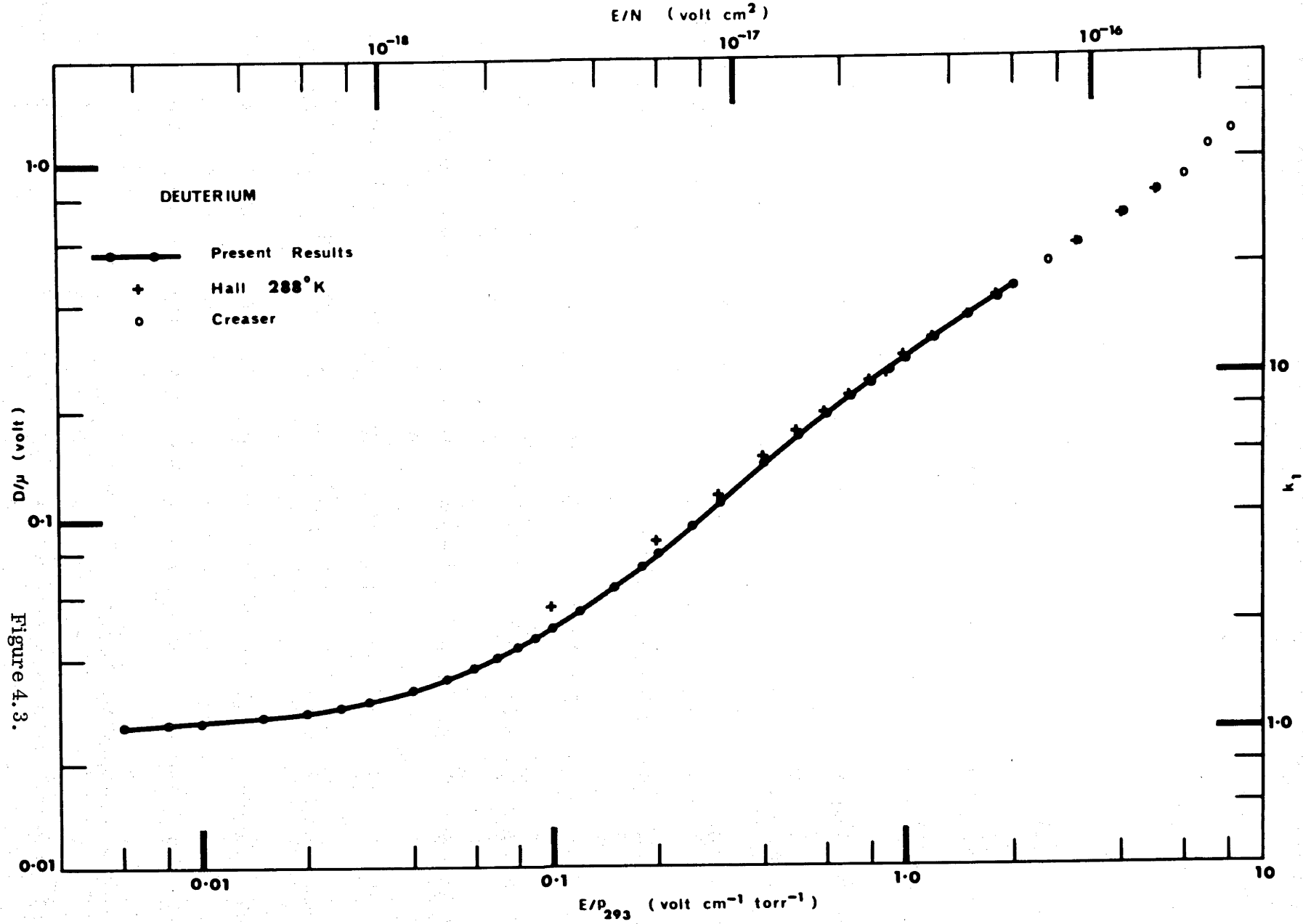
E/N (volt cm²)
10⁻¹⁸
10⁻¹⁷
10⁻¹⁶
DEUTERIUM
Present Results
Hall 288°K
Creaser
D/μ (volt)
k⁻¹
1·0
0·1
0·01
10
1·0
0·01
0·1
1·0
10
E/p293 (volt cm⁻¹ torr⁻¹)

Figure 4.3.

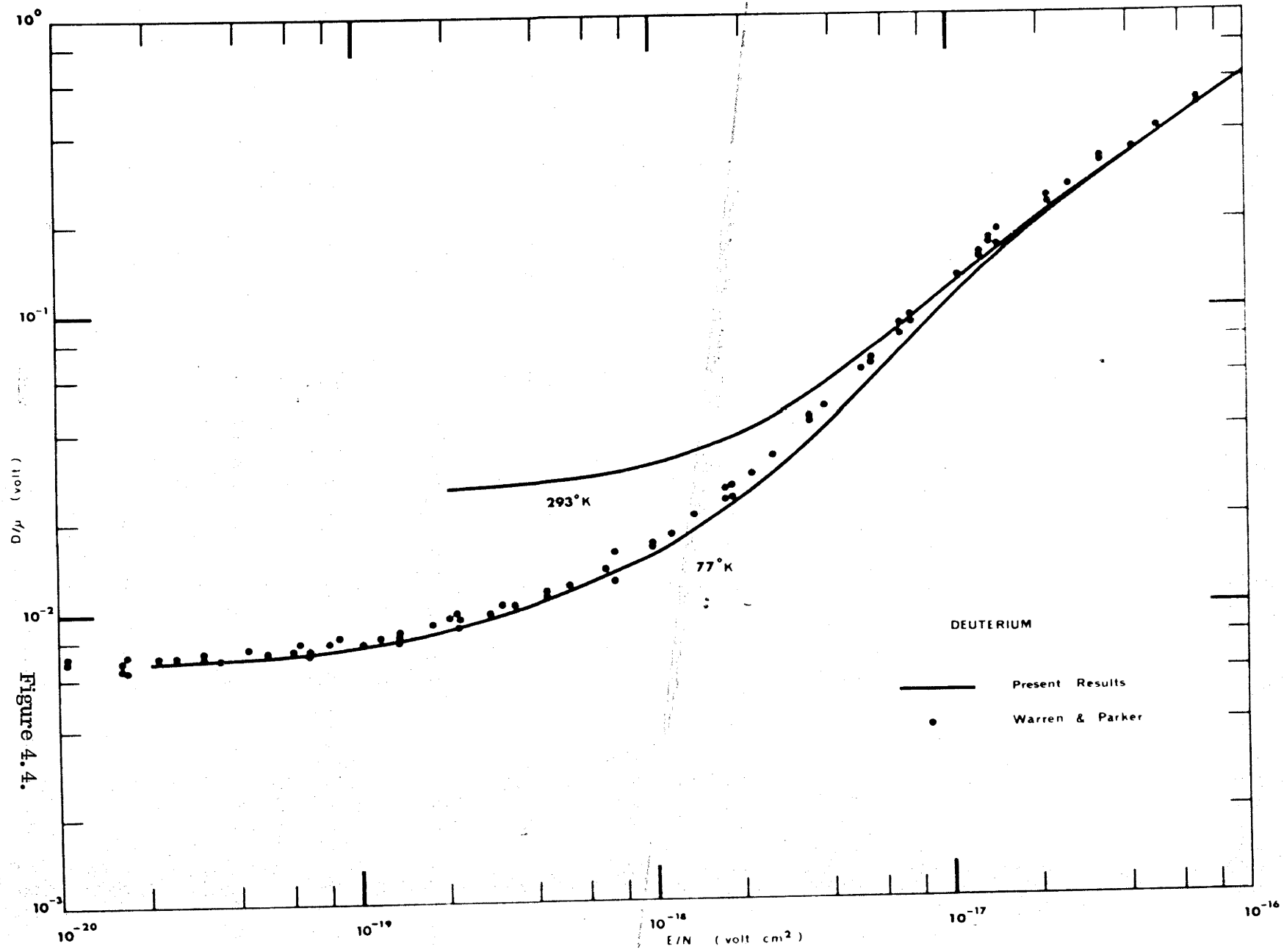
10^{0}
10^{-1}
10^{-2}
10^{-3}
D/μ (volt)
293°K
77°K
DEUTERIUM
Present Results
Warren & Parker
10^{-20}
10^{-19}
10^{-18}
10^{-17}
10^{-16}
E/N (volt cm^2)

Figure 4.4.

4.4 Results for para-Hydrogen.

4.4.1 At $77^{o}K$. $2.0 \times 10^{-20} \leq E/N \leq 5 \times 10^{-17}$ V cm^{2}.

Results in pure para-hydrogen were taken after establishing the reliability of the apparatus with normal hydrogen. The para-hydrogen gas was prepared using the apparatus and techniques described in Appendix I. Using the analyser described in Appendix I the para-concentration of the gas sample was found to be in excess of 98%. Since changing the para-concentration from 25% in normal hydrogen to 100% in pure para-hydrogen causes, at most, a 20% change in the value of D/μ at a given value of E/N, any errors from the possible 2% of unconverted gas are completely negligible.

The use of the Americium source in place of the platinum filament used in hydrogen and deuterium resulted in a smaller rise in the mean temperature of the apparatus as the pressure was lowered. The factors used for interchange between D/μ and k_1 in para hydrogen were:

$2 \times 10^{-20} \leq E/N < 1 \times 10^{-17}$ $\quad T = 77.28^{o}K$ $\quad kT/e = 0.006659$

$1 \times 10^{-17} \leq E/N \leq 5 \times 10^{-17}$ $\quad T = 77.47^{o}K$ $\quad kT/e = 0.006675.$

A total of 66 individual data points were taken and when these were plotted on a graph similar to that used for hydrogen and deuterium, all but one point lay within $\pm$ 1% of the line of best fit drawn through the data. As in the case of deuterium, the graphs were plotted in terms of k_1 for $D/\mu < 10$ kT/e but D/μ for $D/\mu \geq 10$ kT/e. The values of D/μ and k_1 corresponding to the required values of E/N are shown in Table 4.11.

4.4.2 Comparison with Other Data.

There have been no previous measurements of electron transport coefficients in para-hydrogen. A comparison between the values of D/μ measured in para-hydrogen and in normal hydrogen is shown in Figure 4.5 and discussed in the following section. The small difference between the values of D/μ for $2 \times 10^{-20} < E/N < 1 \times 10^{-19}$ is considered significant but, being about 2%, is less than the combined experimental error.

Table 4.11

D/μ and k_1 in para-hydrogen at 77.3°K.

E/N	D/μ	k_1
2.0×10^{-20}	0.00686	1.03(0)
2.5	0.00692	1.03(9)
3.0	0.00698	1.04(8)
3.5	0.00705	1.05(8)
4.0	0.00711	1.06(8)
4.5	0.00717	1.07(7)
5.0	0.00724	1.08(7)
6.0	0.00740	1.11(1)
7.0	0.00759	1.14(0)
8.0	0.00778	1.16(8)
9.0	0.00796	1.19(5)
1.0×10^{-19}	0.00814	1.22(3)
1.2	0.00852	1.27(9)
1.4	0.00888	1.33(3)
1.6	0.00924	1.38(7)
1.8	0.00960	1.44(1)
2.0	0.00996	1.49(6)
2.5	0.0108(1)	1.62(3)
3.0	0.0116(4)	1.74(8)
3.5	0.0123(9)	1.86(0)
4.0	0.0131(1)	1.96(8)
4.5	0.0137(2)	2.06
5.0	0.0143(2)	2.15
6.0	0.0153(2)	2.30
7.0	0.0163(1)	2.45
8.0	0.0170(5)	2.56
9.0	0.0177(1)	2.66

E/N	D/μ	k_1
1.0×10^{-18}	0.0184(5)	2.77
1.2	0.0197(8)	2.97
1.4	0.0211	3.17
1.6	0.0224	3.36
1.8	0.0236	3.54
2.0	0.0247	3.71
2.5	0.0272	4.09
3.0	0.0302	4.54
3.5	0.0334	5.01
4.0	0.0365	5.48
4.5	0.0396	5.95
5.0	0.0428	6.43
6.0	0.0497	7.46
7.0	0.0567	8.52
8.0	0.0639	9.60
9.0	0.0679	10.1(9)
1.0×10^{-17}	0.0792	11.8(7)
1.2	0.0946	14.1(7)
1.4	0.109(7)	16.4(3)
1.6	0.124(9)	18.7(1)
1.8	0.139(8)	20.9
2.0	0.154(4)	23.1
2.5	0.189(4)	28.4
3.0	0.221	33.1
3.5	0.249	37.3
4.0	0.275	41.2
4.5	0.301	45.1
5.0	0.325	48.7

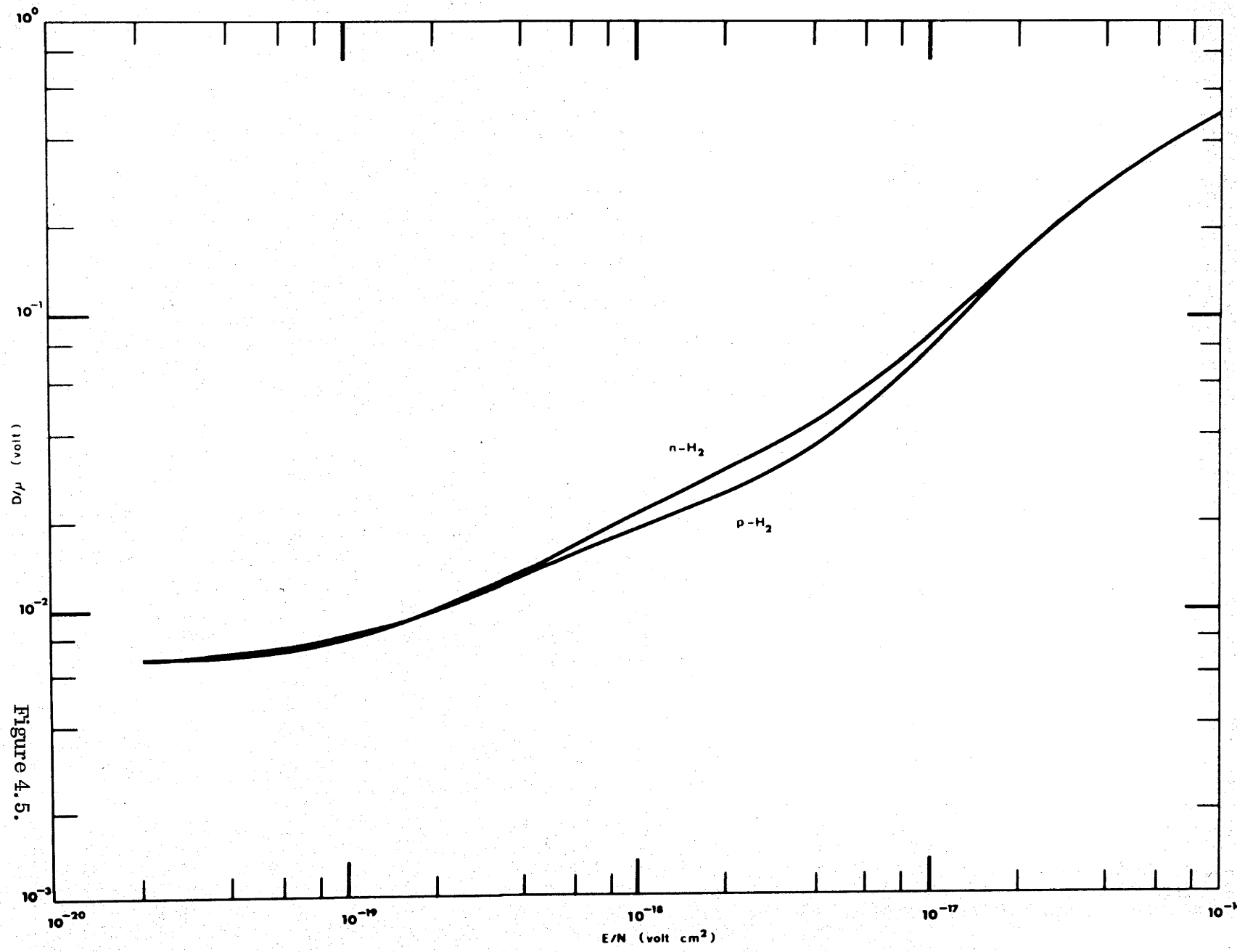
10^{0}
10^{-1}
10^{-2}
10^{-3}
D/μ (volt)
n-H_2
p-H_2
10^{-20}
10^{-19}
10^{-18}
10^{-17}
10^{-16}
E/N (volt cm^2)

Figure 4.5.

4.5 General Discussion of Results at 77°K.

In addition to the comparison made in Figure 4.5, a comparison between the values of D/μ in normal hydrogen and deuterium is shown in Figure 4.6. A qualitative description of these curves can be given in terms of the various collision processes occurring. Reference should be made to Appendix I for a discussion of the rotational quantum numbers, allowable transitions and the proportions of ortho- and para- molecules in each case. The momentum transfer cross section is the same in all three gases.

Comparing the curves for normal hydrogen and normal deuterium (Figure 4.6) it is seen that the value of D/μ initially rises more rapidly in hydrogen than it does in deuterium. This occurs because the first rotational threshold in deuterium is at approximately 0.02β eV and, at 77°K, the $J \neq 0$ level in deuterium is occupied by approximately 60% of the molecules (see Appendix I). Even when the electrons are in thermal equilibrium with the gas their mean energy is 0.01 eV and there are a significant number whose energy exceeds 0.02β eV. As the value of E/N is increased most of the energy received by the electrons from the field is used in exciting the $J = 0$ to $J = 2$ transition and, as a result, the mean electron energy rises only slowly. In the case of hydrogen, not only does the first rotational transition have a threshold at the higher value of 0.045 eV, but only 25% of the hydrogen molecules occupy the $J = 0$ level. An appreciable change in the slope of the D/μ v E/N curve therefore does not occur until a considerable proportion of the electrons in the swarm have an energy in excess of 0.075 eV which corresponds to the threshold of the $J = 1$ to $J = 3$ transition.

In both gases the rotational cross sections become only slowly rising functions of the electron energy after the rapid rise in the near threshold region. This behaviour, coupled with the very small populations of excited rotational states and the fact that cross sections for rotational excitation involving a change in quantum number of 4 or more are very small, results in the steady rise of the mean electron energy with E/N until a significant number of electrons have enough energy to cause vibrational excitation of the molecules. The thresholds for vibrational excitation occur at 0.360 eV and 0.516 eV in deuterium and hydrogen

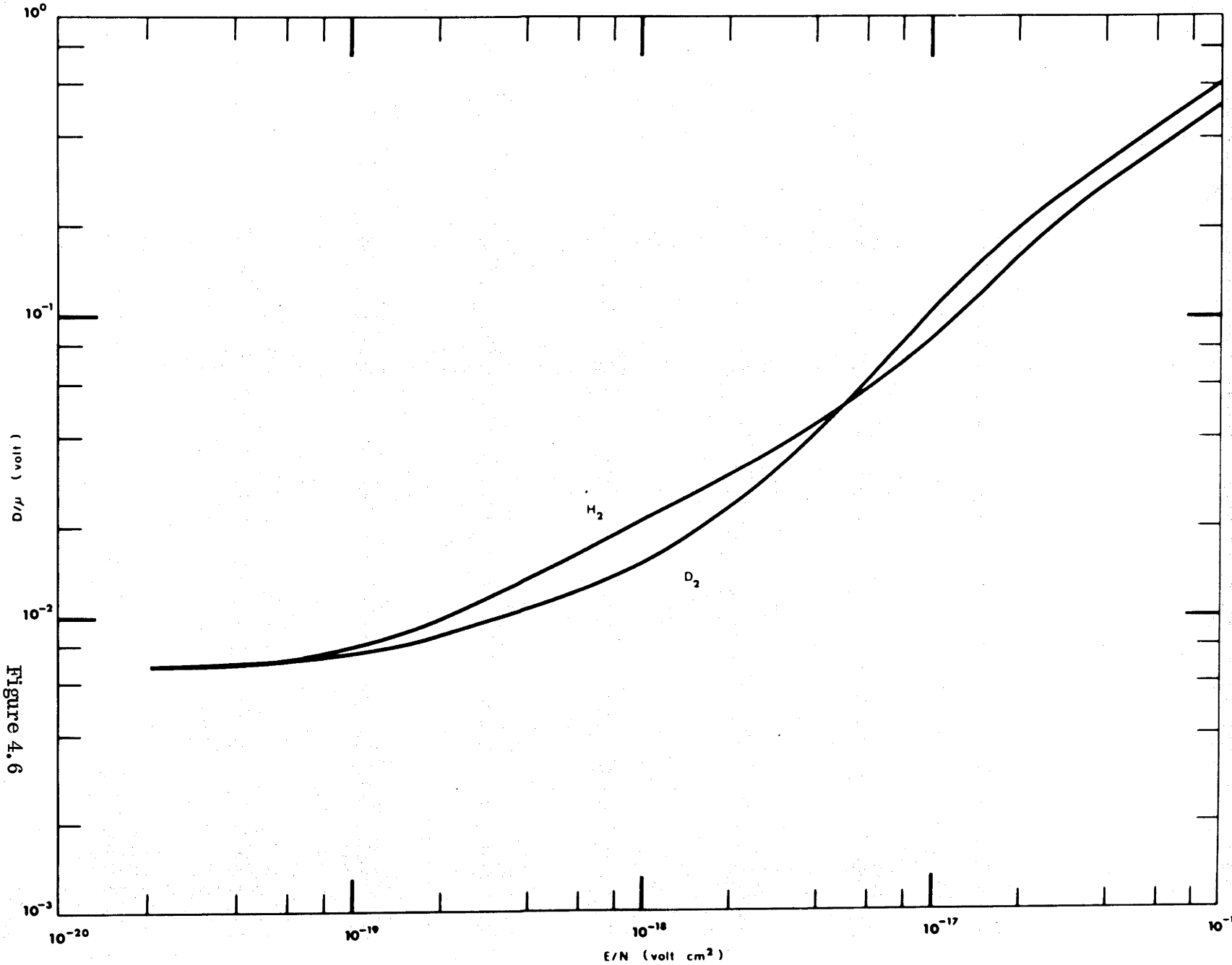
10^{0}
10^{-1}
10^{-2}
10^{-3}
D/μ (volt)
H_2
D_2
10^{-20}
10^{-19}
10^{-18}
10^{-17}
10^{-16}
E/N (volt cm^2)

Figure 4.6

respectively. The vibrational states act as effective energy "absorbers" and cause a decrease in the slope of the D/μ v E/N curve.

A similar comparison between the results for normal and para-hydrogen can be given, the differences this time being due to the different statistical weights of the rotational levels. At sufficiently high values of E/N when the mean electron energy approaches 0.5 eV, the values of D/μ are identical in the two gases because the vibrational excitation cross section is so much larger than the rotational cross sections that the differences in the rotational states are unimportant.

CHAPTER 5.

APPARATUS AND EXPERIMENTAL TECHNIQUES IN THE DRIFT VELOCITY EXPERIMENT.

In this chapter the apparatus and techniques used in the drift velocity experiments are described. Two different apparatuses were used for the measurements of drift velocities, one for the measurements in deuterium at 293^{o}K and the other for the measurements at low temperature. These apparatuses will be referred to as apparatus A and apparatus B.

Some of the material in this chapter is based on the papers of Lowke (1963), Crompton and Jory (1965) and Elford (1966).

5.1 Design Considerations.

The design of an apparatus to measure drift velocities is considerably simpler than that of a lateral diffusion apparatus because the measurements are much less sensitive to the presence of small amounts of field distortion. Furthermore, the rigid mechanical tolerances on the collecting electrode of the lateral diffusion apparatus are not essential in the construction of the collecting electrode of a drift velocity apparatus.

The factors of importance in the design of a drift tube are discussed in following sections.

5.1.1 Uniformity of the Electric Field.

In a series of experiments Lowke (1963) showed that, provided the correct d.c. potentials are applied to the electrical shutters, the measured drift velocities are relatively insensitive to distortion of the electric field between them. Even when incorrect potentials were deliberately applied to the electrodes between the shutters only small changes in the measured drift velocities were observed. To obtain results which are unaffected by field distortion it is therefore not necessary to use the guard ring structure which was shown in section 3.1.2 to give the most highly uniform field. The guard ring structure of apparatus A was, however, identical to that of the lateral diffusion apparatus

described in section 3.1.3 and the results obtained in it were therefore free from any errors due to field distortion. Apparatus B was subject to greater mechanical stresses because of the temperature range it was designed to withstand and it was not practicable to use the same guard ring structure as in apparatus A. Details of the design of apparatus B and of the field distortion within it will be given in section 5.3.1.

Lowke (1963) found that with a spacing between the shutter wires of 0.5 mm he could not observe any distortion of the main field due to the a.c. signals applied to the shutters. The errors caused by distortion of the a.c. voltages themselves will be discussed in section 5.4.3.

5.1.2 Choice of Dimensions of the Apparatus.

Lowke (1962) showed that the resolving power is proportional to $h^{\frac{1}{2}}$, where h is the distance between the planes of the shutters (see section 2.2.2). The resolving power is a measure of the sharpness of the current peaks and should therefore be as large as possible for accurate drift velocity measurements, i.e. the distance between the planes of the shutters should be made as large as possible. Similarly, equation (2.8) derived by Lowke to describe the effects of diffusion on drift velocity measurements shows that h should be as large as possible to minimize errors from this source.

Less important considerations are that the length should be kept small to minimize the quantity of high purity gas needed and that, if it is intended to take results in gases in which electron attachment occurs, the shutter separation should be short enough to ensure that adequate electron current reaches the second shutter.

The combination of these factors resulted in the choice of a nominal 10 cm shutter separation in apparatus A and a nominal 5 cm in apparatus B.

The diameter of the chamber is dictated by the requirements that the electron concentration be negligible at the cylindrical boundary of the chamber and that the electric field be sufficiently uniform. The internal diameter of the guard electrodes of apparatus A was 9 cm. In apparatus B examination of the

field plots to be described in section 5.3.1 resulted in the choice of 6 cm as the internal diameter of the apparatus.

5.1.3 Elimination of Contact Potential Differences.

The lack of sensitivity of the results to field distortion means that the effect of contact potential differences is primarily to falsify the total potential between the planes of the shutters. The interior of apparatus A was gold plated and the shutter wires were flashed with gold. Measurements of the contact potential differences on such surfaces (Crompton, Elford and Gascoigne, 1965) suggest that errors from this source would be less than 1% if the electric field strength was not less than 2.0 V cm^{-1}. The results to be presented in chapter 6 show that errors which could be attributed to contact potential differences within the chamber were less than 0.4% at E = 2.0 V cm^{-1}.

Since it was not intended that apparatus B should yield data with errors of less than 1% it was not considered necessary to coat the whole interior with gold. The shutter wires were, however, flashed with gold to minimize any falsification of the total potential. The results to be given in chapter 6 show some evidence of errors due to contact potential differences but these errors were negligible at field strengths of 8 V cm^{-1} or greater.

5.2 Construction of Apparatus A.

Apparatus A has been described by Jory (1965).

A schematic diagram of the apparatus is shown in Figure 5.1. The guard ring structure was the thick ring type discussed in 3.1.2, eight modules each of 1.66 cm being used. The copper electrodes were separated by ground glass spacers and mounted on four stainless steel tie rods. The internal diameter of the guard rings was 9 cm. The shutters, separated by a nominal 10 cm, were mounted between two "half-rings" with the wires of the shutters being accurately located at the mid-plane of the guard rings.

The shutter wires were 0.0033" nichrome sealed under tension between two soda glass frames. The spacing between the wires was 0.4 mm. Details of the construction of the shutters and of the method of mounting them in

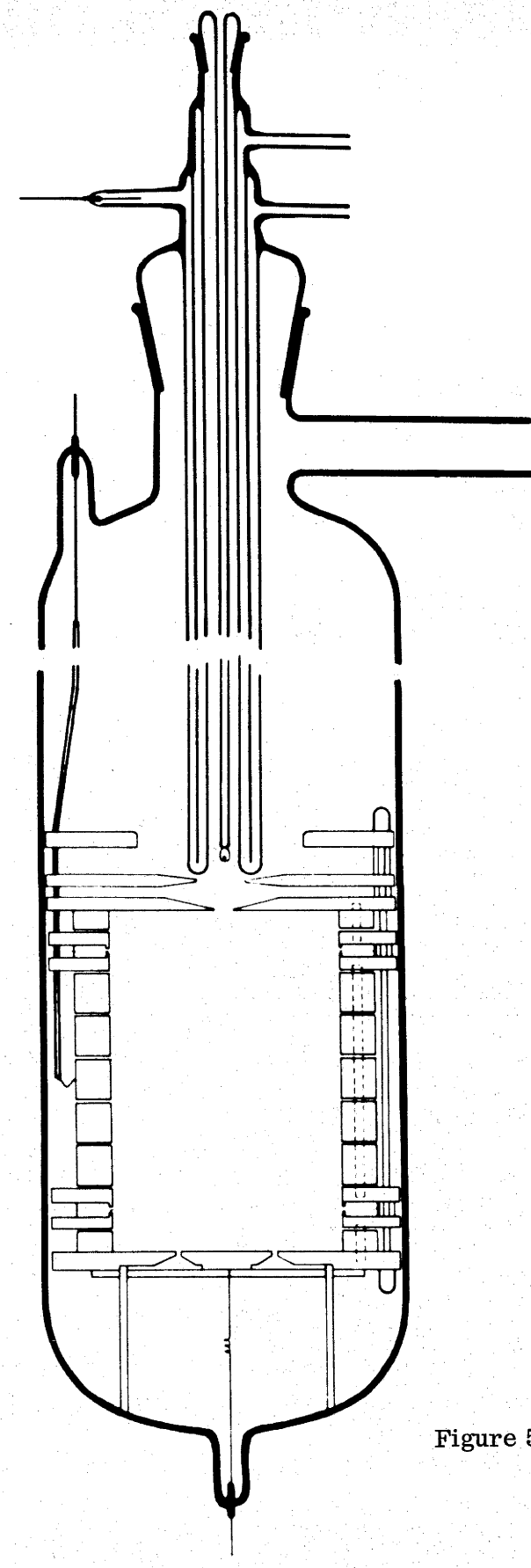

Figure 5.1.

the guard rings were described by Jory (1965).

The apparatus was mounted inside a Pyrex glass envelope similar to that used for the lateral diffusion apparatus of section 3.1.3. The demountable seals were made with W 100 wax. The receiving electrode consisted of a plane metal electrode with a central insulated disc of radius 3.8 cm. Electrons entered the chamber through a 0.5 cm radius hole in the source electrode. The critical dimensions of the apparatus were :

guard ring thickness	1.6149 ± 0.0002 cm
spacer thickness	0.0508 ± 0.0002 cm
total chamber length	13.324 ± 0.008 cm
shutter separation	9.991 ± 0.003 cm.

5.3 Construction of Apparatus B.

This apparatus was designed by Dr. M. T. Elford primarily for the measurement of electron drift velocities in ultra-pure gases at low temperature. The drift tube was therefore made as small as possible and constructed in a form suitable for relatively high temperature bakeout to achieve the required low outgassing rates.

5.3.1 The Guard Ring Structure.

The guard ring structure used can be seen in the sketch of the complete apparatus, Figure 5.2. The electrodes were machined from vacuum melted copper and were lapped and polished to a high degree of flatness and surface finish. The electrodes were separated by glass spacers and mounted on ceramic tie rods. All sharp edges and sudden changes of contour were eliminated to minimize the possibility of electrical breakdown.

Field plots of the proposed electrode structure were made with Teledeltos conducting paper and a plotting device manufactured by Servomex Controls Ltd. Several configurations were tried before the final design was chosen. The changes included the thickness of the guard rings, their separation and internal diameter and the shape of the electrodes adjacent to the shutters. The trial configurations were also examined for their effectiveness in preventing

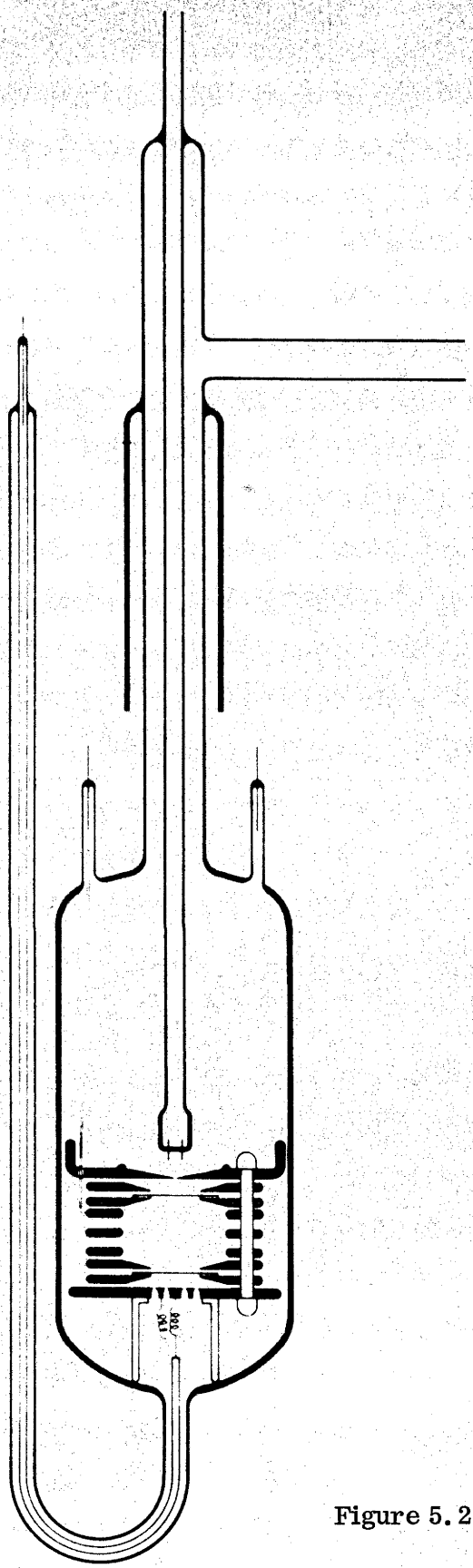

Figure 5.2.

field distortion within the chamber from external sources (Elford, 1957). The final design shown in Figure 5.2 was virtually free of field distortion over the important central region. Small amounts of field distortion were present off the central axis.

A comparison of results obtained in apparatus B with those obtained in apparatus A, which was known to yield highly accurate data, showed that there was a systematic error in apparatus B of approximately 0.3%. If the distance between the planes of the shutters was taken to be 5.014 cm instead of the measured value of 5.008 cm, the agreement between the two sets of data was to within 0.2% at all electric field strengths greater than 8 V cm^{-1}. The empirical figure was used in subsequent measurements and no further discrepancies between the measured values and the results taken in apparatus A or by Lowke (1963) were observed.

5.3.2 Construction of the Shutters.

The shutters were constructed of 0.0033" nichrome wires, separated by 0.4 mm and mounted on ceramic rings of internal and external diameters 3 cm and 5.5 cm respectively. The wires were sealed to the ceramic with Pyro-ceram cement obtained from Corning Glass Works Pty Ltd.

5.3.3 General Details.

Figure 5.2 shows the apparatus mounted inside the permanently sealed Pyrex glass envelope. Hollow Kovar tube seals were used to bring the electrical leads through the glass.

Unlike the lateral diffusion apparatus of chapter 3, the entire apparatus was immersed in liquid nitrogen to a depth just above the bottom of the glass skirt on the filament stem shown in Figure 5.2. Total immersion of the apparatus reduced the pressure variations caused by oscillations in the level of the refrigerant. The temperature gradient between the top and bottom of the apparatus was also much less than it had been in the lateral diffusion apparatus. The liquid nitrogen was contained in a copper can insulated from the outer stainless steel jacket by approximately $3\frac{1}{2}$" of "Insulwool". This material can withstand

temperatures of 250°C and the apparatus can therefore be baked at a moderately high temperature without removing the liquid nitrogen container and its insulating jacket.

The electrical leads through the glass skirt shown in Figure 5.2 were sealed with silicone rubber thereby ensuring that the space between the filament stem and the glass skirt was hermetically sealed. This arrangement prevented condensation and ice formation on the leads.

5.4 Electrical Equipment.

5.4.1 Power Supplies.

The potentials applied to the electrodes were derived from a highly accurate resistance chain across either a Fluke model 301E or a Keithley model 241 power supply. The output of both supplies was accurate and stable to within 0.1%. The actual voltage applied between the shutters was checked with a Fluke model 801R differential voltmeter which was accurate to within 0.05%. Additional potentials between the filament or Americium source and the top plate of the apparatus were supplied either by dry cells or by small stabilized power supplies.

5.4.2 The Electron Sources.

A platinum filament was used as the electron source in the deuterium experiments and the Americium source was used in the para-hydrogen measurements. Both of these sources were identical to those described in 3.2.2.

5.4.3 The A.C. Supplies.

Lowke (1963) examined the effects of distortion in the a.c. signals applied to the shutters of a Bradbury and Nielsen type apparatus. He found that many of the errors introduced were largely self-cancelling to a first order, but that the following ideal characteristics should be approximated as closely as possible;

(a) the phase difference between the two voltages applied to the shutter should be 180°.

(b) there should be no phase difference between the corresponding voltages applied to each shutter.

(c) the amplitude of the two signals applied to the halves of a single shutter should be equal.

(d) the amplitude of the signal should remain constant as the frequency is varied.

(e) the RMS voltage of the signal should be high enough for at least 80% of the current to be collected by the shutter wires when the signal is at its peak.

With the exception of (d) all these requirements are met with the equipment used. It was not possible to produce a combination of oscillator and amplifier with constant output over the whole of the required frequency range. The signal applied to the shutters was therefore monitored on an oscilloscope; by expanding the oscilloscope signal and monitoring only the peaks of the trace very small changes in voltage could be detected. When such changes were observed the oscillator output was adjusted to maintain a constant voltage at all frequencies. Over most of the range used no adjustment was necessary, but for frequencies in excess of 150 Kc/sec or less than 2 Kc/sec continual adjustment was required. The voltages applied to the shutters were also monitored for distortion, e.g. in apparatus A the signal became distorted from a sine wave when the peak to peak voltage applied to the shutters was greater than 25 volts.

The oscillator used was a Hewlett-Packard model 233A audio oscillator with a range 50 c/sec to 500 Kc/sec. The output of the oscillator was amplified by a conventional solid-state amplifier before being applied to the shutters. A resistor-capacitor network was used to superimpose the a.c. signals on the d.c. voltage of each shutter.

The frequencies of the signals were measured with either of two counters: a Venner type TSA, 1035 useful for frequencies less than 150 Kc/sec or a Hewlett-Packard model 3734 A useful up to 5000 Kc/sec. The accuracy of both instruments was $\pm$ 1 count. At frequencies less than 2 Kc/sec the period of the signal was measured rather than its frequency, thus preventing errors due to rounding off.

5.4.4 Electrometry.

Electron currents of 10^{-10} A or less were used. They were measured with a Vibron model 62A electrometer in conjunction with either a 10^{10} or 10^{11} Ω resistor. The time constant of the electrometer circuit was kept small to allow rapid scanning of the current peaks.

5.5 Gas Handling Techniques.

The vacuum systems and gas handling techniques were essentially similar to those described in section 3.5. The outgassing rate of apparatus A was less than 0.1 micron in 10 hours; over the same period of time the contamination of a 500 torr sample of gas was therefore less than 0.2 ppm. The corresponding outgassing rate and impurity concentration in apparatus B were at least four times smaller.

5.5.1 Pressure Measurement.

Unlike the ratio of diffusion coefficient to mobility, the drift velocity is strongly dependent on the value of E/N even at very small values of this parameter. As a result the gas pressure must be measured as accurately as possible over the entire pressure range and it was not possible to use the capsule gauges for pressures greater than 250 torr as had been the case for the lateral diffusion measurements.

The quartz manometer described in section 3.5 was used to measure all pressures. This instrument is essentially a null manometer with a range of a little over 250 torr. A hollow quartz spiral forms the pressure sensitive element and the deflection of this spiral when operated in an evacuated reference volume is a measure of the absolute pressure. For pressures in the range 250 to 500 torr the gauge is operated with the reference pressure held accurately at 250 torr. Stability of the pressure in the reference volume was improved by the addition of a 5 litre ballast volume immersed in a water bath.

5.6 Temperature Control and Measurement.

Apparatus A was immersed in a water bath whose temperature was stable to within 0.1^{o}C per hour. The gas temperature was measured to

within 0.1°C with a copper constantan thermocouple.

Apparatus B was used only at 77°K. Because of an accident during the final assembly only the thermocouple which was attached to the electrode adjacent to the top shutter could be used. Since the lower half of the apparatus was in excellent thermal contact with the liquid nitrogen bath, the single thermocouple would still have shown the existence of any temperature gradients. Only very small temperature gradients were observed; details are given in sections 6.3.2 and 6.4.1.

The thermocouples were prepared and calibrated in the manner described in section 3.6, and their e.m.f's were measured with the combination of Leeds and Northrup K3 potentiometer and electronic null detector described previously.

5.7 Experimental Procedures.

Each experimental observation consisted of the determination of the transit time of the electron pulse and the temperature and pressure of the gas. These data, together with the electric field strength and the distance between the shutters, allow the calculation of W and E/N for each observation.

It was only possible to obtain accurate results if the electron current was stable during the measurement of each current peak. The power supply for heating the filaments was highly stabilized and short term fluctuations from this source were negligible. There were no significant fluctuations in the electron current produced by the Americium source. Any changes in the electron current because of variations with frequency of the amplitude of the a.c. signal applied to the shutters were eliminated by adjusting the a.c. signal as described in 5.4.3 above.

The determinations of the frequencies of the maxima in the current-frequency curves were made in accordance with the methods described by Elford (1966). Thus the frequencies on each side of the peak for pre-determined proportions (roughly 50%, 70% and 90%) of the total peak height were measured. The averages of these pairs of frequencies gave three estimates of the frequency

corresponding to the current maximum. Any trend in these estimates would indicate asymmetry of the peak but in no set of measurements was this observed.

The frequencies corresponding to both the first and second peaks in each current-frequency system were determined. Since the frequency of the second peak should be exactly twice that of the first an excellent experimental check on the accuracy and repeatability of the measurement is provided.

CHAPTER 6.

RESULTS FROM THE DRIFT VELOCITY EXPERIMENTS.

Results obtained for the drift velocity of electrons in deuterium at $293^{o}K$ and $77^{o}K$ and in para-hydrogen at $77^{o}K$ are presented in this chapter. The drift velocities of electrons in hydrogen have been measured accurately by Lowke (1963) and these data are used in the remainder of the present work.

6.1 General Results.

In the Bradbury and Nielsen shutter method a graph of the transmitted current as a function of the frequency of the signal applied to the shutters shows a series of maxima and minima, the amplitude of which decreases with increasing frequency. At constant E/p these maxima and minima should occur at integral multiples of a characteristic frequency f_o such that $1/2\ f_o$ is the transit time of the electrons between the shutters. For each value of E/p and p the frequencies corresponding to the first two maxima were determined. In the results presented in following sections the two values of the drift velocity found in this way were always in agreement to within 0.2%; in about 90% of the observations the agreement was to within 0.1%. The cases where the agreement was to within 0.2% were in either of two categories: (a) at the very lowest values of E/p where the current was small and electrometry noise made accurate estimations of the current peaks more difficult, or (b) at the lowest pressures used when the current pulses were greatly broadened by effects of diffusion.

Throughout this chapter reference is made to the diffusion errors considered by Lowke (1962) and summarised in section 2.2.2. Lowke found that, to a good approximation, the observed drift velocity W' is related to the true drift velocity W through the relation

$$W' = W\ [\ 1 + 3\ /\ (hW/\ D)\ ] \qquad (6.1)$$

in which h is the distance between the planes of the shutters and D is the diffusion coefficient. It has been found (Elford, 1966, McIntosh, 1966, Crompton, Elford and Jory, 1966) that the term 3/(hW/D) overestimates the effects of

diffusion and that a more accurate estimate of the drift velocity is obtained by applying only half of the correction implied by equation (6.1). In practice the difference between these two corrections is insignificant except at the highest values of E/p at room temperature where results could be obtained only with pressures of 5 and 2 torr. At the remaining values of E/p at 293°K and at all the values of E/p used at 77°K, results were obtained at sufficiently high gas number density that the difference between W' and W was less than 0.25% whichever correction was applied.

As in the lateral diffusion experiments, the data taken at 293°K were measured at predetermined values of E/p_{293} with units of V cm^{-1} $torr^{-1}$. Corrections to the values of W' corresponding to small departures ($< \frac{1}{2}\%$) of the actual value of E/p from the desired value were made numerically. A similar procedure was followed at 77°K, with the data being taken at pre-determined values of E/N. The low temperature data were treated in this way rather than graphed as in the case of the D/μ results because the experimental scatter was only $\pm$ 0.15% compared with the $\pm$ 1% for the D/μ results.

6.2 Lowke's Results for Hydrogen.

6.2.1 At 293°K. $0.004 \leq E/p_{293} \leq 18$ V cm^{-1} $torr^{-1}$.

Lowke's results (1963) were taken under similar experimental conditions and with the same techniques as the present results. He placed an error limit of $\pm$ 1% on his "Best Estimate" values. Taking into account the 0.37% difference between the torr and the 20°C mm of mercury used by Lowke in determining his values of E/p, Lowke's results were plotted on a graph with scales sufficiently large to allow both co-ordinates to be read with an error not exceeding 0.3%. The values of W were then read off at integral values of E/N. The results obtained in this way are listed in Table 3 of Appendix II.

6.2.2 At 77°K. $0.001 \leq E/p_{293} \leq 3.0$ V cm^{-1} $torr^{-1}$

Lowke's 77°K data were analysed in the same way as his room temperature results. The values so obtained are given in Table 4 of Appendix II. Lowke placed an error limit of $\pm$ 2% on his original data.

6.3 Results for Deuterium.

6.3.1 At $293^{o}K$. $0.006 \leq E/p \leq 5.0$ V cm^{-1} $torr^{-1}$.

The measured values of W' are listed in Table 6.1. The agreement of the values taken at the same E/p but different p is good, but it is made even better by correcting the results for the effects of diffusion using equation (6.1). The "Best Estimate" values of W were obtained by the application of equation (6.1) to the result taken at the highest pressure for each value of E/p since these results are less subject to diffusion errors and to errors from contact potential differences within the chamber. Although it was later found that a better estimate of W could be obtained by applying only half of the diffusion correction, the full correction term has been used with the data in Table 6.1. This was done because the discrepancies involved are less than 0.25% except at the highest values of E/p where they do not exceed 0.6% and because the data in Table 6.1 have been published previously (McIntosh, 1966) with the whole correction applied. Where results were taken over a sufficiently wide range of pressures, values of W identical to the "Best Estimate" figures could be obtained by plotting W' against p^{-1} and extrapolating to $p^{-1} = 0$. An error limit of $\pm$ 1% is placed on the "Best Estimate" figures for $0.006 \leq E/p \leq 1.2$ and of $\pm$ 2% for $1.2 < E/p \leq 5.0$.

It should be emphasized that the corrections made to the values of W' are very small: for each value of $E/p \leq 0.5$ the discrepancy between the "Best Estimate" and the result taken at the highest pressure is less than 0.25%; for $0.5 < E/p \leq 1.2$ the discrepancy remains less than 0.5%, while for $E/p > 1.2$ it ranges from 0.8% to 1.2%. The fact that the corrections made to the measured values of W' for $E/p > 1.2$ are greater than 0.5% is the only reason for the increased error limit placed on these data.

The values of W at integral values of E/N were found by the graphical method described earlier and are listed in Table 5 of Appendix II.

6.3.2 At $77^{o}K$. $7.970 \times 10^{-20} \leq E/N \leq 9.564 \times 10^{-17}$ V cm^{2}.

Several room temperature measurements were made in apparatus B before proceeding to the $77^{o}K$ experiments. The results obtained agreed with the data given in the previous section (obtained in apparatus A) to within $\pm$ 0.2%.

Table 6.1

Drift velocity of electrons in Deuterium at 293°K.

E/p	Values of W' x 10^{-5} (cm sec^{-1}) when p (torr) of :									Best Estimate
(V cm^{-1} $torr^{-1}$)	500	400	300	200	100	50	20	10	5	of W x 10^{-5} (cm sec^{-1})
.006	.281(9)	.282(1)								.281(2)
.007	.328	.328								.327
.008	.373	.373								.372
.009	.418	.418								.417
.010	.463	.463	.464							.462
.012	.551	.552	.552							.550
.015	.679	.679	.680	.683						.678
.018	.802	.803	.804	.807						.802
.020	.882	.884	.884	.887						.882
.025	1.076	1.076	1.077	1.079						1.075
.03	1.258	1.258		1.260	1.266					1.257
.04	1.593	1.594	1.596	1.601	1.604					1.592
.05	1.896	1.897	1.898	1.904	1.907					1.895
.06	2.17(0)	2.17(0)	2.17(1)	2.17(8)	2.18(1)	2.18(4)				2.16(9)
.07	2.41(7)	2.41(8)	2.42(1)	2.42(6)	2.42(8)	2.43(2)				2.41(6)
.08		2.64(6)	2.64(7)	2.65(4)	2.65(6)	2.65(9)				2.64(5)
.09		2.85(3)	2.85(5)	2.86(0)	2.86(6)	2.86(8)				2.85(2)
.10			3.05	3.05	3.06	3.06				3.05
.12			3.38	3.39	3.40	3.40				3.38
.15				3.82	3.82	3.83	3.83			3.81
.18				4.17	4.17	4.18	4.19			4.17
.20					4.38	4.38	4.39			4.37
.25					4.82	4.82	4.83			4.81
.3					5.19	5.19	5.20	5.24		5.18
.4						5.84	5.85	5.86		5.82
.5						6.42	6.43	6.45		6.41
.6							6.99	7.00	7.04	6.95
.7							7.51	7.54	7.56	7.48
.8							8.02	8.03	8.07	7.98
.9							8.50	8.53	8.55	8.46

	500	400	300	200	100	50	20	10	5	Best Estimate
1.0							8.96	8.98	9.01	8.93
1.2							9.84	9.86	9.88	9.80
1.5								11.06	11.10	10.98
1.8								12.18	12.20	12.10
2.0								12.85	12.91	12.77
2.5								14.47	14.50	14.38
3									16.01	15.86
4									18.73	18.59
5									21.2(9)	21.1(3)

When apparatus B was cooled to liquid nitrogen temperature the thermocouple attached to the electrode just below the top shutter agreed with the bath temperature to $0.1^{o}K$. At all pressures in excess of 50 torr no temperature rise was recorded by the thermocouple. At pressures of 50 torr and below a temperature rise of as much as $1^{o}K$ was observed. In the data which follows it was assumed that the lower half of the apparatus was always maintained at the bath temperature; the gas temperature used to calculate the values of E/N was taken to be the average of the bath temperature and the temperature recorded by the top thermocouple.

Since W is dependent on the gas temperature as well as E/N the temperature to which the data refer must be selected carefully from the range of temperatures observed. The temperature chosen was $77.0^{o}K$ since this was the mean temperature of all the results taken at $p \geq 100$ torr. Over this pressure range deviations from $77.0^{o}K$ were less than $0.15^{o}K$. Although deviations of as much as $1^{o}K$ were observed at 20, 10 and 5 torr, the values of E/N used at these pressures were sufficiently high for W to be substantially independent of the gas temperature. Provided the correct temperatures are used to calculate the values of E/N no significant errors are incurred by these departures from the standard temperature.

Three experimental runs were made in deuterium. Deviations of the actual values of E/N from the chosen values were always less than 1%, most being less than 0.5%. The observed values of W' were corrected numerically to those corresponding to the chosen values of E/N.

Results obtained at $E = 3$ V cm^{-1} showed variations of as much as $\pm$ 0.75% but the experimental scatter at high values of E was only $\pm$ 0.15%. It was concluded that the scatter at low field strengths was due to variations in contact potential differences within the apparatus. Only results taken with field strengths of 5 V cm^{-1} were included in the final table of results. The measured values of W' are shown in Table 6.2. Each entry is the average of at least two results differing by no more than 0.3%, a large proportion of the differences between the sets of results being only 0.1% or 0.2%.

Table 6.2

Drift velocity of electrons in Deuterium at 77°K.

E/N ($V\ cm^2$)	Values of W'($cm\ sec^{-1}$) when p (torr) of :									Best Estimate of W ($cm\ sec^{-1}$)
	500	400	300	200	100	50	20	10	5	
7.970×10^{-20}	$2.69(7)\times10^{4}$									
9.564	3.19									
1.195×10^{-19}	3.90	3.91×10^{4}								
1.435	4.58	4.59	4.61×10^{4}							
1.594	5.01	5.02	5.04							
1.992	6.07	6.07	6.09	6.14×10^{4}						
2.391	7.07	7.08	7.10	7.16						
3.188	8.95	8.97	9.00	9.06						
3.985	1.072×10^{5}	1.072×10^{5}	1.077×10^{5}	1.083×10^{5}	1.090×10^{5}					
4.782	1.237	1.239	1.243	1.250	1.257					
5.579	1.393	1.395	1.400	1.407	1.414					
6.376	1.540	1.543	1.548	1.555	1.563					
7.173	1.681	1.682	1.687	1.697	1.704					
7.970	1.814	1.816	1.820	1.831	1.838	1.846×10^{5}				
9.564	2.06(1)	2.06(2)	2.06(7)	2.07(6)	2.08(5)	2.09(4)				
1.195×10^{-18}		2.39(1)	2.39(6)	2.40(6)	2.41(5)	2.42(4)				
1.435			2.69(5)	2.69(5)	2.70(4)	2.71(4)				
1.594			2.86(0)	2.86(5)	2.87(6)	2.88(7)				

E/N	500	400	300	200	100	50	20	10	5	Best Estimate
1.992				3.25	3.25	3.26	3.29×10^{5}			
2.391				3.56	3.57	3.58	3.59			
3.188					4.06	4.07	4.08			
3.985					4.43	4.44	4.45	4.46×10^{5}		
4.782					4.72	4.73	4.74	4.74		4.72×10^{5}
5.579						4.96	4.97	4.98		4.96
6.376						5.16	5.17	5.19		5.16
7.173						5.34	5.35	5.36		5.34
7.970						5.50	5.51	5.52		6.50
9.564						5.79	5.79	5.81		5.78
1.195×10^{-17}							6.20	6.21		6.19
1.435							6.59	6.61		6.58
1.594							6.85	6.87	6.88×10^{5}	6.84
1.992							7.51	7.52	7.54	7.50
2.391							8.15	8.16	8.19	8.14
3.188								9.36	9.39	9.34
3.985								1.044×10^{6}	1.047×10^{6}	1.042×10^{6}
4.782								1.146	1.148	1.144
5.579									1.244	1.240
6.376									1.331	1.326
7.173									1.416	1.411
7.970									1.497	1.492
9.564									1.651	1.646

At high values of E/N and low pressures the term 3/(hW/D) of equation (6.1) overestimates the effects of diffusion whereas one half of this correction yields values of W which are independent of pressure to within 0.2%. The "Best Estimate" values of W in Table 6.2 were obtained by applying one half of the diffusion correction to the value of W' observed at the highest pressure at each value of E/N. The corrections made were less than 0.2% for $3.985 \times 10^{-18} \leq E/N \leq 3.985 \times 10^{-17}$ and less than 0.35% at higher values of E/N. An error limit of $\pm$ 1.5% is placed on the "Best Estimate" values in Table 6.2.

Below $E/N = 3.985 \times 10^{-18}$ the values of W' increase more rapidly as the pressure is lowered than can be accounted for by the influence of diffusion; consequently no "Best Estimate" values of W are given. For example, the increase in W' at $E/N = 9.564 \times 10^{-19}$ ($\sim$ 1.5%) is more than 10 times greater than expected from the effects of diffusion. Similar behaviour, but on a larger scale, was observed by Lowke (1963) in his measurements in nitrogen at 77.6°K. However, Lowke did not observe any unexpected pressure dependence of his results in hydrogen at low temperature. To check that the pressure dependence in deuterium was genuine and not instrumental, results were taken in hydrogen at $E/N = 7.970 \times 10^{-19}$ and 9.564×10^{-19} over the same range of pressures as is deuterium. Once again W' was found to increase more rapidly with decreasing pressure than can be accounted for by diffusion. However at $E/N = 7.970 \times 10^{-19}$ the increase was only three times that predicted by equation (6.1) and since the discrepancy not accountable for by diffusion was only 0.5%, it is doubtful that Lowke using a smaller range of pressures and less accurate pressure gauges would have detected so small a difference.

Values of W at integral values of E/N were found graphically from the data of Table 6.2 and are listed in Table 6 of Appendix II.

6.3.3 Comparison with Other Data.

The only other results for the drift velocity of electrons in deuterium are those of Pack, Voshall and Phelps (1962) who used gas temperatures of 300°K and 77°K.

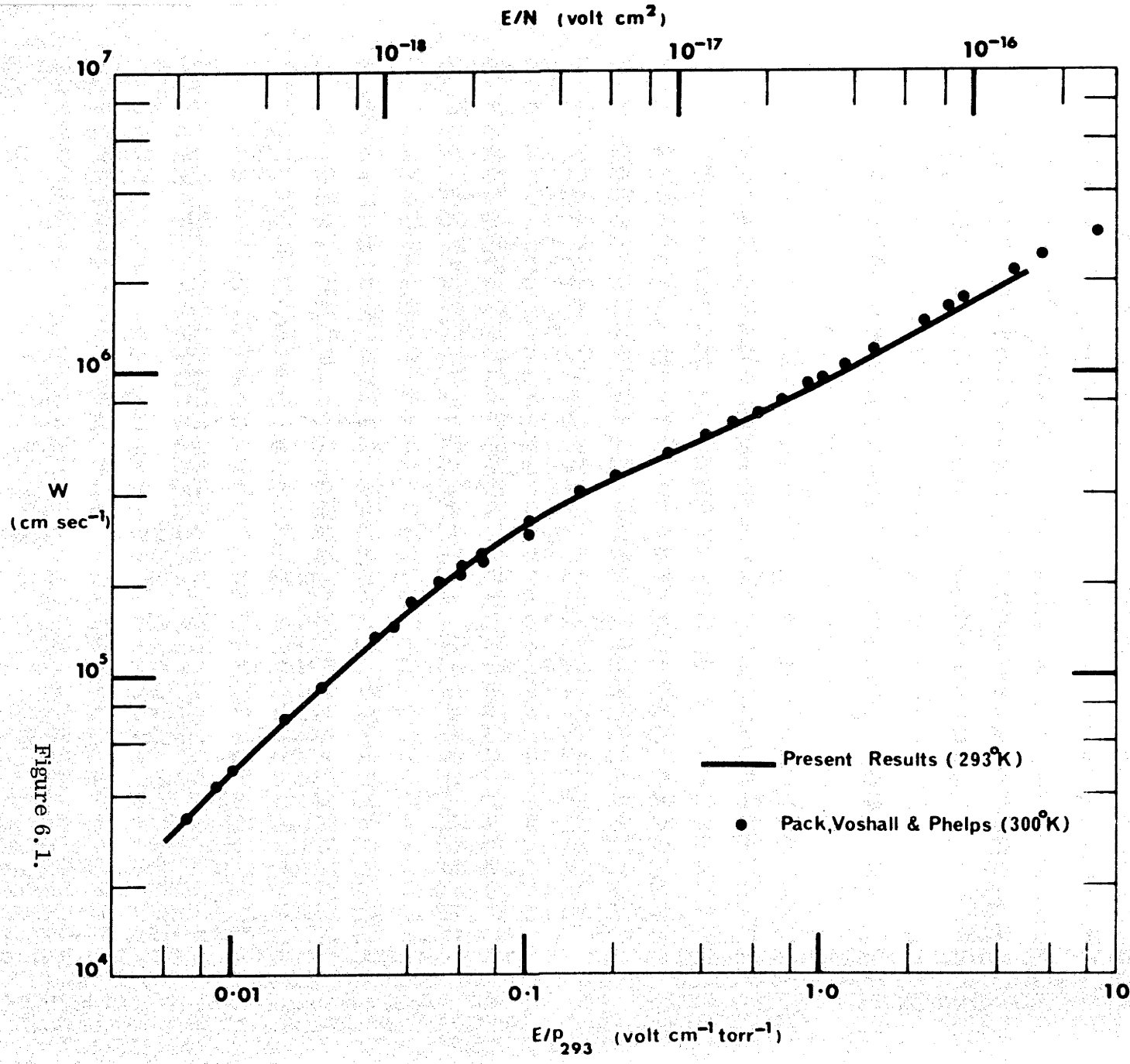
E/N (volt cm^2)
10^{-18}
10^{-17}
10^{-16}
10^7
10^6
10^5
10^4
W
(cm sec^{-1})
Present Results (293°K)
Pack, Voshall & Phelps (300°K)
0·01
0·1
1·0
10
E/p_{293} (volt cm^{-1} torr^{-1})

Figure 6.1.

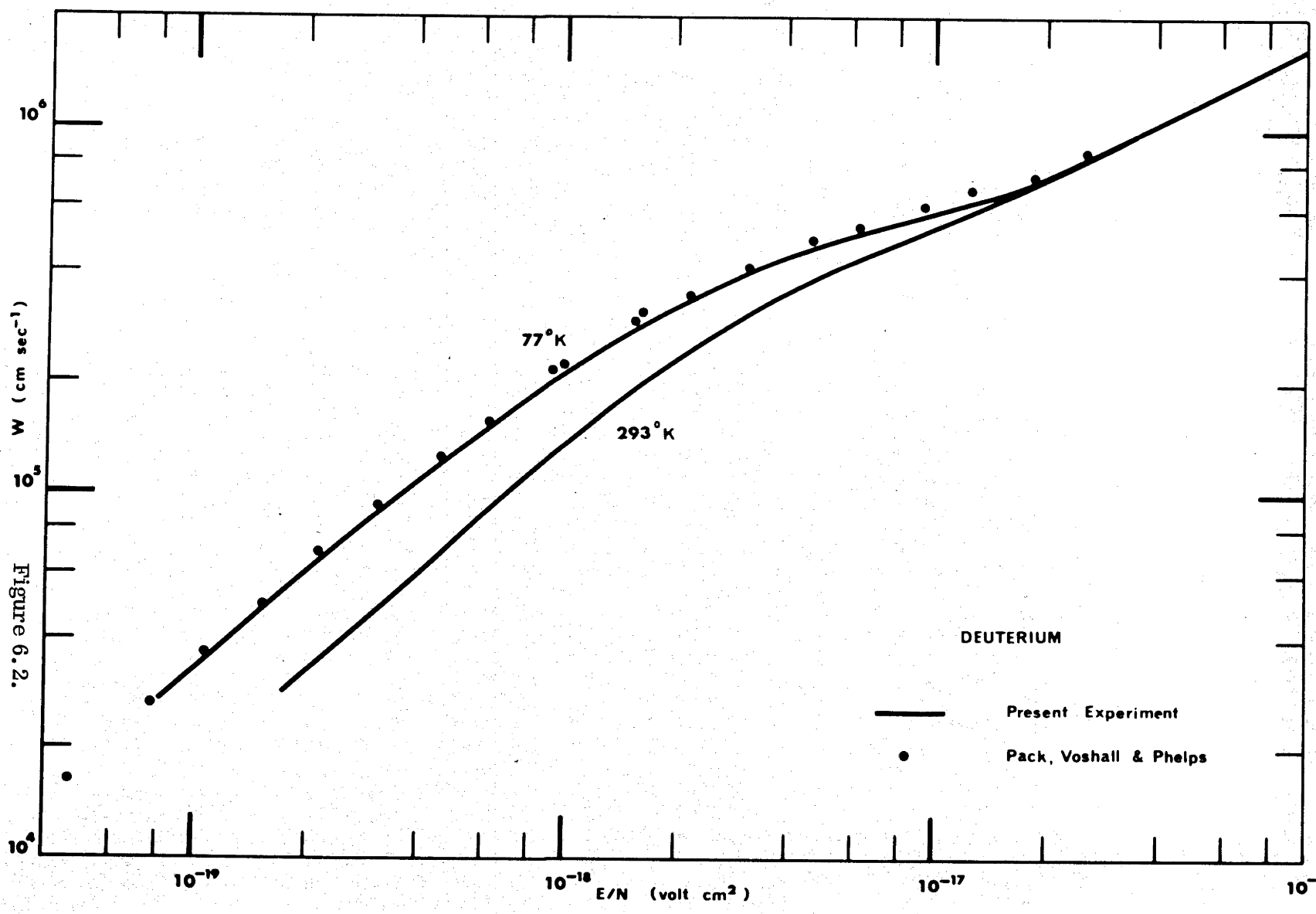
10^6
10^5
10^4
W (cm sec^{-1})
77°K
293°K
DEUTERIUM
Present Experiment
Pack, Voshall & Phelps
10^{-19}
10^{-18}
E/N (volt cm^2)
10^{-17}
10^{-16}

Figure 6.2.

Figure 6.1 shows the present 293°K results and the 300°K results of Pack, Voshall and Phelps plotted as a function of E/p_{293} or E/N. The present results are not plotted individually since all of the "Best Estimate" values are contained within the thickness of the line. The 7°K temperature difference between the present results and those of Pack, Voshall and Phelps has been taken into account only in converting their values of E/p_{300} to values of E/N since the direct influence on the values of W would be much less than the experimental error. The two sets of data are in good agreement at low values of E/N but appear to diverge by as much as 7% at higher values of E/N, the magnitude of the discrepancy being masked to some extent by the scatter in the data of Pack et al. The results for hydrogen of Pack and Phelps (1961) who used the same apparatus and experimental techniques as Pack, Voshall and Phelps, show a similar discrepancy when compared with the data of Lowke (1962) and Bradbury and Nielsen (1936).

Hall (1955) measured the magnetic drift velocity W_M. This is not the true drift velocity (Huxley, 1960, Jory, 1965) and therefore no reference to her data is made in Figure 6.1

A comparison of the present 77°K results with those of Pack, Voshall and Phelps for 77°K, and with the present results for 293°K is shown in Figure 6.2. The individual data points for the present 77°K data are not shown since they all lie within the thickness of the line plotted. On the log-log plot the observed pressure dependence below $E/N = 3.985 \times 10^{-18}$ cannot be seen. From $E/N = 4 \times 10^{-17}$ upwards the values of W are independent of temperature, this observation agreeing well with the temperature independence of the values of D/μ noted in section 4.3.3. The agreement between the 77°K results of the present experiment and those of Pack, Voshall and Phelps is fair; their values are approximately 7% above the present data over the whole range of E/N studied.

6.4 Results for para-Hydrogen.

6.4.1 At 77°K. $1.195 \times 10^{-19} \leq E/N \leq 9.564 \times 10^{-17}$ V cm^2.

Before taking measurements in para-hydrogen a series of results was taken in normal hydrogen to check that if any differences between the drift

velocities in the two gases were observed, the differences would be genuine and not instrumental. The agreement with Lowke's values was always better than 1%.

The para-hydrogen content of the gas samples used was greater than 98% (see Appendix I). Two experimental runs were taken, one covering the pressure range $10 \leq p \leq 250$ torr and the other the range $10 \leq p \leq 350$ torr. At the pressures common to the two runs the agreement between the two sets of data was always better than 0.3%, and this agreement suggests that the data taken at pressures of 300 and 350 torr can also be considered reliable.

The measured values of W' are shown in Table 6.3 for the range $1.195 \times 10^{-19} \leq E/N \leq 9.564 \times 10^{-17}$. The mean temperature of the results taken at pressures greater than 100 torr has been used as the gas temperature to which the measurements refer; as in the measurements in deuterium this temperature was $77.0^{o}K$. At higher values of E/N, W is substantially independent of temperature and no significant errors are incurred by the $0.5^{o}K$ departures from $77.0^{o}K$ observed at pressures of 50 torr and less. The departures from $77.0^{o}K$ at low pressures were less in para-hydrogen than they were in deuterium because of the use of the Americium source instead of the platinum filament.

The "Best Estimate" values of W in Tables 6.3 were found by applying one half of the correction of equation (6.1) to the result taken at the highest pressure at each value of E/N. An error limit of $\pm$ 1.5% is placed on the "Best Estimate" values in this Table. The maximum difference between the "Best Estimate" and the value of W' taken at the highest pressure was 0.15% at $E/N = 5.579 \times 10^{-17}$. Below $E/N = 3.985 \times 10^{-18}$ no "Best Estimate" values of W are given because, as in deuterium, the values of W' increase more rapidly as p is lowered than can be accounted for by the effects of diffusion. As expected, the discrepancy is less than it is in deuterium. The differences not accountable for by diffusion are about 0.5% for $E/N \sim 10^{-18}$ at which values it was possible to take the results over the widest range of pressures. These differences are very small but are considered significant when compared with the experimental scatter which was everywhere less than 0.15%.

Table 6.3

Drift velocity of electrons in para-hydrogen at 77.0°K

E/N	Values of W' (cm sec^{-1}) when p (torr) of :								Best Estimate of W (cm sec^{-1})
(V cm^2)	350	300	250	200	100	50	20	10	
1.195x10^{-19}	3.78x10^4								
1.435	4.40	4.41x10^4							
1.594	4.80	4.80	4.80x10^4						
1.992	5.73	5.73	5.73	5.72x10^4					
2.391	6.58	6.58	6.58	6.57					
3.188	8.14	8.14	8.14	8.13					
3.985	9.57	9.58	9.59	9.58	9.57x10^4				
4.782	1.094x10^5	1.094x10^5	1.096x10^5	1.095x10^5	1.095x10^5				
5.579	1.226	1.227	1.230	1.229	1.230				
6.376	1.356	1.357	1.359	1.360	1.362				
7.173	1.483	1.485	1.487	1.487	1.491				
7.970	1.606	1.608	1.611	1.612	1.615	1.614x10^5			
9.564	1.846	1.848	1.850	1.852	1.857	1.858			
1.195x10^{-18}	2.18(3)	2.18(8)	2.19(0)	2.19(2)	2.19(7)	2.20(1)			
1.435	2.49(8)	2.50(2)	2.50(6)	2.50(8)	2.51(5)	2.52(1)			
1.594	2.69(6)	2.70(1)	2.70(5)	2.70(7)	2.71(4)	2.71(8)			
1.992	3.15	3.16	3.16	3.16	3.17	3.18	3.17x10^5		
2.391	3.56	3.57	3.57	3.57	3.58	3.59	3.58		
3.188		4.26	4.27	4.27	4.28	4.29	4.28		
3.985			4.84	4.85	4.85	4.86	4.86		4.84x10^5

E/N	350	300	250	200	100	50	20	10	Best Estimate
4.782				5.33	5.33	5.33	5.33		5.33
5.579					5.73	5.73	5.73		5.73
6.376					6.07	6.08	6.07		6.07
7.173					6.37	6.38	6.37		6.37
7.970					6.64	6.65	6.64		6.64
9.564					7.09	7.10	7.09		7.09
1.195×10^{-17}						7.64	7.64		7.64
1.435						8.09	8.09		8.09
1.594						8.36	8.36		8.36
1.992						8.96	8.97		8.96
2.391							9.53	9.54	9.52
3.188							1.064×10^{6}	1.066×10^{6}	1.063×10^{6}
3.985							1.174	1.178	1.173
4.782							1.282	1.286	1.281
5.579								1.389	1.387
6.376								1.487	1.485
7.173								1.582	1.580
7.970								1.675	1.673
9.564								1.850	1.848

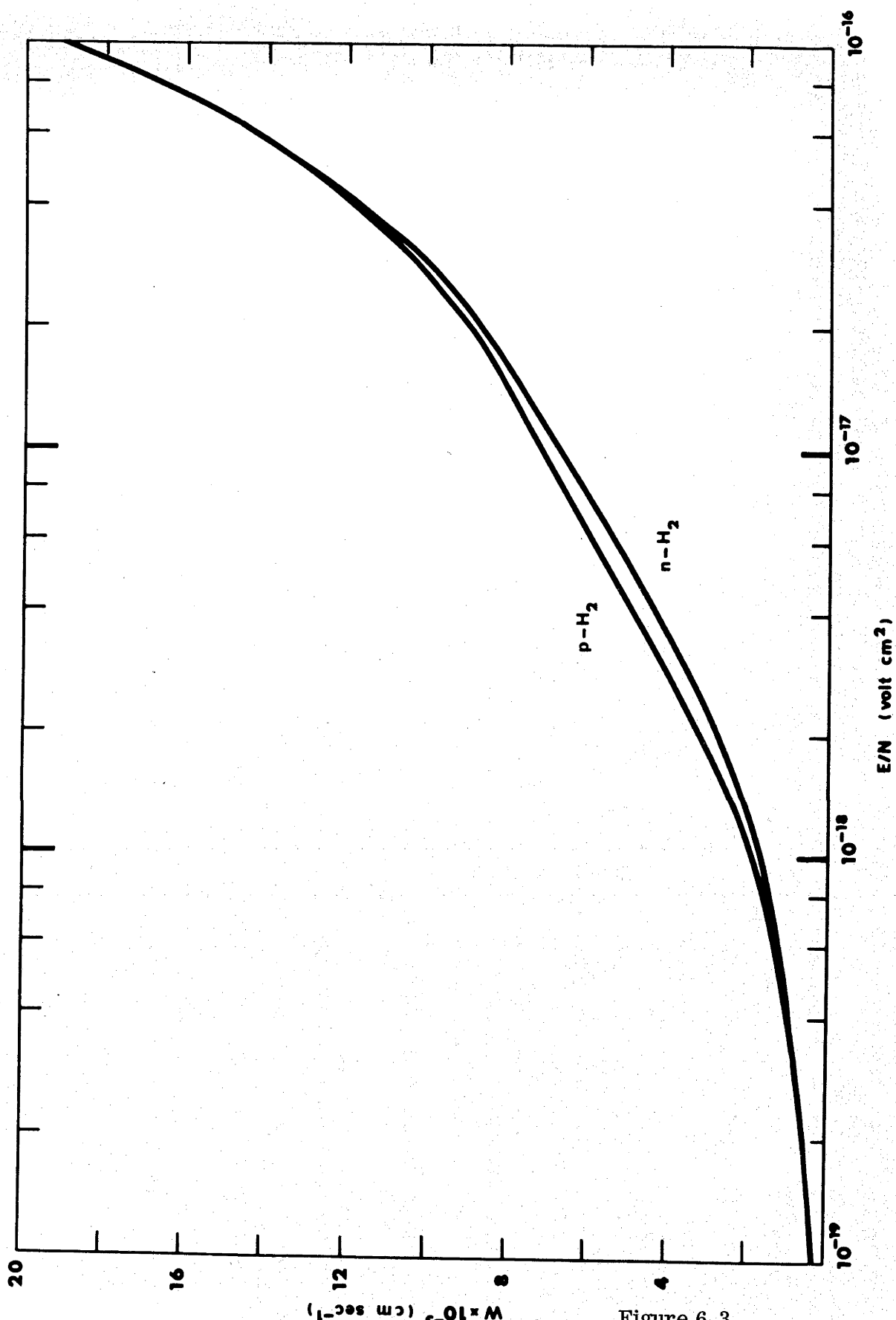
10^{-16}
10^{-17}
10^{-18}
10^{-19}
E/N (volt cm^2)
$n-H_2$
$p-H_2$
20
16
12
8
4
W x10^{-5} (cm sec^{-1})

Figure 6.3.

6.4.2 Comparison with Other Data.

There have been no previous measurements of electron drift velocities in para-hydrogen. A comparison of drift velocities of electrons in normal and para-hydrogen is shown in Figure 6.3 and discussed in the following section.

6.5 General Discussion of Results at 77^{o}K.

In addition to the comparison made in Figure 6.3, a comparison between the drift velocities in normal hydrogen and deuterium is shown in Figure 6.4. It should be noted that in Figure 6.3 the drift velocities are plotted on a linear scale to show more clearly the small differences between the two sets of data.

Taken with Figures 4.5 and 4.6, the drift velocity results provide confirmation of the self-consistency of all the sets of data. Thus, considering the comparisons between normal hydrogen and deuterium it is seen (a) that significant differences between the two sets of results appear at about $E/N = 10^{-19}$ in both W and D/μ, (b) that the cross-over point between the curves for hydrogen and deuterium occurs at exactly the same E/N in both the W and D/μ data, and (c) that the differences between the two W curves are very nearly half the differences between the D/μ curves at each value of E/N. This last result is expected from equations (2.30) and (2.32) which, for a constant momentum transfer cross section, show that D/μ is proportional to $\overline{c^2}$ (where c is the electron speed) and W is proportional to $[\ \bar{c}\ ]^{-1}$. Similar remarks apply to Figures 4.5 and 6.3 which show the differences between normal and para-hydrogen. Thus the differences are approximately twice as great for D/μ as they are for W, they first become significant at $E/N \sim 6 \times 10^{-19}$ and they disappear completely at $E/N \sim 3 \times 10^{-17}$.

A discussion of the shape of the curves 6.3 and 6.4 can be given in terms of the various collision processes occurring as was done in section 4.5.

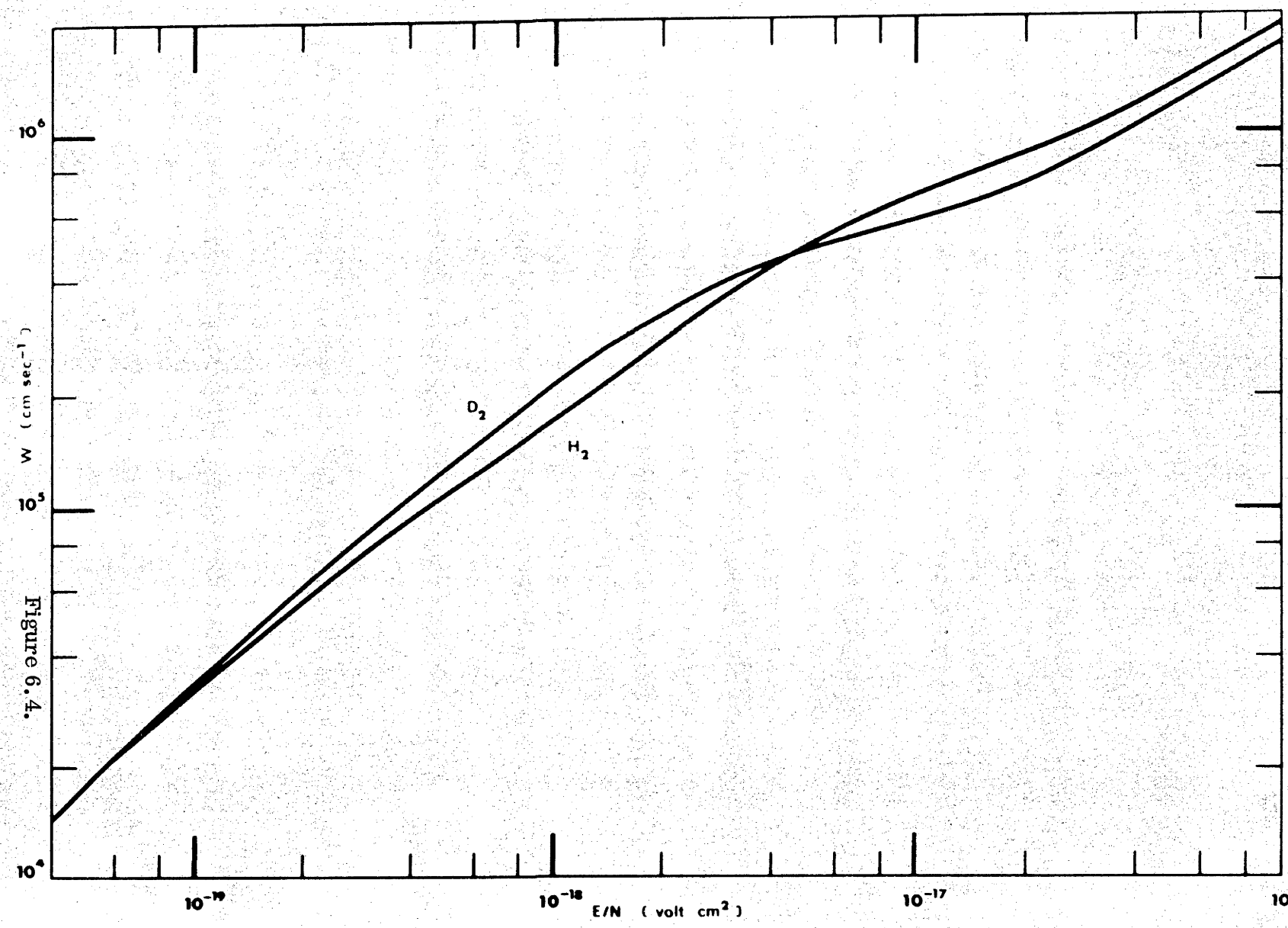

Figure 6.4.

CHAPTER 7.

DETERMINATION OF CROSS SECTIONS: THEORY.

A detailed derivation and analysis of the Boltzmann equation is beyond the scope of this thesis. The particular concern of this chapter is the solution of the form of the Boltzmann equation appropriate to electrons drifting and diffusing through a neutral background gas under the influence of (a) a d.c. electric field, (b) and a.c. electric field, or (c) mutually perpendicular d.c. electric and magnetic fields. The effects of elastic and inelastic collisions are included. The fields considered are "weak" and collisions of the second kind are excluded from the present analysis although an indication of how they could be included is given.

Before discussing the details of the particular solution employed a general form of the Boltzmann equation is presented. It is then written in a form appropriate to the present problem and transformed to a form amenable to solution by numerical computation.

The method of solution and the basic computer program used are based almost entirely on the papers of Dr. A.V. Phelps and Dr. A.G. Engelhardt of the Westinghouse Research Laboratories. Appropriate references are given in the text below. Private communications from these authors to Dr. R.W. Crompton have also been of great assistance.

7.1 The Boltzmann Equation.

The rigorous kinetic theory of gases is based on the knowledge of the distribution function $f_i(\underline{r}, \underline{c}, t)$ for each of the species of particles present. Here $\underline{r}$ is the radial distance from the origin, $\underline{c}$ is the velocity and f is defined as in chapter 2. The Boltzmann equation describes the effect of applied forces and collisions on the distribution function.

Consider a single species of particles of number density n and let f be position and time dependent. The definition of f requires that at any time t the number of particles within the volume element dx dy dz and

with velocity components between c_x and $c_x + d c_x$, c_y and $c_y + d c_y$, and c_z and $c_z + d c_z$, should be

$$n f (c_x , c_y , c_z , x , y , z , t) \; d c_x \; d c_y \; d c_z \; dx \; dy \; dz. \qquad (7.1)$$

If the law of distribution of f is known at time t it is possible to follow the motion of each group of particles and so to obtain f at the time t + dt, and similarly at any subsequent time. Thus f is determined for all time when its value is given at any one instant. It follows that n f must satisfy a characteristic equation of such a form that d/dt (n f) is given as depending on n f. Furthermore, for a steady state, n f must satisfy an equation which is derived from the previous equation by putting d/dt (n f) = 0.

Suppose the particles move in a field of force so that the components of the force per unit mass acting on the particles are F_x, F_y and F_z. If no collisions occur then at the end of the time interval dt the co-ordinates of each particle will have increased by c_x dt, c_y dt and c_z dt, while its velocity components will have increased by F_x dt, F_y dt and F_z dt. Thus after an interval d t, the original particles will have velocities within a small range $d c_x \; d c_y \; d c_z$ surrounding the values $c_x + F_x dt$, $c_y + F_y dt$, $c_z + F_z dt$ and co-ordinates lying within a small element dx dy dz surrounding the point $x + c_x dt$, $y + c_y dt$, $z + c_z dt$. In the absence of collisions these, and only these, particles were formerly in the volume element dx dy dz about the point x, y, z and had velocity components c_x, c_y, c_z. Hence, expressing this mathematically,

$$n f (c_x , c_y , c_z , x , y , z , t) \; d c_x \; d c_y \; d c_z \; dx \, dy \, dz$$

$$= n f (c_x + F_x dt, \ldots , x + c_x dt, \ldots , t + dt) \; d c_x \; d c_y \; d c_z \; dx \, dy \, dz \qquad (7.2)$$

i. e.

$$n f = n f (c_x + F_x dt, \ldots , x + c_x dt, \ldots t + dt)$$

$$\doteqdot n f + \left\{ F_x \frac{\partial}{\partial c_x} + F_y \frac{\partial}{\partial c_y} + F_z \frac{\partial}{\partial c_z} + c_x \frac{\partial}{\partial x} + c_y \frac{\partial}{\partial y} + c_z \frac{\partial}{\partial z} \right\} (nf) \, dt$$

from which it follows that

$$\frac{\partial}{\partial t}(nf) = -\left\{ F_x \frac{\partial}{\partial c_x} + \ldots + c_z \frac{\partial}{\partial z} \right\} (nf) \qquad (7.3)$$

A similar equation can be written for each particle type i in the gas.

Changes in n f are also brought about by collisions between the particles of type i with themselves and with particles of type j. The effect of these collisions is to change the velocity of the particles and so remove them from the element of velocity space under consideration. The "collision term" which accounts for this term is, in general, complex. It is, in effect, the sum of N integrals where N is the number of different species in the gas and each integral gives the rate of change of f for species i caused by collisions with particles of species j. If the collision term is represented as $[\partial (nf)/\partial t]_{coll}$, then the equation which n f must satisfy is

$$\frac{\partial (nf)}{\partial t} = -\left\{ F_x \frac{\partial}{\partial c_x} + \ldots + c_z \frac{\partial}{\partial z} \right\} (nf) + \left[\frac{\partial}{\partial t} (nf) \right]_{coll} \qquad (7.4)$$

Equation (7.4) is known as the Boltzmann equation.

7.2 Form of the Boltzmann Equation Appropriate to the Present Problem.

The energy distribution of electrons in a gas subject to an electric field has been treated by many authors, e.g. Holstein (1946), Margenau (1946) and Allis (1956). The particular form of the Boltzmann equation derived by Holstein (1946) is the form used in the present chapter, but once again a detailed derivation is beyond the scope of this thesis. Holstein's derivation requires the following conditions or assumptions:

(a) the electric field is uniform or is spatially uniform and of high frequency

(b) ionizing collisions are negligible compared to excitation collisions.

(c) the densities of electrons and excited molecules are low compared with the density of unexcited molecules.

(d) the elastic collision cross section is very large compared with the inelastic electron-molecule collision cross sections

(e) the mean free path for elastic collisions is small compared with the size of the discharge region.

Holstein also assumed that the molecular velocities were zero but the additional term to include the effect of the molecular velocity distribution has been derived by Margenau (1946) and by Allis (1956).

Following Frost and Phelps (1962), the results of Holstein are extended to include that of Margenau and to include the effects of inelastic collisions of the second kind thereby leading to the following form of the Boltzmann equation:

$$\frac{E^2}{3}\frac{d}{d\epsilon}\left(\frac{\epsilon}{N q_m}\frac{df}{d\epsilon}\right) + \frac{2m}{M}\frac{d}{d\epsilon}\left(\epsilon^2 N q_m f\right) + \frac{2mkT}{Me}\frac{d}{d\epsilon}\left(\epsilon^2 N q_m \frac{df}{d\epsilon}\right)$$

$$+ \sum_k \left[(\epsilon + \epsilon_k) f(\epsilon + \epsilon_k) N q_k(\epsilon + \epsilon_k) - \epsilon f(\epsilon) N q_k(\epsilon) \right]$$

$$+ \sum_k \left[(\epsilon - \epsilon_k) f(\epsilon - \epsilon_k) N q_{-k}(\epsilon - \epsilon_k) - \epsilon f(\epsilon) N q_{-k}(\epsilon) \right] = 0 \qquad (7.5)$$

This equation describes the motion of a swarm of electrons drifting through a gas at temperature T under the influence of a uniform electric field E ($V\,cm^{-1}$). N is the gas number density, $q_m(\epsilon)$ is the momentum transfer cross section for electron-molecule collisions as a function of the electron energy ϵ, and $q_k(\epsilon)$ is a rotational, vibrational or electronic excitation cross section with an excitation energy of ϵ_k. The other symbols are e, the electronic charge, m the electronic mass, M the molecular mass and k Boltzmann's constant. The electron energy ϵ is in eV so that $\epsilon = mc^2/2e$ where c is the electron speed.

The term $\frac{2mkT}{Me}\frac{d}{d\epsilon}\left(\epsilon^2 N q_m \frac{df}{d\epsilon}\right)$ is the one derived

by Margenau (1946) to account for the molecular velocities. The last term in equation (7.5) expresses the effect of collisions of the second kind in which thermally excited molecules impart their energy of excitation to the electrons. It is assumed in the derivation of equation (7.5) that the gas density is sufficiently high for terms due to electron density gradients to be neglected.

Each term in the equation has particular physical significance in relation to the gain or loss of energy due to one of the processes being considered. Thus the first term represents the effect of the energy input to the electrons from the field, the second the energy loss in elastic collisions, the third the energy gain in elastic collisions, the fourth the energy loss in inelastic collisions and the last the energy gain in inelastic collisions of the second kind.

Although equation (7.5) is written in terms of a d.c. electric field E, Allis (1956) has shown that for high frequency electric fields or mutually perpendicular d.c. electric and magnetic fields, the electric field E may be replaced by E_ϵ where

$$(E_\epsilon)^2 = \frac{q_m(\epsilon)^2 E^2}{q_m(\epsilon)^2 + \left(\frac{\Omega}{N}\right)\frac{m}{2\epsilon}} \qquad (7.6)$$

When the applied field is a high frequency electric field of radian frequency ω, $\Omega = \omega$. In the case of mutually perpendicular d.c. electric and magnetic fields, $\Omega = e B/m$ where B is the magnetic field strength.

Near thermal equilibrium the electron energy distribution function is Maxwellian. In this case the energy lost in elastic collisions is exactly balanced by the energy gained in elastic collisions. A similar situation exists for inelastic collisions and it is possible to write (Mitchell and Zemansky, 1934, Frost and Phelps, 1962)

$$(\epsilon - \epsilon_k)\, q_{-k}(\epsilon - \epsilon_k) = \exp(-\epsilon_k e/kT)\, \epsilon\, q_k(\epsilon_k) \text{ for } \epsilon \geq \epsilon_k \qquad (7.7)$$

thus showing that collisions of the second kind can be written in terms of inelastic

collisions of the first kind.

For computational purposes it is convenient to use normalized variables. Equation (7.5) is transformed using

$$z = \epsilon\, kT/e \qquad \theta(z) = q_m(\epsilon)/q_o \qquad \eta_{\pm k} = M\, q_{\pm k}(\epsilon)/(2\, m\, q_o)$$

$$\alpha = \frac{M}{6\, m}\left(\frac{E\, e}{N\, q_o\, kT}\right)^2$$

in which q_o is the value of q_m at some reference energy.

This gives

$$\frac{d}{dz}\left[\left(\frac{\alpha}{\theta} + z\,\theta\right) z \frac{df}{dz} + z^2\,\theta\, f\right]$$

$$+ \sum_k \left[(z + z_k)\, f(z + z_k)\, \eta_k(z + z_k) - z\, f(z)\, \eta_k(z)\right]$$

$$+ \sum_k \left[(z - z_k)\, f(z - z_k)\, \eta_{-k}(z - z_k) - z\, f(z)\, \eta_{-k}(z)\right] = 0 \qquad (7.8)$$

On integrating (7.8) with respect to z and making use of (7.7) and the Boltzmann relation for the relative population of excited states, the following equation is obtained (Frost and Phelps, 1962) :

$$\left(\frac{\alpha}{\theta} + z\,\theta\right) z \frac{df}{dz} + z^2\,\theta\, f$$

$$+ \sum_k \int_z^{z+z_k} z\, \eta_k(z)\left[f(z) - \exp(-z_k)\, f(z - z_k)\right] dz = c$$

Sherman (1960) has shown the integration constant c is zero, i.e.

$$\left(\frac{\alpha}{\theta} + z\,\theta\right) z \frac{df}{dz} + z^2 \theta f +$$

$$+ \sum_k \int_z^{z+z_k} z\, \eta_k(z) \left[f(z) - \exp(-z_k) f(z - z_k) \right] dz = 0 \qquad (7.9)$$

The approximation is now made that collisions of the second kind may be neglected. This is a good approximation in hydrogen and deuterium at $77^{\circ}K$ since the lowest rotational levels occur at energies well above the thermal energy and will therefore be only slightly populated. The currents used in the present experiments are so small that the population of excited levels due to electron-molecule collisions is completely negligible. When collisions of the second kind are neglected equation (7.9) becomes

$$\left(\frac{\alpha}{\theta} + z\,\theta\right) z \frac{df}{dz} + z^2 \theta f + \sum_k \int_z^{z+z_k} z\, \eta_k(z) f(z)\, dz = 0 \qquad (7.10)$$

Two further substitutions can be made

$$h(z) = \frac{z}{\theta(z)} \left(\alpha + z\,\theta^2(z) \right) \qquad (7.11)$$

$$g(z) = \frac{z\,\theta^2(z)}{\alpha + z\,\theta^2(z)} \qquad (7.12)$$

leading to

$$h(z) \left[\frac{df}{dz} + g(z) f(z) \right] + \sum_k \int_z^{z+z_k} z\, \eta_k(z) f(z)\, dz = 0 \qquad (7.13)$$

7.3 Solution of the Boltzmann Equation.

7.3.1 Conditions for Solution.

The conditions for the solution of equation (7.10) have been examined by Sherman (1960). He shows that a solution exists provided :

(a) $\lim_{z \to \infty} \inf \; z^{m} \; \theta(z) > 0$

(b) $f(z) \geq 0$

(c) $\int_0^\infty z^{\frac{1}{2}} f(z)\, dz = 1$

(d) $\int_0^\infty z\, f(z)\, dz < \infty$.

These mathematical conditions imply (Francey, 1966, private communication) that $\theta(z)$ and $\eta_k(z) \longrightarrow 0$ as $z \longrightarrow \infty$, that f(z) is always a positive quantity and that $f(z) \longrightarrow 0$ as $z \longrightarrow \infty$. Solutions exist if the asymptotic behaviour of $\theta(z)$ is well behaved as $z \longrightarrow \infty$ i.e. $\theta(z) \longrightarrow 0$ slowly for large z. The normalization of f(z) is $\int_0^\infty z^{\frac{1}{2}} f(z)\, dz = 1$.

7.3.2 Principle of the Method of Solution.

The method of solution developed by Sherman relies on the fact that at sufficiently high energies the distribution function is governed by the elastic collisions, i.e. f(z) takes the form of equation (2.18). Sherman writes:

$$f(z) = v(z)\, \gamma(z) \qquad (7.14)$$

where $\gamma(z)$ is the distribution function for eleastic scattering and where $v(z) = 1$ for $z \geq \delta$ and δ is sufficiently large. Starting with the known solution, $\gamma(z)$, at high energies, the solution f(z) is prolonged backwards to the origin by solving equations involving the inelastic terms to find the value of v(z) at each point.

The distribution function $f(\epsilon)$ for elastic scattering was given in section 2.3.1 as

$$f(\epsilon) = A \exp\left\{ -\int_0^{\epsilon} \left[\frac{M}{6m} \left(\frac{E}{N q_m} \right)^2 \frac{1}{\epsilon} + \frac{kT}{e} \right]^{-1} d\epsilon \right\} \qquad (7.15)$$

If equation (7.15) is written in a normalized form consistent with equation (7.8) and if, as in equation (7.14), $\gamma(z)$ is the normalized distribution function for elastic scattering, then

$$\gamma(z) = \exp\left[- \int_0^z \frac{y\,\theta^2(y)\,dy}{\alpha + y\,\theta^2(y)} \right] \qquad (7.16)$$

7.3.3 Solution Neglecting Collisions of the Second Kind.

Equation (7.16) can be differentiated to give

$$\frac{d\gamma(z)}{dz} = - \frac{z\,\theta^2(z)}{\alpha + z\,\theta^2(z)}\,\gamma(z) \qquad (7.17)$$

If the substitutions

$$h(z) = \frac{z}{\theta(z)}\,(\alpha + z\,\theta^2(z))$$

and

$$f(z) = v(z)\,\gamma(z)$$

are made in equation (7.10) it becomes

$$h(z)\,v(z)\,\frac{d\gamma(z)}{dz} + h(z)\,\gamma(z)\,\frac{dv(z)}{dz} + z^2\,\theta(z)\,v(z)\,\gamma(z)$$

$$+ \sum_k \int_z^{z+z_k} z\,\eta_k(z)\,v(z)\,\gamma(z)\,dz = 0 \qquad (7.18)$$

Dividing throughout by $h(z)\,\gamma(z)$, equation (7.18) becomes

$$\frac{dv(z)}{dz} + \frac{v(z)}{\gamma(z)}\,\frac{d\gamma(z)}{dz} + z^2\,\theta(z)\,\frac{v(z)}{h(z)}$$

$$+ \frac{1}{h(z)\,\gamma(z)} \sum_k \int_z^{z+z_k} z\,\eta_k(z)\,v(z)\,\gamma(z)\,dz = 0 \qquad (7.19)$$

For convenience equation (7.19) is split into two parts, one containing the first three terms and the other the summation. In the first three terms use is made of (7.17) to give

$$\frac{d\,v\,(z)}{d\,z} - \frac{v\,(z)}{\gamma\,(z)} \cdot \frac{z\,\theta^2\,(z)\,\gamma\,(z)}{\alpha + z\,\theta^2\,(z)} + \frac{z^2\,\theta\,(z)\,v\,(z)}{h\,(z)}$$

or

$$\frac{d\,v\,(z)}{d\,z} - \frac{v\,(z)\,z\,\theta^2\,(z)}{\alpha + z\,\theta^2\,(z)} + \frac{z^2\,\theta\,(z)\,v\,(z)\,\theta\,(z)}{z\,(\,\alpha + z\,\theta^2\,(z)\,)}$$

giving, finally,

$$\frac{d\,v\,(z)}{d\,z} \tag{7.20}$$

Taking now the summation term of equation (7.19),

$$\frac{1}{h\,(z)\,\gamma\,(z)} \sum_k \int_z^{z+z_k} z\,\eta_k\,(z)\,v\,(z)\,\gamma\,(z)\,d\,z$$

the substitution x = z is made to give

$$\frac{1}{h\,(z)\,\gamma\,(z)} \sum_k \int_z^{z+z_k} x\,\eta_k\,(x)\,v\,(x)\,\gamma\,(x)\,d\,x \tag{7.21}$$

Combining the results (7.20) and (7.21), equation (7.19) has become

$$\frac{d\,v\,(z)}{d\,z} + \frac{1}{h\,(z)\,\gamma\,(z)} \sum_k \int_z^{z+z_k} x\,\eta_k(x)\,v\,(x)\,\gamma\,(x)\,d\,x = 0 \tag{7.22}$$

Equation (7.22) must be solved by numerical methods. The mesh size for the computation is taken to be h_o, and the various values of z in the computation mesh are represented by z_i. The values of z_k are then given by $N_k\,h_o$ and the value of δ by $N\,h_o$.

If equation (7.22) is written in the form

$$\frac{d\,v(z)}{d\,z} + s\,(z) = 0 \tag{7.23}$$

then

$$\int_{z_{i-1}}^{z_{i+1}} \frac{d\,v\,(z)}{d\,z} = v\,(z_{i+1}) - v\,(z_{i-1})$$

$$= - \int_{z_{i-1}}^{z_{i+1}} s\,(z)\,d\,z \qquad (7.24)$$

Applying Simpson's three point integration rule to the right hand side of (7.24)

$$v\,(z_{i+1}) - v\,(z_{i-1}) = - \frac{h_o}{3} \left[s\,(z_{i+1}) + 4\,s\,(z_i) + s\,(z_{i-1}) \right] \qquad (7.25)$$

Re-arranging terms this becomes

$$v\,(z_{i-1}) = v\,(z_{i+1}) + \frac{h_o}{3} \left[s\,(z_{i+1}) + 4\,s\,(z_i) + s\,(z_{i-1}) \right] \qquad (7.26)$$

with

$$s\,(z_i) = \sum_k \int_{z_i}^{z_i+z_k} \frac{v\,(x)\,x\,\eta_k\,(x)\,\gamma\,(x)\,d\,x}{h\,(z_i)\,\gamma\,(z_i)} \qquad (7.27)$$

For convenience the function $\phi\,(x,\,z_i)$ is introduced, where

$$\phi\,(x,\,z_i) = \frac{x\,v\,(x)\,\eta_k\,(x)\,\gamma\,(x)}{h\,(z_i)\,\gamma\,(z_i)} \qquad (7.28)$$

Using this definition

$$s\,(z_i) = \sum_k \int_{z_i}^{z_i+z_k} \phi\,(x,\,z_i) \qquad (7.29)$$

$$= \sum_k \left\{ \int_{z_i}^{z_{i+1}} \phi\,(x,\,z_i)\,d\,x + \int_{z_{i+1}}^{z_{i+1}+z_k} \phi\,(x,\,z_i)\,d\,x - \int_{z_i+z_k}^{z_{i+1}+z_k} \phi\,(x,z_i)\,dx \right\}$$

(7.30)

From the definition of $\phi\,(x,\,z_i)$, equation (7.28),

$$\phi(x, z_{i+1}) = \frac{x\, v(x)\, \eta_k(x)\, \gamma(x)}{h(z_{i+1})\, \gamma(z_{i+1})}$$

$$= \frac{h(z_i)\, \gamma(z_i)}{h(z_{i+1})\, \gamma(z_{i+1})}\, \phi(x, z_i) \qquad (7.31)$$

This last result and equation (7.29) can be used to show that

$$\sum_k \int_{z_{i+1}}^{z_{i+1}+z_k} \phi(x, z_i) = \frac{h(z_{i+1})\, \gamma(z_{i+1})}{h(z_i)\, \gamma(z_i)} \sum_k \int_{z_{i+1}}^{z_{i+1}+z_k} \phi(x, z_{i+1})$$

$$= \frac{h(z_{i+1})\, \gamma(z_{i+1})}{h(z_i)\, \gamma(z_i)}\, s(z_{i+1}) \qquad (7.32)$$

Using equation (7.32), equation (7.30) can be re-written as

$$s(z_i) = \frac{h(z_{i+1})\, \gamma(z_{i+1})}{h(z_i)\, \gamma(z_i)}\, s(z_{i+1}) + \sum_k \int_{z_i}^{z_{i+1}} \phi(x, z_i)\, dx$$

$$- \sum_k \int_{z_i+z_k}^{z_{i+1}+z_k} \phi(x, z_i)\, dx \qquad (7.33)$$

The equations derived above allow the calculation of $v(z_i)$ by the method of backward prolongation. The values of $v(z_i)$ effectively give the values of the distribution function since $f(z_i) = v(z_i)\gamma(z_i)$ and the calculation of $\gamma(z_i)$ is straightforward. The high energy solution is $v(z_i) = 1$ for $z_i \geq \delta$ and this is prolonged backwards to lower energies, i.e. $v(z_{i-1})$ is calculated in terms of $v(z_i)$, $v(z_{i-2})$ in terms of $v(z_{i-1})$ and so on.

However, inspection of equations (7.26) and (7.27) shows that calculation of $v(z_{i-1})$ requires knowledge of $s(z_{i-1})$ but this, in turn, requires prior knowledge of $v(z_{i-1})$. A cyclic procedure is therefore used. Knowing $v(z_{i+1})$ and $v(z_i)$ a first approximation to $v(z_{i-1})$ can be found by linear

extrapolation:

$$v(z_{i-1}) = v(z_i) - (v(z_{i+1}) - v(z_i))$$

$$= 2v(z_i) - v(z_{i+1}) \qquad (7.34)$$

The approximation to $v(z_{i-1})$ found from equation (7.34) is used in equation (7.33) to find the corresponding value of $s(z_{i-1})$. The value of $s(z_{i-1})$ found in this way is substituted in equation (7.26) to find a second approximation to $v(z_{i-1})$ and so on. Cycling between equations (7.26) and (7.33) is continued until the difference between successive approximations to $v(z_{i-1})$ is a specified small value ($\sim$1 part in 10^6).

The cyclic procedure is then repeated for $v(z_{i-2})$ and so on until the values of v have been found at every mesh point in the computation.

7.4 Computation of Solution.

The steps involved in the complete calculation of the transport coefficients from a trial set of elastic and inelastic cross sections are as follows:

(a) Select a trial value of δ. Experience shows that at a particular value of E/N δ should be, in general, about 7-8 times the corresponding value of D/μ.

(b) Select the appropriate number of mesh points and the mesh size so that $\delta = N h_o$ and $z_k = N_k h_o$. The mesh size should be chosen to be considerably smaller than the first inelastic threshold so that no loss of accuracy through a coarse-grained mesh is incurred. At the same time the mesh size should be chosen so that each inelastic threshold occurs at an integral number of times the mesh size. In practice this is difficult to achieve and a compromise value must be selected. Experience shows that the thresholds calculated from $z_k = N_k h_o$ should be within 1% of the actual values of z_k for satisfactory results to be obtained.

(c) Use repeated application of Simpson's rule to calculate $\gamma(z_i)$ for $1 \leq i \leq N + N_k$ (max). In practice computational efficiency is improved

by rewriting the value of $\gamma\ (z_{i+1})$ in terms of $\gamma\ (z_i)$ as follows:

$$\gamma\ (z_i) = \exp\left[- \int_0^{z_i} \frac{y\ \theta^2\ (y)\ d\ y}{\alpha + y\ \theta^2\ (y)} \right]$$

$$\gamma\ (z_{i+1}) = \exp\left[- \int_0^{z_{i+1}} \right]$$

$$= \exp\left[- \int_0^{z_i} \right] \exp\left[- \int_{z_i}^{z_{i+1}} \right]$$

$$= \gamma\ (z_i) \exp\left[- \int_{z_i}^{z_{i+1}} \right] \qquad (7.35)$$

Experience shows that a 6 point integration of the integral on the right hand side of (7.35) is sufficient.

(d) Put $v(z_i) = 1$ for $i \geq N$. This corresponds to the step $v(z) = 1$ for $z \geq \delta$.

(e) Calculate the values of $v(z_i)$ for $1 \leq i < N$ using the cyclic procedure outlined in the previous section. The integrations on the right hand side of (7.33) are evaluated using the trapezoidal rule.

(f) Calculate the values of $f(z_i) = v(z_i)\ \gamma\ (z_i)$.

(g) Evaluate the transport integrals. Equations (2.27) and (2.28) become, when written in the normalized form of the computation (Frost and Phelps, 1962) :

$$D = \frac{2\ (kT/m)^{\frac{1}{2}}}{3\ N\ q_o} \int_0^{\infty} \frac{z}{\theta} f(z)\ d\ z \qquad (7.36)$$

$$\mu = \frac{e\ (2/kTm)^{\frac{1}{2}}}{3\ N\ q_o} \int_0^{\infty} f(z) \frac{d}{d\ z} \left(\frac{z}{\theta} \right) d\ z$$

$$= - \frac{e\ (2/kTm)^{\frac{1}{2}}}{3\ N\ q_o} \int_0^{\infty} \frac{z}{\theta} \frac{d\ f}{d\ z}\ d\ z \qquad (7.37)$$

(h) Adjust the value of δ until the resultant change in the transport integrals is satisfactorily small.

7.4.1 Computer Program.

The computer program used was based on one supplied by Dr. A.G. Engelhardt (Engelhardt, 1963). Changes in this program have been made to suit the requirements of the available computer.

7.5 Separation between Effects of Elastic and Inelastic Collisions.

Frost and Phelps (1962) introduced two combinations of transport coefficients which effectively separate the effects of momentum transfer and inelastic collisions.

The first of these is the effective frequency for momentum transfer on "elastic" collisions which is defined by

$$\nu_m / N = \frac{e}{m} \frac{E/N}{W} \qquad (7.38)$$

In the special case when the true frequency of momentum transfer collisions is constant, i.e. $N q_m(c) c$ is constant, equation (2.30) shows that the frequency of elastic collisions is given exactly by equation (7.38). In cases where $N q_m(c) c$ is not constant, ν_m/N nevertheless remains a good measure of the frequency of elastic collisions.

The combination of transport coefficients characteristic of inelastic collisions was deduced by Frost and Phelps by writing the power balance for an average electron. Thus the power input per electron due to the electric field, $e E W$, is equal to the frequency of inelastic collisions times the fractional energy exchanged per inelastic collision. If D/μ is taken as the measure of the electron energy (section 2.3.4) then

$$\nu_u / N = \frac{(E/N) W}{D/\mu - kT/e} \qquad (7.39)$$

Frost and Phelps called ν_u the "energy exchange collision frequency".

Frost and Phelps (1962) and Engelhardt and Phelps (1963) have confirmed the usefulness of the quantities ν_m/N and ν_u/N as defined above. When ν_m/N and ν_u/N were plotted as a function of D/μ, these workers found that a small change in the magnitude of q_m resulted in a proportional change in ν_m/N but a much smaller change in the ν_u/N v D/μ curve. Some effect on the values of ν_u/N is expected because of the contribution of elastic scattering to the energy loss of the electron. Similarly, small changes in the inelastic cross sections produced proportional changes in the values of ν_u/N but did not alter the ν_m/N v D/μ curve. Further confirmation was provided by the fact that calculations neglecting inelastic collisions yielded values of ν_m/N which were in excellent agreement with the original ν_m/N v D/μ curve.

In the present investigation the quantities ν_m/N and ν_u/N were used as aids in finding the required cross sections. However, the ultimate comparison between the calculated and experimental results was made in terms of the values of W and D/μ at each value of E/N.

CHAPTER 8.

DETERMINATION OF CROSS SECTIONS: RESULTS.

The techniques described in section 2.3.6 and in chapter 7 are now applied to the problem of deducing cross sections for momentum transfer and rotational and vibrational excitation in hydrogen and deuterium. In general the initial values of the cross sections for such an analysis are based on previous theory and experiment; in the present instance some of the values are taken to be the momentum transfer and vibrational excitation cross sections deduced in an earlier analysis by Engelhardt and Phelps (1963). It was pointed out in the Introduction that it does not seem possible to infer unique values for the inelastic cross sections directly from the experimental data. An assumed inelastic cross section can, however, be tested for consistency with the experimental data. The theory of Gerjuoy and Stein (1955) for rotational excitation of homonuclear diatomic molecules is widely accepted, particularly when the polarization correction of Dalgarno and Moffet (1962) is taken into account. The rotational cross sections examined in the present analysis are based on their theory. The same theory was incorporated in the analysis of Engelhardt and Phelps (1963) but the experimental data available were subject to both systematic and random errors to such an extent that no firm conclusions could be drawn from them.

8.1 Restrictions on the Range of Data Analysed.

Because collisions of the second kind are neglected in the present treatment, only the data obtained from the experiments performed at 77^{o}K can be analysed. At 293^{o}K the thermal energy is sufficiently large for there to be appreciable populations of excited rotational states even in hydrogen and deuterium and therefore collisions of the second kind must be taken into account. At 77^{o}K the populations of excited rotational states in these gases are very small and it is essential to take into account collisions of the second kind only when the electron energy is less than the threshold energy of the first inelastic transition (0.045 eV in hydrogen, 0.023 eV in deuterium). Above the first inelastic

threshold collisions of the second kind become less important because their cross sections, which are initially small, continue to fall steadily whereas the cross sections for inelastic collisions of the first kind rise rapidly to relatively high values. The error incurred by the neglect of collisions of the second kind is expected to be small for all energies above the first inelastic threshold and, in the present investigation, to be entirely negligible for values of D/μ greater than 0.08 volt.

The maximum value of D/μ obtained in the $77^{o}K$ measurements in hydrogen and deuterium was about 0.5 volt which corresponds to a mean electron energy of about 0.75eV. As a result there are effectively no electrons with energies above 3 eV (approximately) and no information about cross sections at energies higher than this can be found from the present data. The approximate energy range over which the cross sections can be deduced accurately from an analysis of data in hydrogen and deuterium subject to the present restrictions is, therefore, $0.08 \leq D/\mu \leq 3$ volts.

8.2 Input Cross Sections.

8.2.1 Momentum Transfer Cross Section.

The same momentum transfer cross section was used in hydrogen and deuterium. It is expected (Gerjuoy and Stein, 1955) that this cross section will be the same in both gases. This expectation is confirmed by the results of both Englehardt and Phelps (1963) and the present investigation.

The initial momentum transfer cross section used was identical to that of Engelhardt and Phelps. It was subsequently altered as described below to obtain a better fit to the experimental data.

8.2.2 Vibrational Excitation Cross Section.

The threshold for vibrational excitation occurs at 0.516 eV in hydrogen and 0.360 eV in deuterium (Herzberg, 1950). The initial and final values of the vibrational cross section used were identical to those of Engelhardt and Phelps.

8.2.3 Rotational Excitation Cross Section.

The cross sections used for rotational excitation in hydrogen and deuterium were based on the theory of Gerjuoy and Stein (1955), as modified by Dalgarno and Moffet (1962).

Gerjuoy and Stein examined the problem of rotational excitation by considering it to be the result of pure electric quadrupole interaction. Their calculations were based on the Born approximation despite the fact that the electrons are of very low energy. They argued that the principal contribution to the cross section arises when the impact parameter is large and therefore where the wave function is only slightly distorted from its incident form. This argument leads to the inference that the Born approximation probably improves with decreasing incident electron energy.

Gerjuoy and Stein found that the cross sections in which the rotational quantum number J changes by $\pm$ 2 were given by

$$\sigma_{J,\,J+2}(\epsilon) = \frac{(J+2)(J+1)}{(2J+3)(2J+1)} \frac{8\pi Q^2 a_o^2}{15} \left[1 - \frac{(4J+6) B_o}{\epsilon}\right]^{\frac{1}{2}} \tag{8.1}$$

$$\sigma_{J,\,J-2}(\epsilon) = \frac{J(J-1)}{(2J-1)(2J+1)} \frac{8\pi Q^2 a_o^2}{15} \left[1 + \frac{(4J-2) B_o}{\epsilon}\right]^{\frac{1}{2}} \tag{8.2}$$

Here ϵ is the electron energy in eV, Q is the electric quadrupole moment in units of $e a_o^2$, a_o is the Bohr radius, and B_o is the rotational constant of the molecule.

In the collision for which the cross section is $\sigma_{J,\,J+2}$, the energy lost by the electron is

$$\epsilon_J = (4J+6) B_o \tag{8.3}$$

The cross section rises rapidly near threshold and for large energies asymptotically approaches a constant value.

Equation (8.2) gives the cross section for the collision of the second kind in which the electron gains an energy of

$$\epsilon_{-J} = (4J - 2) B_o \qquad (8.4)$$

To obtain the effective cross section $q_{J, J+2}(\epsilon)$ for rotational excitation of molecules from the Jth to the (J+2)th level, the cross sections of Gerjuoy and Stein must be multiplied by the fraction of molecules in the Jth rotational level:

$$q_{J, J+2}(\epsilon) = \frac{p_J}{p_r} \exp(-E_J/kT)\, \sigma_{J, J+2} \qquad (8.5)$$

Here p_J is calculated as in Appendix I and differs for hydrogen and deuterium because of the difference in the nuclear spin,

$$p_r = \sum_J p_J \exp(-E_J/kT) \qquad (8.6)$$

and

$$E_J = J(J+1) B_o \qquad (8.7)$$

The value of B_o is 0.00754 eV for hydrogen and 0.00377 for deuterium (Herzberg, 1950).

In Appendix I the fractional populations for the rotational levels of hydrogen, para-hydrogen and deuterium at 77°K are calculated. The results are summarised in Table 8.1.

Table 8.1

Fractional populations of rotational levels at 77°K.

J =	0	1	2	3
Hydrogen	24.87%	75.00%	0.13%	-
para-Hydrogen	99.46%	0.0 %	0.54%	-
Deuterium	57.21%	33.07%	9.45%	0.26%

Dalgarno and Moffett (1962) pointed out that although Gerjuoy and Stein's calculations showed that coupling to other rotational levels of the molecule was unimportant, the coupling to excited electronic levels should have been taken into account. This coupling is due to the polarization interaction resulting from the reaction of the bound electrons to the field of the much slower free electron. If the polarization is taken into account the cross sections of Gerjuoy and Stein should be multiplied by the factor $f_R(\epsilon)$ where

$$f_R(\epsilon) = 1 + \frac{p_\alpha (4\epsilon - \epsilon_J)}{\epsilon^{\frac{1}{2}}} + \frac{9}{4} p_\alpha^2 (2\epsilon - \epsilon_J) \qquad (8.8)$$

with

$$p_\alpha = \frac{\pi (\alpha_{||} - \alpha_\perp)}{24 Q R^{\frac{1}{2}}}$$

In equations (8.8) and (8.9), $\alpha_{||}$ and $\alpha_\perp$ are the parallel and perpendicular polarization constants of the molecule and R is the Rydberg constant.

The effect of the polarization correction is to allow the rotational cross sections to rise steadily with increasing energy rather than to approach the asymptotic value given by equation (8.1). The effective rotational cross section for the J = 0 to J = 2 transition in hydrogen is increased by about 10% near threshold and by about 45% near the onset of vibrational excitation at 0.52 eV.

Only one form of rotational cross section has been examined in the present analysis. This cross section was calculated from equations (8.5) and (8.8) using the fractional populations of Table 8.1. The most recent and reliable values of Q , $\alpha_{||}$ and $\alpha_\perp$ have been used. These values are :

$$Q = 0.49 , \qquad \alpha_{||} = 6.88 , \qquad \alpha_\perp = 4.81$$

(Sampson and Mjolness, 1965, based on the data of Kolos and Wolniewicz, 1964, and Bridge and Buckingham, 1964). The same quadrupole moments and polarization constants have been used in hydrogen and deuterium.

8.3 Results and Discussion.

Inserting the inelastic cross sections described in the previous section and the momentum transfer cross section of Engelhardt and Phelps, the calculated values of ν_m/N and ν_u/N for hydrogen were compared with those found from the experimental values of W and D/μ . The inelastic cross sections were not altered in subsequent iterations because (a) in the case of rotational excitation the aim was to provide an unambiguous test of the theory described above, and (b) in the case of vibrational excitation the results showed that the curves of Engelhardt and Phelps were not significantly in error. The momentum transfer cross section was, however, adjusted in successive iterations to obtain the best possible fit to the values of ν_m/N. The final values of the cross sections in hydrogen are shown in Figure 8.1, while a comparison between the experimental and calculated values of W and D/μ is shown in Figure 8.2.

The same momentum transfer and vibrational excitation cross sections and the same theory for rotational cross sections but with the appropriate fractional populations from Table 8.1 were then used to predict the values of W and D/μ in para-hydrogen. The resulting comparison with the experimental data is shown in Figure 8.3.

Finally, the same momentum transfer cross section and theory of rotational excitation have been used with the vibrational excitation cross section of Engelhardt and Phelps to calculate the values of W and D/μ in deuterium. Figure 8.4 shows the comparison between calculated and experimental values in this gas. The cross sections used in deuterium are plotted in Figure 8.5.

It should be pointed out that the anomalies to be described in subsequent paragraphs make any discussion of Figures 8.2, 8.3 and 8.4 complicated. However these anomalies are expected to disappear when a later analysis provides a more realistic form of the rotational cross sections.

Figure 8.2 shows a comparison of the calculated and experimental values of W and D/μ in hydrogen at $77^{o}K$. The agreement between the calculated and experimental values of W is excellent, the discrepancies being less than 3% everywhere. This agreement is, of course, expected because of the way q_m

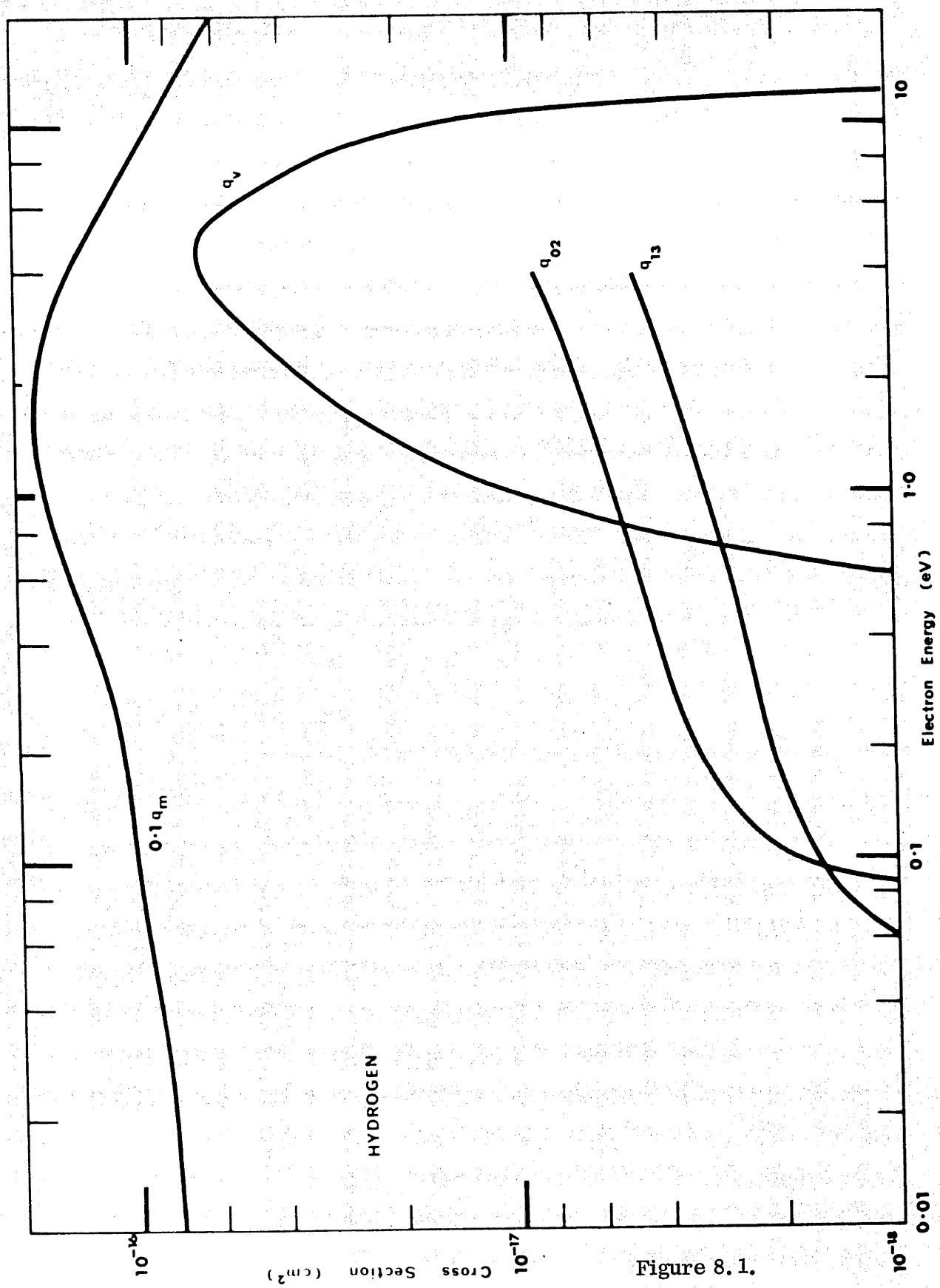
HYDROGEN
q_v
q_{02}
q_{13}
$0{\cdot}1\,q_m$
Cross Section (cm^2)
10^{-16}
10^{-17}
10^{-18}
Electron Energy (eV)
10
1·0
0·1
0·01

Figure 8.1.

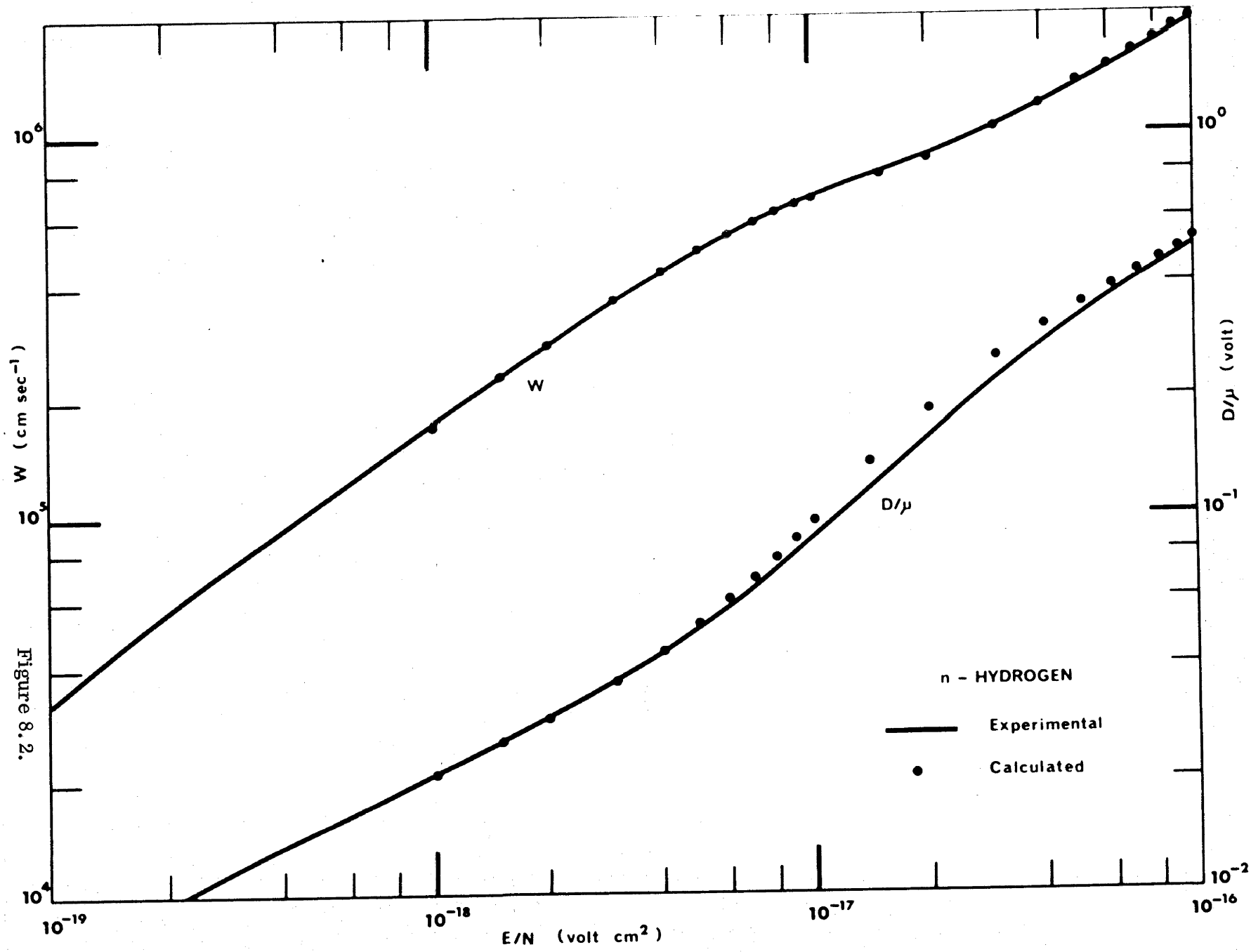
W (cm sec^{-1})
D/μ (volt)
E/N (volt cm^2)
W
D/μ
n - HYDROGEN
Experimental
Calculated
10^6
10^5
10^4
10^0
10^{-1}
10^{-2}
10^{-19}
10^{-18}
10^{-17}
10^{-16}

Figure 8.2.

has been adjusted to give the best fit to the values of ν_m/N or, through equation (7.38), to the values of W. The agreement between the calculated and experimental values of D/μ is less satisfactory. In the energy range where rotational excitation is of greatest importance discrepancies of up to 18% are observed. The agreement with the experimental values at low energies suggests that Gerjuoy and Stein's cross sections are not significantly in error in the near threshold region. The agreement between the calculated and experimental values of D/μ is also quite good above 0.35 eV. In this energy range the values of D/μ are largely controlled by the cross section for vibrational excitation which is much larger than the cross sections for rotational excitation. The vibrational cross section used was deduced by Engelhardt and Phelps from values of W and D/μ corresponding to $5 < E/p_{293} < 20$ (approximately) where the measurements of W and D/μ are less subject to experimental difficulties and there is general agreement among the results of most experimenters. Since the present experimental data are in general agreement with the earlier data in this range of E/p it is not surprising that the vibrational cross section deduced by Engelhardt and Phelps should also lead to good agreement between the calculated and experimental values of D/μ in the present investigation.

The momentum transfer cross section shown in Figure 8.1 is probably too small between 0.2 and 0.6 eV. The small values of q_m at these energies result from the way in which q_m was adjusted to force agreement between the calculated and experimental values of ν_m/N. If a rotational cross section which gives better agreement with the experimental values of D/μ can be used in a later analysis, a smoothly rising curve for q_m should result. Later analyses should not significantly alter the q_m curve shown in Figure 8.1 above 0.6 eV or below 0.1 eV. Above 3 eV the present curve has been smoothly connected to that of Engelhardt and Phelps.

Figure 8.3 shows a comparison of the calculated and experimental values of W and D/μ in para-hydrogen at $77^{\circ}K$. A discussion of these curves is essentially similar to that for normal hydrogen. The agreement of the values of W and the disagreement of the values of D/μ at intermediate energies are

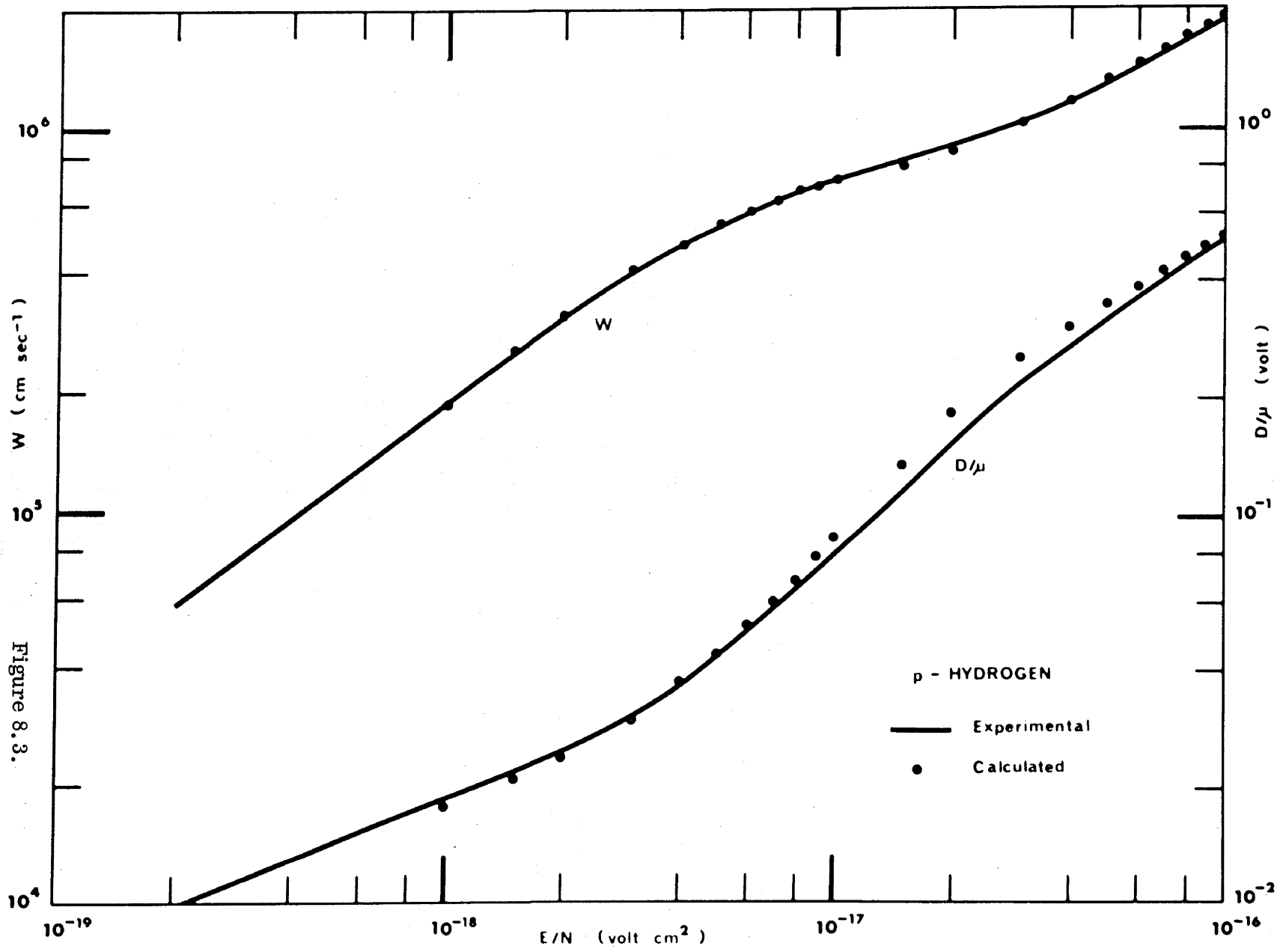
W (cm sec^{-1})
D/μ (volt)
E/N (volt cm^2)
W
D/μ
p - HYDROGEN
Experimental
Calculated
10^6
10^5
10^4
10^0
10^{-1}
10^{-2}
10^{-19}
10^{-18}
10^{-17}
10^{-16}

Figure 8.3.

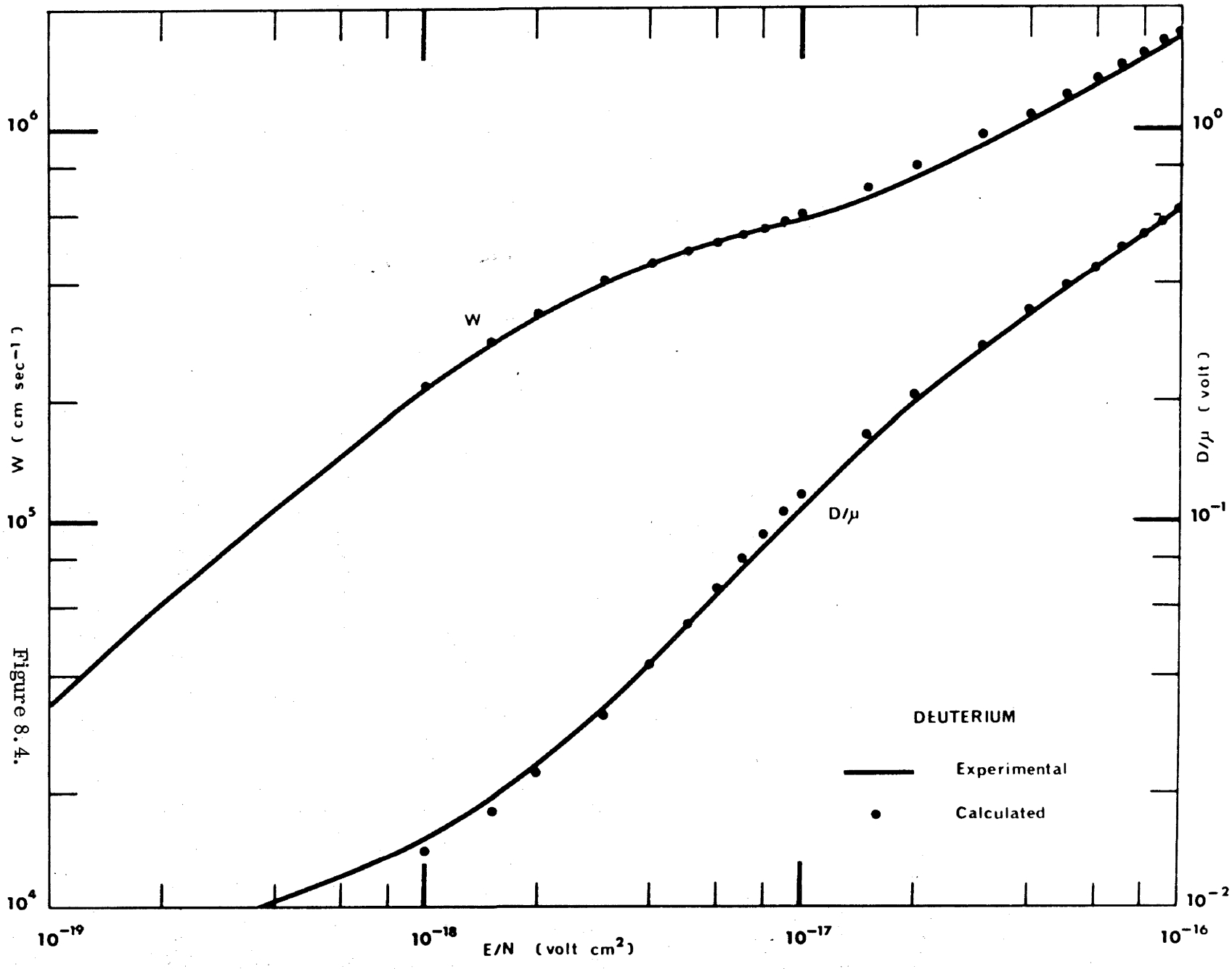
W (cm sec^{-1})
D/μ (volt)
E/N (volt cm^2)
W
D/μ
DEUTERIUM
Experimental
Calculated
10^6
10^5
10^4
10^0
10^{-1}
10^{-2}
10^{-19}
10^{-18}
10^{-17}
10^{-16}

Figure 8.4.

of exactly the same order as in normal hydrogen. The importance of the para-hydrogen results in a future analysis to determine more realistic rotational cross sections is discussed below.

A comparison of the calculated and experimental values of W and D/μ in deuterium at $77^{o}K$ is given in Figure 8.4. It is seen that the agreement between the values of W is good except in the energy range where q_m is thought to be too small. If the smoothly rising curve for q_m suggested above were used the calculated values of W would be lowered and the agreement with the experimental data greatly improved. This lowering of the values of W would be accompanied by an increase in the values of D/μ; the disagreement between the calculated and experimental values of this quantity would then be of the same order as it is in hydrogen and para-hydrogen. At energies in the vicinity of the vibrational cross section the agreement between the calculated and experimental values of D/μ is again quite good. As in hydrogen, this is a reflection of the accuracy of the cross section derived by Engelhardt and Phelps and of the comparative ease of measurement of the required values of W and D/μ. At very low energies the calculated values of D/μ fall below the experimental curve. This is due to the neglect of collisions of the second kind which are more important in deuterium than they are in hydrogen. This can be seen from equations (8.1) and (8.2) and Table 8.1. The ratio of the energy-independent J terms of the equations is 1/5 for the 2,0 and 0,2 transitions, while from Table 8.1 the ratio of the populations of the J = 2 and J = 0 levels is $\sim 4 \times 10^{-3}$ for hydrogen and ~ 0.15 for deuterium. Thus, neglecting the polarization correction, in the high energy limit the ratio of $q_{2,0}$ to $q_{0,2}$ is $\sim 10^{-3}$ for hydrogen but ~ 0.03 for deuterium.

To summarise, it is clear from the above discussion that (a) the rising part of the vibrational cross sections derived by Engelhardt and Phelps for hydrogen and deuterium is not significantly in error, (b) a suitable variation of q_m can be found, and (c) Gérjuoy and Stein's theory of rotational excitation is not consistent with the experimental results although it was shown during the course of the analysis that the inclusion of the polarization correction of Dalgarno

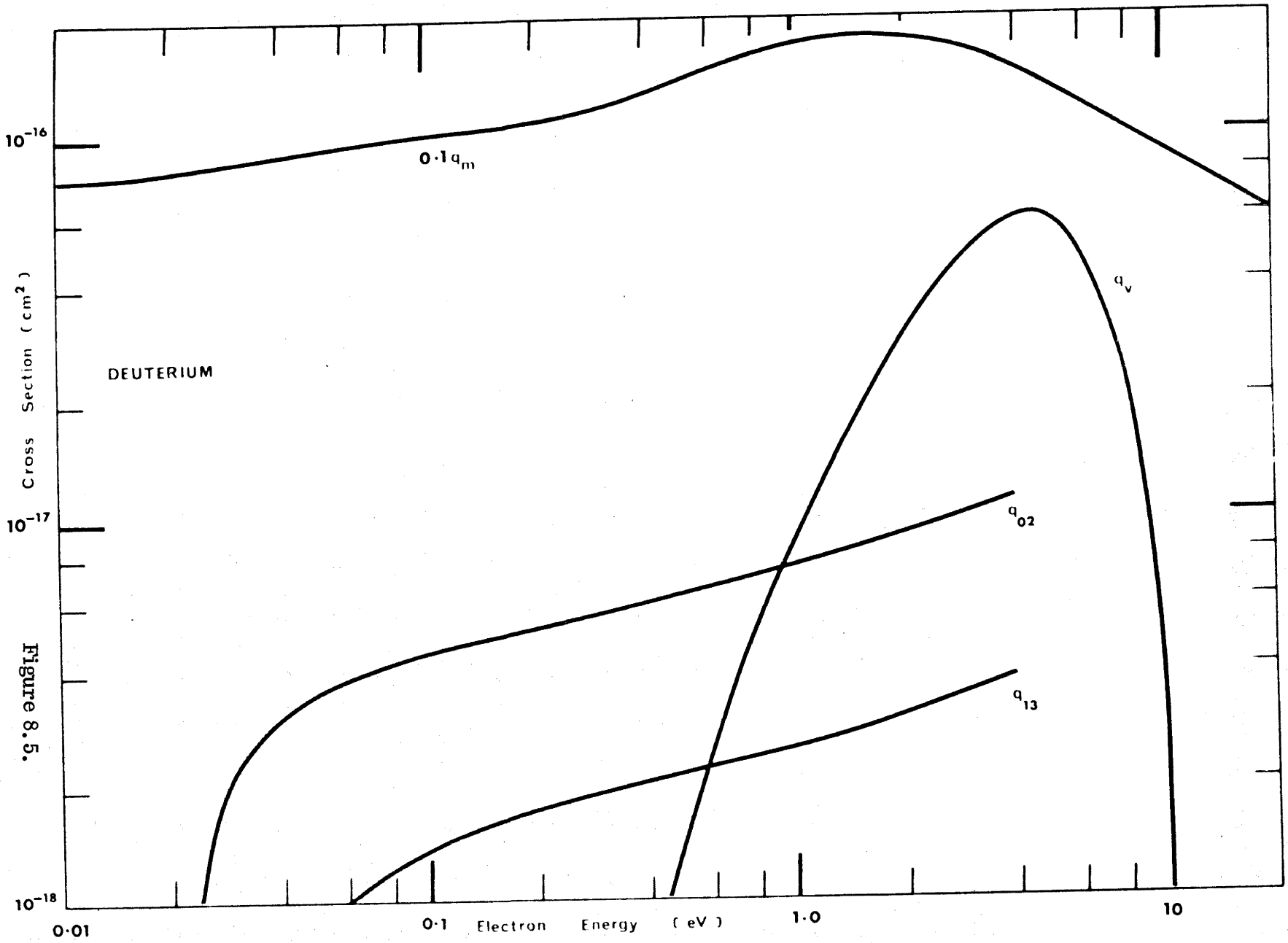
10^{-16}
10^{-17}
10^{-18}
Cross Section (cm^2)
DEUTERIUM
$0{\cdot}1q_m$
q_v
q_{02}
q_{13}
0·01
0·1
1·0
10
Electron Energy (eV)

Figure 8.5.

and Moffett leads to a better fit to the experimental data. If no polarization correction is included the rotational cross sections are smaller and the calculated values of D/μ are higher, i.e. in poorer agreement with the experimental results. Cross sections which rise more rapidly with energy than those shown in Figures 8.1 and 8.5 would seem likely to give a better fit to the experimental data. Such cross sections have been proposed by Sampson and Mjolness (1965) and Takayanagi and Geltman (1965) both of whom use distorted wave calculations.

Engelhardt and Phelps were able to obtain a "satisfactory" fit to the previously available experimental data by the use of a simple scaling factor with Gerjuoy and Stein's cross sections. Trial calculations of this type in the present investigation suggest that it would be possible to obtain a fit to the values of D/μ to within 5 - 7% everywhere, but only at the expense of nowhere having agreement to within the experimental error of $\pm$ 2%. Although Engelhardt and Phelps were justified in using this approach with the data of Warren and Parker (1962) which are subject to systematic and random errors of at least $\pm$ 5%, further investigation along these lines does not appear profitable with the accurate experimental data provided by the present experiments.

A comparison between the momentum transfer cross section of the present analysis and that of Engelhardt and Phelps is given in Figure 8.6. As explained above, the present curve is not expected to be altered by more than a few percent by later analyses with a better rotational cross section, except in the range 0.1 to 0.6 eV where the present values are thought to be too low. The vibrational cross sections of the present analysis are identical to those of Engelhardt and Phelps. A comparison between the rotational cross sections is not useful since the present analysis shows that neither cross section is valid. The electric quadrupole moment used by Engelhardt and Phelps was 0.473 e a_o^2 and their rotational cross sections were therefore smaller than those used in the present analysis by approximately 7%. The value of $(\alpha_{\parallel} - \alpha_{\perp})$ used by them was apparently smaller than that used in the present calculation because in their case the polarization correction increases Gerjuoy and Stein's cross section by

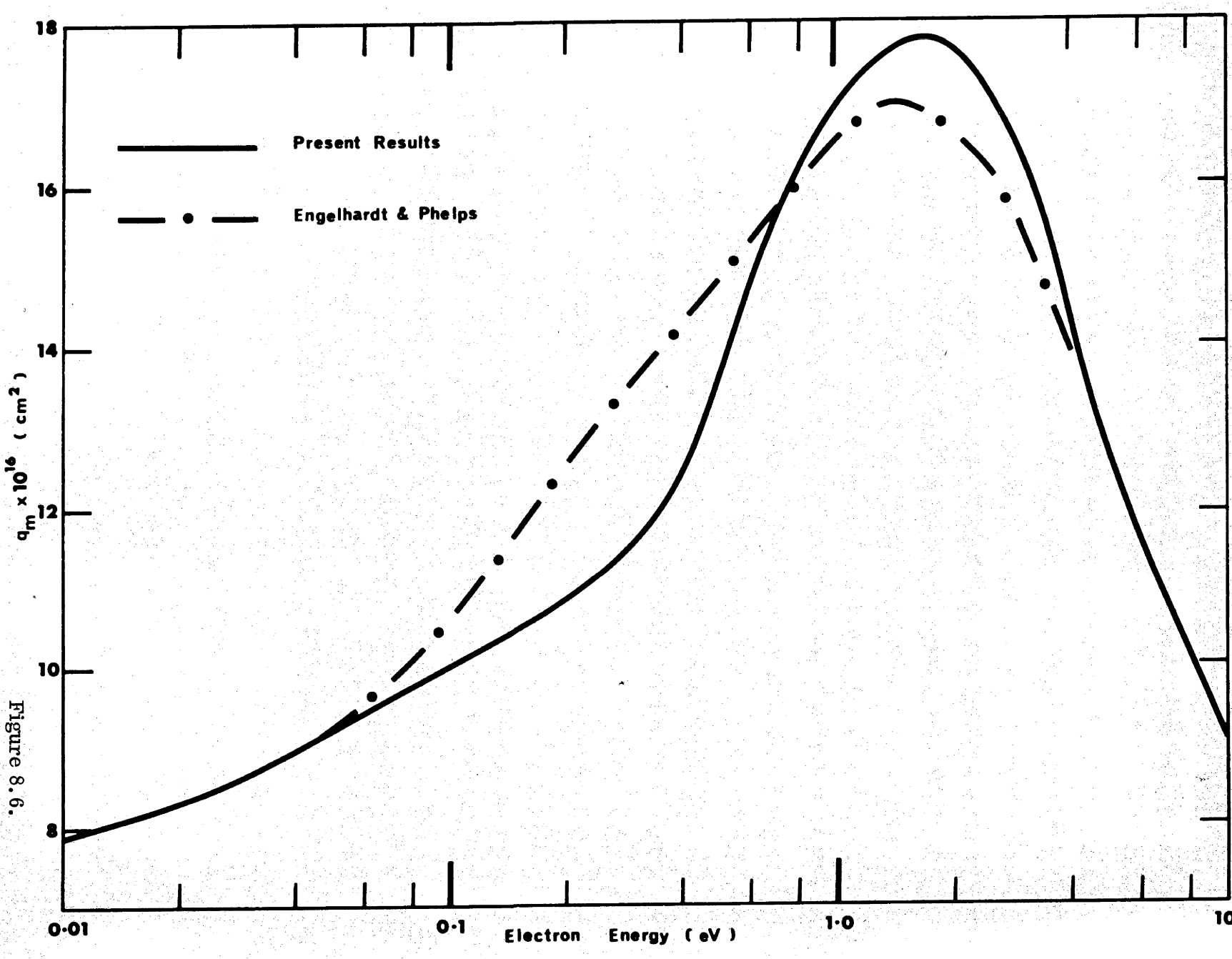
Present Results
Engelhardt & Phelps
$q_m \times 10^{16}$ (cm^2)
18
16
14
12
10
8
0·01
0·1
1·0
10
Electron Energy (eV)

Figure 8.6.

30% at 0.52 eV instead of the 45% found using the present values of $\alpha_{\parallel}$ and $\alpha_{\perp}$.

An error in equations (14) and (15) of Engelhardt and Phelps's paper should be noted because it appears responsible for their use of incorrect fractional populations for the rotational levels of deuterium. Table 8.1, which is based on formulae set out in Appendix I, shows that the fractional populations of the J = 0 and J = 1 states in normal deuterium are approximately 57% and 33%. The high energy limit of the square bracket term in equation (8.1) is unity, whereas the energy independent J term of this equation is 2/3 for the J = 0, 2 transition and 2/5 for the J = 1, 3 transition. If the polarization correction is neglected, the high energy limits of the 0,2 and 1,3 cross sections of deuterium are therefore in the approximate ratio of 3 : 1. Since the 0,2 transition has the lower threshold energy and the larger cross section at high energies, the curves for $q_{0,2}$ and $q_{1,3}$ can never cross in deuterium as they do in hydrogen. This statement should be contrasted with Figure 2 of Engelhardt and Phelps's paper where the rotational cross sections for deuterium are shown as having the same general form as they do for hydrogen, i.e. with $q_{1,3}$ intersecting $q_{0,2}$ at about 0.05 eV. Equations (14) and (15) of their paper also disagree with paragraph II c of Frost and Phelps (1962) where the correct formulae are given. It seems likely that this error is largely responsible for Engelhardt and Phelps's failure to find as good agreement between the calculated and experimental transport coefficients in deuterium as they found in hydrogen.

8.4 Further Work.

The present investigation should be extended in two ways: (a) to find a form of the rotational cross section which is consistent with all the experimental data, and (b) to take into account collisions of the second kind which have been ignored in the present analysis.

The task of finding a set of rotational cross sections which are consistent with the experimental data involves modifying the computer program described in chapter 7. It is suggested that this be done in such a way that the

rotational cross sections be read into the computer as tabulated values. An alternative approach would be to modify the program so that the cross sections are calculated according to given formulae, e.g. those of Sampson and Mjolness (1965). This approach has two main disadvantages. Firstly, if Sampson and Mjolness's formulae are used the computer time involved is likely to be excessive. Secondly, if this particular cross section is found to be inconsistent with the experimental data then a further modification to the computer program would be required. The suggested method of reading in tabulated cross sections also contains some difficulties. These are :

(a) the problem of interpolating between tabulated values when the cross section is a rapidly changing function of energy. This difficulty could be overcome by tabulating the cross sections at smaller energy intervals but there are computer limitations to the total number of points which can be used.

(b) the problem of ensuring that consistent cross sections are used for each of the allowed transitions. In any theoretical treatment the shape of the 1,3 cross section will be related to that of the 0,2 cross section and this relation must be preserved when testing the theory. The values of W and D/μ in para-hydrogen will be of particular importance in overcoming this problem. Table 8.1 shows that only the 0,2 transition is significant in para-hydrogen at $77^{o}K$ and it should therefore be possible with the present data to obtain a unique cross section for this process. In para-hydrogen the tabulated cross section can be arbitrarily adjusted to give a unique cross section which leads to agreement with the experimental data to within the experimental error. In no other gas is this possible.

The second extension of the present analysis of the experimental data is to take into account collisions of the second kind by following the solution of the Boltzmann equation outlined by Frost and Phelps (1962). The development of this solution would allow data in the near thermal region at both $77^{o}K$ and

293^{o}K to be analysed and therefore extend the energy range over which reliable cross sections can be deduced.

PART B.

THE EXTENSION OF D/μ MEASUREMENTS TO HIGHER ENERGIES

CHAPTER 9.

INTRODUCTION AND EXPERIMENTAL TECHNIQUES

9.1 Introduction.

The general techniques described in Part A of this thesis have been applied by Engelhardt and Phelps (1963) to hydrogen and deuterium to obtain the relevant cross sections for electron energies of greater than 3 eV. Since the dissociation, photon excitation and ionization cross sections must be added to the list of cross sections which are deduced from the relatively limited experimental data, it is not surprising that some inconsistencies have arisen at higher energies. These inconsistencies suggest that not all of the experimental data are of comparable accuracy.

A case in point is the available data for the transport coefficients in hydrogen for $E/p > 20$ V cm^{-1} torr^{-1}. Analysis of these data by Engelhardt and Phelps lead them to suggest that the early data for D/μ of Townsend and Bailey (1921) were approximately 25% too low to be consistent with the numerous values of α_T, the first Townsend ionization coefficient. Because of their distrust of Townsend and Bailey's D/μ data, Engelhardt and Phelps decided to use α_T as the measure of the correctness of their input cross sections in their analysis of swarm data. This decision meant that they were unable to obtain any separation between the effects of elastic and inelastic collisions, i.e. they were not able to use the quantities ν_m/N and ν_u/N described in chapter 7, and consequently the inelastic cross sections found were to some extent dependent on the value of the momentum transfer cross section chosen.

Since Engelhardt and Phelps's paper was published, Lawson and Lucas (1965) have reported values of D/μ over the range $10 \leq E/p \leq 100$

which are less than 10% higher than the early data. Since at lower energies Townsend and Bailey's data have been found to be reliable it was thought unlikely that their data would have been in error by as much as 25% at higher values of E/p. At the same time, if accurate values of D/μ for $E/p > 20$ were available it would be possible to overcome the disadvantages of having no separation between the effects of elastic and inelastic collisions. For these reasons it was decided to re-determine the values of D/μ for $10 \leq E/p \leq 100$.

In a Townsend-Huxley lateral diffusion experiment of the type discussed in Part A, the values of D/μ or k_1 have been found to be consistent over a very wide range of pressures. However, in the experiments to be described below this was not always the case, particularly at very high values of E/p. At moderately high pressures, high values of E/p and long chamber lengths, the experimental conditions approach those for which electrical breakdown occurs. If the conditions are such that a self-sustained discharge occurs, each electron leaving the cathode is replaced by one new electron generated by some secondary process such as the impact of photons or positive ions on the cathode. The number of electrons in this distributed source is now exactly equal to the number of primary electrons entering through the 1 mm hole in the cathode. It is clear that as the experimental conditions approach those for which electrical breakdown occurs the effect of the secondary electrons must be taken into account in the analysis of the measured ratios of currents. However, by keeping the pressures low the conditions can be kept sufficiently far from those at which electrical breakdown occurs and in this case it is necessary to consider only the primary ionization within the chamber. The experimental accuracy in such cases is likely to be poor since the pressures required are so low that their accurate measurement is difficult. Moreover the electron mean free path between collisions is long and the electrons may not reach an equilibrium energy distribution before arriving at the anode.

Both approaches to the problem of measuring the values of D/μ in hydrogen for $E/p > 20$ were used in the experiments described below.

9.2 Determination of the Values of D/μ from the Measured Current Ratios.

The geometry of the apparatus in both experiments is similar to that shown in Figure 2.2. Electrons enter the chamber through a 1 mm diameter hole in the cathode and then drift and diffuse through the distance h to the anode which is split into two concentric areas: an inner disc of radius b and an outer region effectively of infinite extent. The ratio of the current reaching the central disc to the total current reaching the anode is measured. In the absence of primary ionization and secondary effects the value of D/μ can then be found from equation (2.25) :

$$R = 1 - h/d \exp (- \lambda (d - h)) \qquad (9.1)$$

9.2.1 Inclusion of the Effect of Primary Ionization.

In an unbounded volume in which an electric field is applied parallel to the z-axis and in which ionization by electrons accompanies the normal processes of drift and diffusion, the electron concentration is described by the differential equation (Huxley, 1959)

$$\nabla^2 n = 2 \lambda \frac{\partial n}{\partial z} - 2 \lambda \alpha_i n \qquad (9.2)$$

In this equation $2 \lambda = W/D$, $\alpha_i = \alpha'/W$ and $n \alpha'$ is the rate of production of electrons by ionization per unit volume when the electron number density is n. If secondary effects are ignored, the solution of this equation analogous to the solution discussed in section 2.1.4 leads to the following expression for the current ratio R (Huxley, 1959) :

$$R = 1 - h/d \exp (- \lambda' (d - h)) \qquad (9.3)$$

where

$$(\lambda')^2 = \lambda^2 - 2 \lambda \alpha_i = (\lambda - \alpha_T)^2 \qquad (9.4)$$

α_T being the Townsend primary ionization coefficient and the other symbols have their usual meaning. Measurements of R therefore yield values of λ' from which the values of λ can be obtained only through knowledge of the values of α_T found from a separate experiment. This experiment could be carried out using

the same apparatus but a different procedure (see for example, Haydon, 1964).

It should be noted that, like λ/p , λ'/p is a function of E/p and not of p alone, so that values of λ'/p obtained from the measured current ratios at a fixed value of E/p should be independent of p.

9.2.2 Inclusion of the Effects of Primary Ionization and Secondary Emission.

Hurst and Liley (1965) reported a comprehensive analysis of the Townsend-Huxley lateral diffusion technique. They were able to derive an expression for R when ionization within the chamber and the emission of secondary electrons at the electrode surfaces accompany the normal processes of drift and diffusion. It will be shown later that for the present experimental conditions virtually all of the secondary electrons are liberated by the impact of photons on the cathode. In this special case the formula for R is (Hurst and Liley, 1965) :-

$$R = b \exp(\lambda' - \lambda) h \left\{ 1 - \frac{2\pi\Delta}{\lambda'} \left[\frac{\exp((\lambda - \lambda')h) - 1}{\lambda - \lambda'} - \frac{\exp(-2\lambda' h)(\exp((\lambda + \lambda')h) - 1}{\lambda + \lambda'} \right] \right\} \times \int_0^\infty I(\ell)\, d\ell \qquad (9.5)$$

where

$$I(\ell) = \frac{J_1(b\ell) \exp(\lambda - (\lambda'^2 + \ell^2)^{\frac{1}{2}} h)}{1 + \Delta M(\ell)} \qquad (9.6)$$

and

$$M(\ell) = \frac{-2\pi}{(\lambda'^2 + \ell^2)^{\frac{1}{2}}} \left\{ \frac{\exp(\lambda - \ell - (\lambda'^2 + \ell^2)^{\frac{1}{2}} h) - 1}{\lambda - \ell - (\lambda'^2 + \ell^2)^{\frac{1}{2}}} - \frac{\exp(-2h(\lambda'^2 + \ell^2)^{\frac{1}{2}})(\lambda - \ell + (\lambda'^2 + \ell^2)^{\frac{1}{2}} h) - 1}{\lambda - \ell + (\lambda'^2 + \ell^2)^{\frac{1}{2}}} \right\} \qquad (9.7)$$

$$\lambda = W/2D \qquad \lambda'^2 = \lambda^2 - 2\lambda\alpha_i \qquad (9.8)$$

$$\Delta = \frac{\lambda' (\lambda - \lambda') (\delta / \alpha_i)}{2 \pi} \qquad (9.9)$$

In these equations $J_1 (b\ell)$ is a Bessel function of the first kind and (δ / α_i) is the number of secondary electrons liberated at the cathode per ionizing collision in the gas. Formulae for the other special case where all the secondary electrons are liberated by positive ion bombardment of the cathode and for the general case when both processes are active can be found in Hurst and Liley.

Equation (9.5) cannot be evaluated explicitly, but R can be calculated numerically from it to any required degree of accuracy by integrating from zero to a sufficiently high root of $J_1 (b\ell)$. Hurst and Liley were able to show that in all practical cases the integration need be made only as far as the third root of $J_1 (b\ell)$.

The calculation is carried out for a series of values of E/p and p for an apparatus of known geometry using published data for α_T and sets of values of λ and the secondary coefficient. At a given value of E/p a comparison of the calculated values of R at a series of pressures with the corresponding experimental values leads to unique values of λ and the secondary coefficient.

9.3 The Apparatus.

The apparatus used for the experiments at low pressure has been described previously by Crompton and Jory (1962). The apparatus used for the experiments at higher pressures was designed by the author.

9.3.1 Apparatus Used for the Experiments at Low Pressures.

Figure 9.1 shows a cross sectional view of the diffusion apparatus used. The effective size of the central disc and the chamber length are variable. The receiving electrode consists of a central disc of radius 0.5 cm and a series of surrounding insulated annuli of external radii 1.0, 1.5, 2.0 and 4.25 cm. Each section of the electrode is mounted on a separate double-ended housekeeper seal to ensure that the sections are accurately concentric with the axis of the apparatus and that each section is highly insulated from the next and from earth.

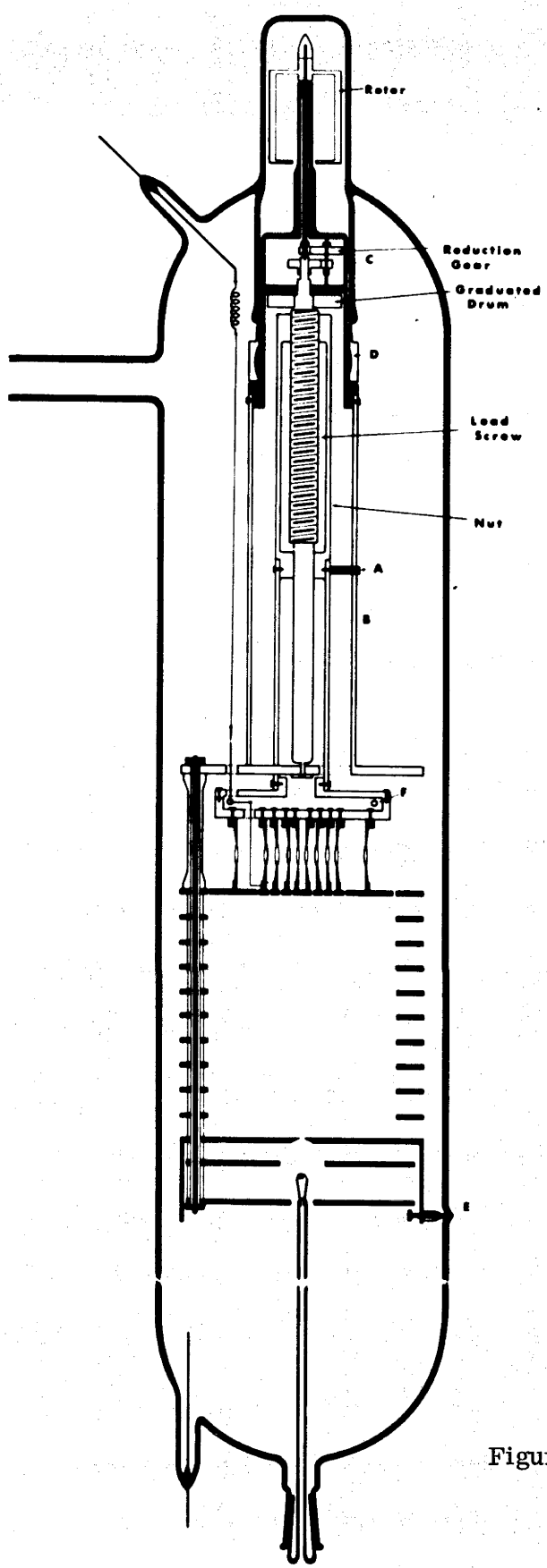

Figure 9.1.

The whole electrode is mounted on a stainless steel thread of 1 mm pitch which enables (Crompton and Jory, 1962) the separation between source hole and receiving electrode to be set at any desired distance in the range 1 to 10 cm. All surfaces of the apparatus exposed to the electron stream were gold coated to minimize errors due to contact potential differences. The Pyrex glass envelope is similar to those described in chapters 3 and 5; the demountable seals were made with W 100 wax.

Using Townsend and Bailey's data as a guide to the expected results, calculations showed that the following experimental conditions would lead to current ratios in the desired range of $0.3 < R < 0.9$:

h = 4 cm	b = 1 cm	p = 0.5, 1.0 and 1.5 torr
h = 3 cm	b = 1 cm	p = 0.5, 1.0 and 1.5 torr
h = 2 cm	b = 1 cm	p = 0.5, 1.0, 1.5 and 2.0 torr.

9.3.2 Apparatus Used for the Experiments at Higher Pressures.

A cross section of the apparatus is shown in Figure 9.2. The electrodes of solid Dural were contoured to a modified Rogowski profile (Bruce, 1947) to minimize the possibility of sparking, other than across the gap, when the conditions approached those for electrical breakdown. The dimensions of the electrodes were chosen to ensure adequate uniformity of the electric field in the central region.

Preliminary calculations showed that a nominal electrode separation of 2 cm together with a central disc of diameter 0.7 cm would be the most useful. With these dimensions it was expected that measurements could be made at any given value of E/p over a significant range of pressure within the limits 2 to 10 torr. Calculations also showed that 99.9% of the current reaching the anode would be collected on a disc of radius 1.0 cm; since this dimension was not critical, the larger radius of the outer annulus of the collecting electrode was made 1.5 cm. Further calculations showed that an error of approximately 1% in k_1 would result from an error of 0.01 cm in h. Errors in h due to inaccuracy of measurement or other causes were less one quarter of this amount.

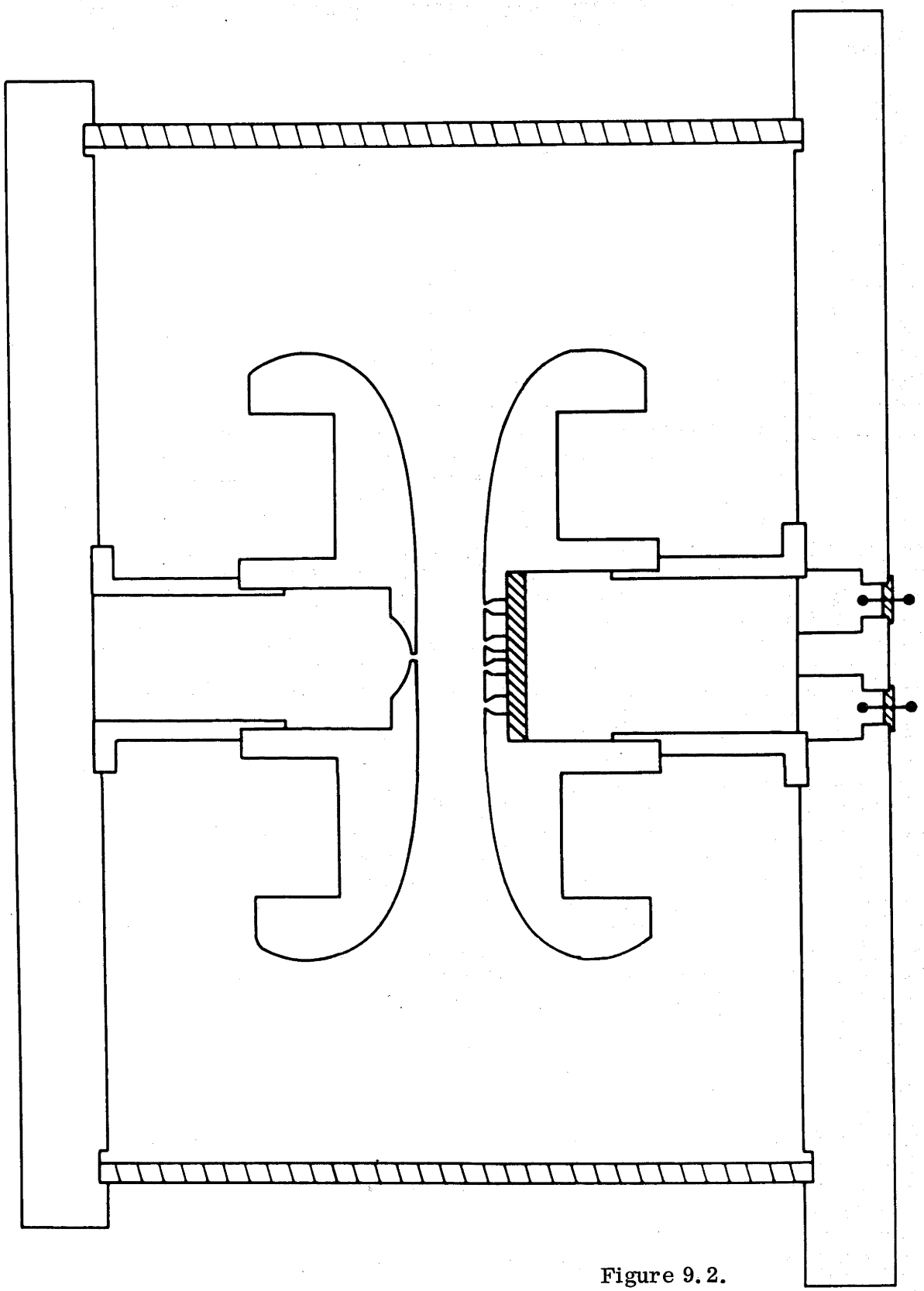

Figure 9.2.

Each electrode was machined from a piece of solid Dural 2" thick and approximately $7\frac{1}{2}$" in diameter. Machining was continued until each electrode fitted an aluminium template accurately constructed according to the formulae of Bruce (1947). The electrodes were polished to a high degree of surface finish and were cut away on the reverse side to reduce the total weight of the apparatus. The segments of the collecting electrode were mounted on a glass backing plate.

The cathode and anode were mounted on brass plates $1\frac{1}{4}$" thick. The thickness of the plates was chosen after consideration of their possible distortion due to atmospheric pressure when the apparatus was evacuated. The end plates were separated by an 8" length of $12\frac{1}{2}$" outside diameter heavy wall Pyrex tubing, the ends of which had been ground flat and parallel to within 0.001". Apiezon W100 wax was used to make the vacuum seal between the end plates and the glass tubing. The electrometer connections to the receiving electrode were made through ceramic to metal seals soldered into the base plate. The filament stem and pumping connection were combined in a $1\frac{1}{2}$" diameter Kovar seal mounted axially on the top plate. The Kovar seal was argon arc welded to a stainless steel flange which in turn was sealed to the brass plate by a pre-outgassed Viton rubber O-ring.

The surfaces of the cathode and anode were gold coated by vacuum deposition to produce surfaces with stable and relatively low photo electric sensitivity. The dimensions of the completed electrode structure were

$$h = 2.016 \text{ cm} \qquad b = 0.3505 \text{ cm}.$$

9.4 Other Experimental Details.

9.4.1 Electrical Supplies, Current Measuring Equipment and Vacuum Systems.

The electrical and current measuring equipment were identical to those described in chapter 3.

The vacuum systems were similar to those described in section 3.5.1 but no second stage pumping was provided. The ultimate pressure reached was of the order of 10^{-4} torr. The rate of pressure rise of the Rogowski profile

apparatus when isolated from the pumping line was typically less than 5×10^{-6} torr/hour. The volume of the chamber was approximately 20 litres. Over the several hours taken for any experimental run this gas influx would lead to an impurity level of 5 ppm in a 2 torr sample of gas and of proportionately less than 5 ppm into higher pressure samples. The impurity levels of the gas samples used in the low pressure experiments were about five times higher than these figures.

9.4.2 Measurement of the Gas Temperature and Pressure.

Neither apparatus contained a water cooler of the type described in section 3.1.3. Both were operated in an air conditioned room maintained at $20 \pm 2^{o}C$. Short term fluctuations in the air temperature appeared to be damped by the bulk of the metal in the apparatuses. Errors in the final values of k_1 due to errors in temperature measurement were thought to be less than $\pm 0.5\%$.

The pressure gauge used in the experiments with the Rogowski profile apparatus was a 0 - 40 torr capsule gauge of the type described by Crompton and Elford (1957). The error in pressure measurement was less than $\pm 0.5\%$ at 5 torr and about $\pm 1.5\%$ at 2 torr.

For the low pressure experiments the error in measuring pressures of 0.5 torr with this gauge would have been about 5%. However, Crompton and Jory (1962) had used the same apparatus but with higher gas pressures to obtain values of k_1 in hydrogen up to $E/p = 5.0$ V cm^{-1} torr^{-1}. They placed an error limit of $\pm 1\%$ on their data. The procedure adopted to set the pressure in the present experiments was therefore to set the voltages accurately to the values required for $E/p = 5.0$ and then to adjust the pressure until the measured value of k_1 was equal to that reported by Crompton and Jory. The reproducibility of this method of setting the pressure was about 1 - 2 %.

CHAPTER 10

RESULTS AND DISCUSSION

The results obtained from both the sets of experiments described in the previous chapter are presented below. In the low pressure experiments values of k_1 were found for the range $10 \leq E/p \leq 100$, while the corresponding range for the experiments in the Rogowski profile apparatus was $10 \leq E/p \leq 70$. An error limit of $\pm$ 5% is placed on both sets of data.

10.1 The Ionization Coefficient.

To proceed with an analysis of the current ratios obtained in either experiment it is necessary to know the values of α_T/p as a function of E/p. The values could have been measured in the present apparatus using the method described by Haydon (1964). However, there is general agreement on the values of the coefficient for $E/p \leq 100$ (see, for example, Golden, Nakano and Fisher, 1965) and this fact suggests that the published data could be used with confidence. The data were therefore not re-determined but taken from the paper of Rose (1956). The values of α_T/p_{293} as a function of E/p_{293} are listed in Table 8 of Appendix 2.

10.2 Results from the Low Pressure Experiments.

The values of k_1 found in the low pressure experiments are shown in Table 10.1. An error limit of $\pm$ 5% is placed on the average values in this Table. A discussion of the results will be given in section 10.4.

10.3 Results from the Higher Pressure Experiments.

Keeping within the limits determined by sparking, two sets of measurements of the ratios were taken in the range $10 \leq E/p \leq 70$ using as wide a range of pressures as possible. Over a period of twelve days no current ratio changed by more than 1%. The averages of these two sets of measurements were used in the subsequent analysis.

If the values of λ' are calculated from these ratios using equation (9.3) which ignores the effect of secondary processes, the quantity λ'/p

Table 10.1

Values of k_1 for electrons in hydrogen at 293°K.

	b/h = 0.5				b/h = 0.333			b/h = 0.25		
p	0.5	1.0	1.5	2.0	0.5	1.0	1.5	0.5	1.0	Aver-age
E/p										
10	43.7	42.4	41.7	41.6	42.2	42.1	42.2	42.1	42.3	42.3
15	61.9	-	60.3	61.7	60.4	61.6	-	61.0	62.2	61.3
20	78.1	78.2	77.9	78.3	76.7	78.2	78.9	76.7	78.9	78.0
25	90.4	90.5	90.7		89.1	90.5	90.7	88.9	90.5	90.2
30	100.6	99.7	100.7		98.8	99.7	99.9	98.6	100.2	99.8
35	108	107	108		106	107		106	106	107
40	116	117	115		114	115		114	114	115
45	124	124	125		121	123		121	119	122
50	132	131			129	131		129	127	130
55	137	137			134			135		136
60	144	145			142			142		143
65	152				147			149		149
70	159				154			157		157
75	165				162			164		164
80	173				169			172		172
85	179				176			181		179
90	185				183			189		186
95	193				192			198		194
100	200				200			208		203

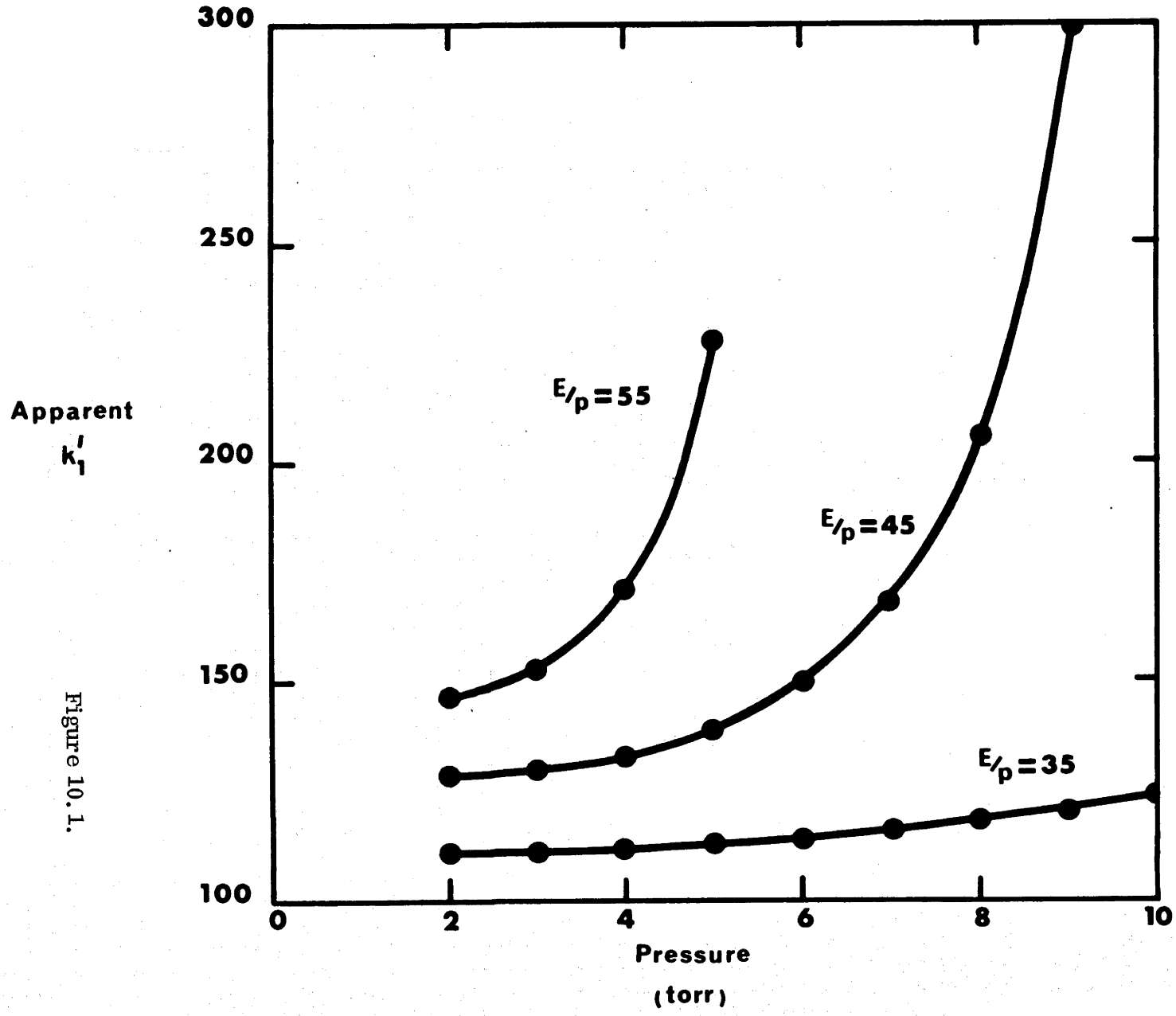
300
250
200
150
100
0
2
4
6
8
10
Apparent
k_1'
Pressure
(torr)
E/p=55
E/p=45
E/p=35

Figure 10.1.

is found to be markedly pressure dependent. This dependence is shown in Figure 10.1 in which the quantity $k_1' = (eE/2kT)/\lambda'$ is plotted as a function of p. It is seen that k_1' increases with increasing p and that this increase becomes more rapid as E/p is increased. The pressure dependence of the results is due to secondary processes at the cathode. To obtain the values of k_1 it is therefore necessary to analyse the measured ratios on the basis of equation (9.5).

The analysis of the results for E/p = 45 is typical of the procedure which was followed to decide which of the secondary processes was more important. From the results of spatial and temporal growth of current experiments (Llewellyn-Jones, 1957, Morgan and Williams, 1965) it is reasonable to assume that the photon effect is dominant over most of the range of E/p used in the present experiments. Accordingly, equation (9.5) was first used with the appropriate values of α_T and trial values of λ and δ/α until the current ratios calculated from it agreed with the ratios measured at the extremes of the pressure range, in this instance 2 and 9 torr. These values of α_T, λ and δ/α were then used to calculate the current ratios at the intermediate pressures and the agreement between theory and experiment examined. A similar procedure was then followed using a formula for R similar to equation (9.5) but appropriate to the positive ion secondary process.

The comparison between theory and experiment is facilitated by converting the current ratios to apparent values of k_1' through equation (9.3). The values of k_1' found in this way are shown in Table 10.2.

Table 10.2

E/p = 45 $\quad \alpha_T/p = 0.266 \quad \delta/\alpha = 2.82 \times 10^{-3} \quad \gamma = 6.64 \times 10^{-3}$

p =	2	3	4	5	6	7	8	9
Apparent k_1' =	128	130	134	139	150	168	208	300
photon calculated k_1' =	130	131	134	138	147	166	205	299
positive ion calculated k_1' =	129	128	129	131	136	148	177	297

From this table it can be seen that the agreement between theory and experiment is excellent when the ratios are calculated on the assumption of a photon secondary effect. On the other hand, when the calculations are based on the assumption of a positive ion process, the agreement is less satisfactory, with discrepancies of up to 15% between theory and experiment. These results support the view that at this value of E/p the secondary process is predominantly a photon rather than a positive ion phenomenon.

The evidence from other experiments and from a consideration of the relative efficiencies of the excitation and ionization processes (Penning, 1938, Druyvesteyn and Penning, 1940, Corrigan and von Engel, 1958) suggests that as E/p is lowered the positive ion effect becomes less important than the photon effect. At low E/p electrons in the swarm have sufficient energy to cause excitation of the gas molecules and hence to create photons, but there are few electrons in the swarm with sufficient energy to cause ionization. Thus the number of photo-electrons per ionizing collision might be expected to be large at low E/p and to decrease as E/p and the mean energy of the electrons rises. At higher values of E/p measurements were not made over a sufficiently wide range of pressure to be able to determine which secondary process was more important, but Morgan and Williams's results show that at E/p = 70 the value of γ (the positive ion secondary coefficient) is still less than 50% of the value of δ/α. For these reasons the experimental current ratios at all values of E/p were analyzed on the assumption that all the secondary electrons were produced by the impact of photons on the cathode. Sample calculations at E/p = 70 using the positive ion formula gave values of k_1 not significantly different to those found assuming the photon process to be dominant. Below E/p = 55 measurements were made over a sufficiently wide range of pressures for the use of the photon formula to be justified by comparisons similar to that of Table 10.2.

At each value of E/p the value of the secondary coefficient which gave k_1 most nearly independent of pressure was found. Table 10.3 shows a typical example of the invariance of k_1 with pressure when the correct value of

the secondary coefficient was used.

Table 10.3

$E/p = 45$ $\quad \alpha_T/p = 0.266$ $\quad \delta/\alpha = 2.82 \times 10^{-3}$

p =	2	3	4	5	6	7	8	9
Apparent k_1' =	129	130	133	139	150	168	206	295
True k_1 =	123	123	124	123	126	126	123	123

The values of the secondary coefficient found in the present investigation are listed in Table 10.4.

Table 10.4

Secondary coefficient δ/α for gold electrodes in hydrogen.

E/p	$\delta/\alpha \times 10^3$	E/p	$\delta/\alpha \times 10^3$
20	48.5	50	2.86
25	13.8	55	2.66
30	8.51	60	2.76
35	5.46	65	2.70
40	3.45	70	2.79
45	2.82		

From the discussion above it would seem likely that some reliance could be placed on the values of δ/α obtained from the present analysis for $E/p < 55$ but that the values obtained at higher values of E/p should be treated with caution.

The values of k_1 found in the same analysis are given in Table 10.5. At each value of E/p the values of k_1 were found to have an overall residual scatter of the order of $\pm$ 1%. At the lower values of E/p measurements could be made over an extended range of pressures and the validity of using equation (9.5) to analyse these results was established. Consequently the values of k_1 can be regarded as reliable. For $E/p > 55$ the range of pressures

Table 10.5

Values of k_1 in Hydrogen at 293°K.

p	2	3	4	5	6	7	8	9	10	
E/p										Average
10	42.2	42.2	42.0	42.3	42.1	42.1	42.1	42.1	42.1	42.1
15	62.3	62.1	62.1	62.1	62.5	62.1	62.0	62.2	62.6	62.2
20	79.1	79.2	79.2	78.9	79.2	78.9	79.2	79.0	79.1	79.1
25	90.4	91.3	91.4	91.3	91.6	91.2	91.4		91.6	91.3
30	100	100	101	101	101	100	101	101	101	101
35	108	108	109	109	109	109	109	109	108	109
40	116	116	117	117	117	117	117	117	116	117
45	123	123	124	125	126	126	125	123		125
50	129	130	130	130	129					130
55	136	137	137	136						137
60	143	143	143							143
65	150	150								150
70	157	157								157

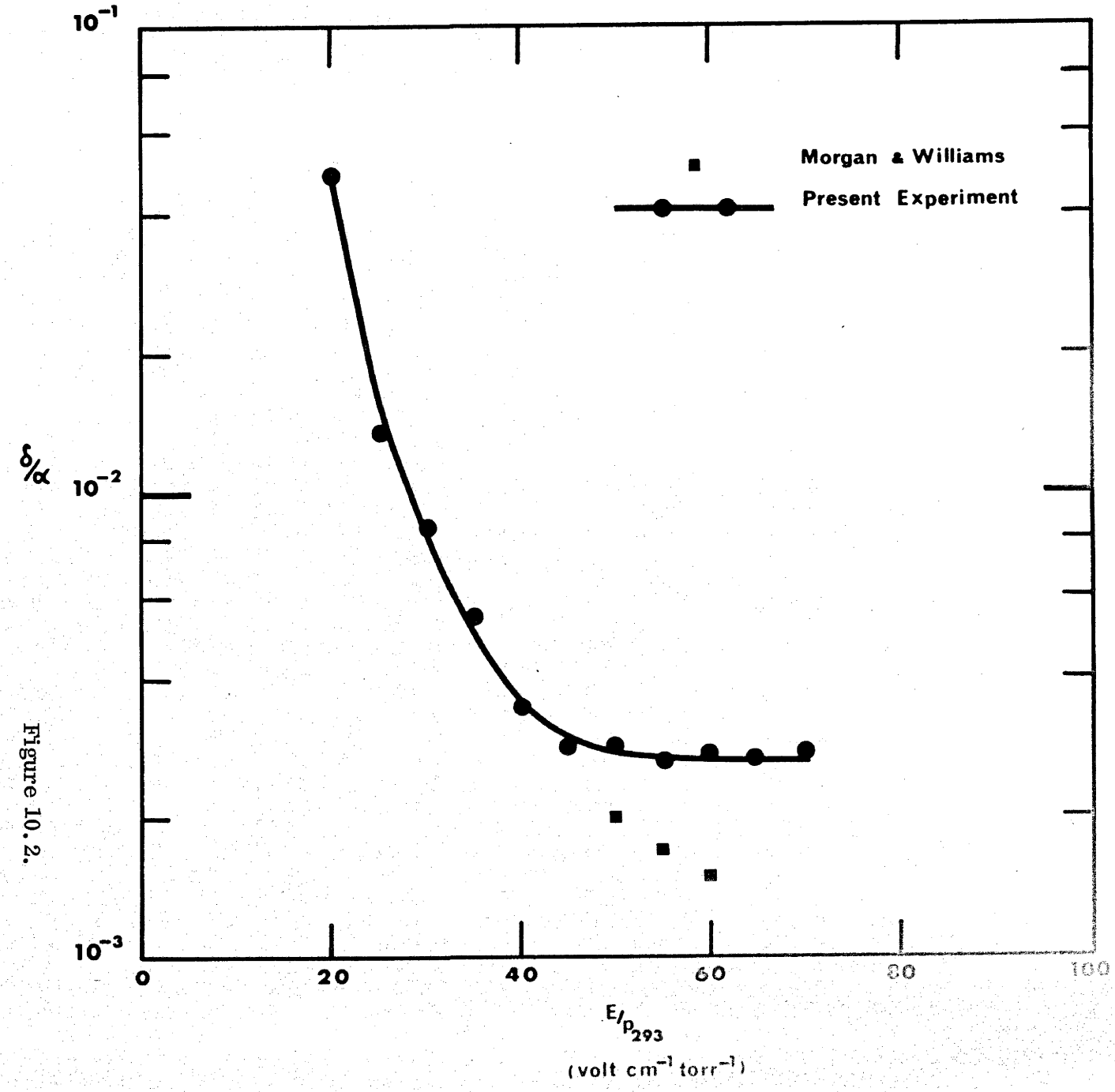
10^{-1}
10^{-2}
10^{-3}
δ/α
Morgan & Williams
Present Experiment
0
20
40
60
80
100
E/p_{293}
(volt cm^{-1} $torr^{-1}$)

Figure 10.2.

was limited but the arguments outlined above and the results themselves suggest that the values of k_1 are subject to an error of less than 5%.

10.4 Comparison with Other Data.

10.4.1 The Secondary Coefficient.

A comparison of results for the secondary coefficient is not generally useful since the actual values of the coefficients vary from experiment to experiment, depending largely on the electrode surfaces. The important results are the variation with E/p of the secondary coefficient and the relative importance of the alternative secondary processes. Nevertheless, it is of interest to compare the present results with the data of Morgan and Williams (1965), which are the only other data for gold electrodes in hydrogen. Figure 10.2 shows that over the common range of E/p there is general agreement between the two sets of data. Morgan and Williams found that at E/p = 52, their lowest value, the photon coefficient was an order of magnitude larger than the positive ion coefficient. There are no other comparable data known to the author which extend to such low values of E/p, but the shape of the present curve is in agreement with the general arguments outlined in section 10.3 above.

10.4.2 The Values of k_1.

Over the common range of E/p the results from the low pressure and Rogowski profile experiments are in excellent agreement, the maximum discrepancy between the two sets of data being about 2%.

The present results are shown plotted as a function of E/p_{293} in Figure 10.3. Also shown in this Figure are the results of Townsend and Bailey (1921), Lawson and Lucas (1965) and the predicted values of Engelhardt and Phelps (1963). A temperature of 15°C has been assumed for Townsend and Bailey's data. Townsend's 1948 values which appear only in his book "Electrons in Gases" are not quoted since they are not in agreement with the values given in the paper cited as their source. Townsend and Bailey's values may at best be regarded as values of k_1' and they have therefore been corrected for the effect of ionization for the purpose of comparison. Lawson and Lucas's values

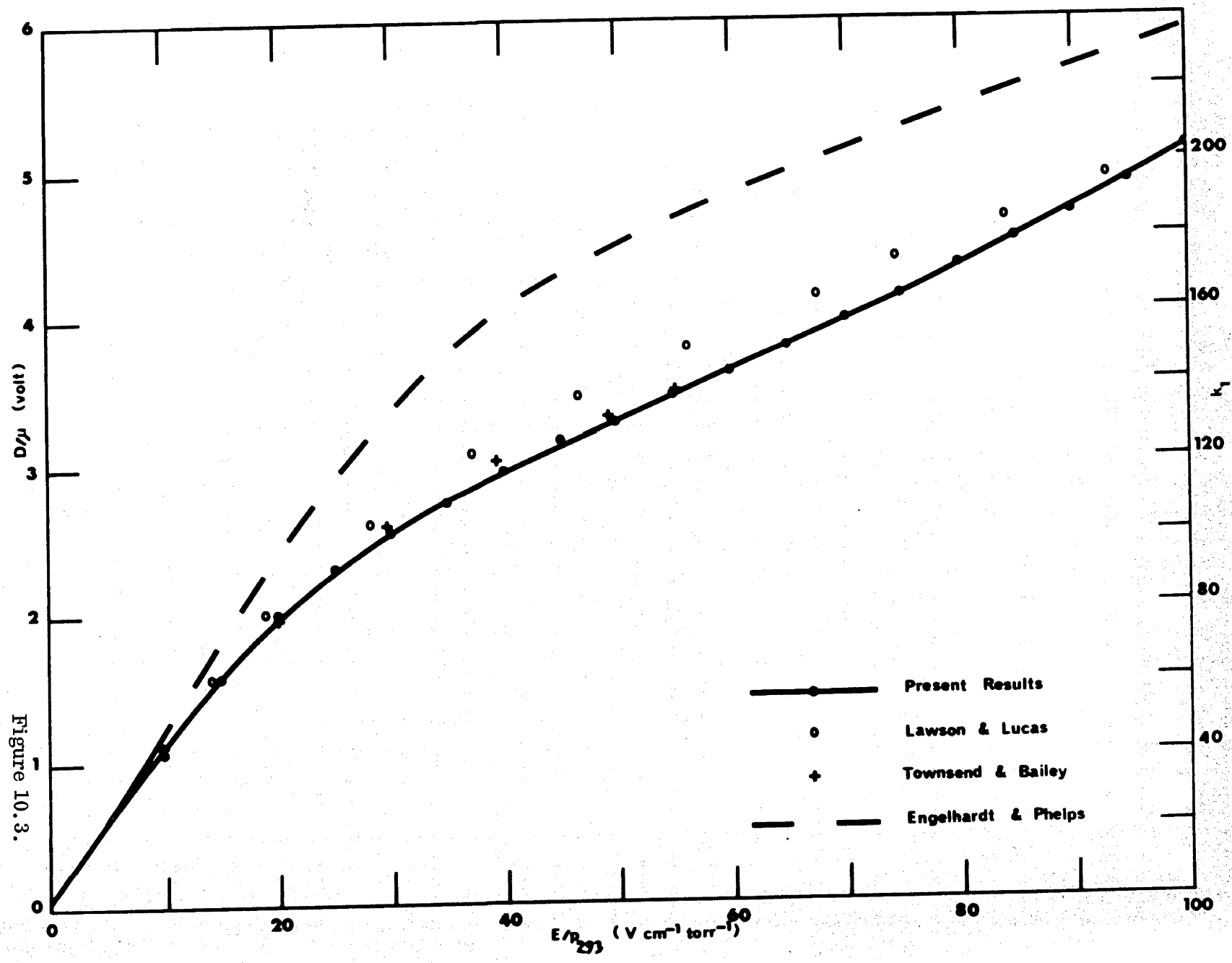
D/μ (volt)
E/p293 (V cm-1 torr-1)
Present Results
Lawson & Lucas
Townsend & Bailey
Engelhardt & Phelps

Figure 10.3.

are consistently about 8% higher than the present results. This percentage discrepancy is present even below $E/p = 20$ where the present results agree well with those of Crompton and Sutton (1952) and those of Townsend and Bailey, and where none of the sets of results are likely to have been influenced by either primary or secondary effects. It therefore seems probable that Lawson and Lucas's measurements are subject to a systematic error of this magnitude throughout.

It should be noted that both Townsend and Bailey and Lawson and Lucas worked at pressures of the order of 1 torr and therefore the effects of secondary processes would be minimized. It is likely, however, that errors from these effects were not always negligible in Townsend and Bailey's experiments. Any correction applied to take account of these processes would lower the values of k_1 reported by them.

Finally, the results of the present experiment are to be compared with the calculated values of Engelhardt and Phelps (1963). Figure 10.3 shows that the present data confirm Townsend and Bailey's data and are therefore also about 25% lower than Engelhardt and Phelps's calculated values. The present results suggest that Townsend and Bailey's data were not seriously in error and were, in fact, too high rather than too low.

Some of the disagreement between the calculated and experimental values of D/μ is due to the fact that Engelhardt and Phelps used the approximation $\alpha_i = \alpha_T$. The values of α_i used by them are therefore too high and lead to calculated values of D/μ which are also too high. Since the difference between α_i and α_T is 4% at $E/p = 70$, and less than this at lower values of E/p, it would seem unlikely that this correction would significantly improve the fit between the calculated and experimental values of D/μ.

By adopting the experimental procedure and analysis described above it is possible to extend considerably the range of E/p over which k_1 can be reliably determined. At the same time an analysis of the data using the complete theory of Hurst and Liley (1965), which takes account of both photon and positive ion secondary effects, provides a new method of determining the coefficients for

these processes. Furthermore, the fact that the present data have confirmed Townsend and Bailey's results shows that further investigation of the inconsistencies found by Engelhardt and Phelps is required.

APPENDIX 1.

THE PROPERTIES OF HYDROGEN, PARA-HYDROGEN AND DEUTERIUM. THE PREPARATION AND ANALYSIS OF PURE PARA-HYDROGEN.

A 1.1 Ortho- and para- Hydrogen.

Both parallel and anti-parallel orientations of the nuclear spin may occur in hydrogen molecules. These different orientations combined with certain values of the rotational quantum number J distinguish the two hydrogen modifications. Para-hydrogen molecules have anti-parallel nuclear spins and even rotational quantum numbers, while ortho-hydrogen molecules have parallel nuclear spins and odd rotational quantum numbers (Farkas, 1935).

There is an equilibrium concentration of ortho- and para-hydrogen characteristic of a given temperature. For $T \geq 293^{o}K$ hydrogen consists of 25% para-hydrogen and 75% ortho-hydrogen; at liquid hydrogen temperature (approximately $20^{o}K$) the equilibrium mixture is very nearly 100% para-hydrogen. However the equilibrium concentration for a given temperature is not reached merely by cooling the gas; if this is done all the para- and ortho-molecules fall to their lowest rotational levels, but the proportion of ortho- to para- molecules remains unchanged at 3 to 1. Such a mixture is known as normal hydrogen. The spontaneous conversion of normal hydrogen to the equilibrium concentration characteristic of a given temperature may take many months. Similarly, once pure para-hydrogen is prepared it does not change spontaneously to the equilibrium mixture corresponding to the temperature at which it is stored but can, in fact, be stored for many weeks with no appreciable reconversion. Paramagnetic substances greatly increase the rate of reconversion. The para-hydrogen is converted to normal hydrogen in contact with metal catalysts such as platinum or nickel at temperatures of several hundred degrees (Farkas, 1935).

It is known from spectroscopic data that in the excitation of rotational levels in hydrogen the rotational quantum number changes only by

± 2, ± 4 etc. (Herzberg, 1950). It is also known that transitions involving a change in J of greater than 2 are extremely rare (i.e. in the context of the present investigation the cross sections for this process are negligibly small) and so the transition rule considered is $\Delta J = \pm 2$.

The thermodynamic equilibrium between ortho- and para-hydrogen is governed by the Boltzmann relation. Thus, of the total number of molecules N_o, the number N_J in the J th rotational state is given by

$$N_J = N_o \, p_J \exp\left(-E_J / kT\right) \qquad \text{(A 1.1)}$$

where p_J and E_J denote the statistical weight and the energy of the state J respectively. It is known from spectroscopic data that

$$E_J = J\,(J+1)\,B_o \qquad \text{(A 1.2)}$$

where B_o is the rotational constant of the molecule. It may be shown that since the hydrogen molecules obey Fermi-Dirac statistics (Farkas, 1935) the statistical weights are given by

$$\begin{aligned} p_J &= 2J+1 \qquad \text{for J even} \\ &= 3\,(2J+1) \qquad \text{for J odd} \end{aligned} \qquad \text{(A 1.3)}$$

Equation (A 1.1) shows that the fraction of the molecules in the J th rotational level is

$$\frac{p_J}{p_r} \exp\left(-E_J / kT\right) \qquad \text{(A 1.4)}$$

with

$$p_r = \sum_J p_J \exp\left(-E_J/kT\right) \qquad \text{(A 1.5)}$$

The application of equations (A 1.2) to (A 1.5) to para-hydrogen is straightforward. Using $B_o = 0.00754$ eV (Herzberg, 1950) and the fact that para-hydrogen contains only rotational levels with even J, it is readily found that at 77°K, 99.46% of the molecules occupy the J = 0 level, while the remaining 0.54% occupy the J = 2 level.

In the case of normal hydrogen, where the proportion of even J to odd J molecules is preserved at the high temperature limit of 1 : 3, the fractional populations are found by calculating the populations for a gas with only even J and for a gas with only odd J ; these two results are then combined by weighting them in the ratio of $\frac{1}{4}$ even J to $\frac{3}{4}$ odd J. Thus, for normal hydrogen at $77^{o}K$ the fractional populations of the rotational levels are found to be:

$$\begin{aligned} J = 0 \qquad & (\tfrac{1}{4} \times 99.46) = 24.87\% \\ J = 1 \qquad & (\tfrac{3}{4} \times 99.99) = 75.00\% \\ J = 2 \qquad & (\tfrac{1}{4} \times 0.54) = 0.13\% \\ J = 3 \qquad & (< \tfrac{3}{4} \times 0.001) = 0.00\% \end{aligned}$$

A 1.2 Deuterium.

Deuterium also contains a mixture of ortho- and para-molecules. Normal deuterium contains 2/3 even J molecules and 1/3 odd J molecules (Farkas, 1935). The nuclear spin of deuterium is 1 (c.f. $\frac{1}{2}$ for hydrogen) and the rotational constant of the molecule is half that of hydrogen, i.e. $B_o = 0.00377$ eV (Herzberg, 1950). Deuterium obeys Bose-Einstein statistics and the statistical weights of its rotational levels are therefore given by (Farkas, 1935) :

$$\begin{aligned} p_J &= 6\,(2J + 1) \qquad \text{for J even} \\ &= 3\,(2J + 1) \qquad \text{for J odd} \end{aligned} \qquad \text{(A 1.6)}$$

Using equation (A 1.6) in place of equation (A 1.3) the fractional populations of the rotational levels in normal deuterium at $77^{o}K$ can be calculated in the same way as those for hydrogen. The results are :

$$\begin{aligned} J = 0 \qquad & (2/3 \times 85.82) = 57.21\% \\ J = 1 \qquad & (1/3 \times 99.21) = 33.07\% \\ J = 2 \qquad & (2/3 \times 14.18) = 9.45\% \\ J = 3 \qquad & (1/3 \times 0.79) = 0.26\% \end{aligned}$$

A 1.3 The Preparation of Pure para-Hydrogen.

As stated above, pure para-hydrogen is not readily obtained by

simply cooling normal hydrogen to 20°K. However, the equilibrium concentration for any given temperature below room temperature can be obtained by cooling normal hydrogen over a simple catalyst. Although many of the early experimenters used activated charcoal as the catalyst, it is now known that a better catalyst for the conversion is unsupported ferric hydroxide of 30-50 mesh size (Barrick, Weitzel and Connolly, 1954, Weitzel and Park, 1956, Buyanov, Zel'dovich and Pilipenko, 1962). The catalyst is activated by baking at approximately 140°C for 24 hours at a pressure of 10 - 20 microns. As long as exposure to air, water vapour or other poisons does not occur the catalyst can be used indefinitely without reactivation (Barrick, Weitzel and Connolly, 1954).

Although para-hydrogen is commonly prepared in liquid form, the requirement of high purity gas for the D/μ measurements at 77°K (where the oxygen concentration must be of the order of 1 part in 10^9 or lower) makes the preparation of 100% para-hydrogen difficult. To prevent contamination of the gas the conversion apparatus and storage tank must form a closed system with a low outgassing rate. It will be shown below that because the para-hydrogen must be prepared in a closed system special precautions must be taken to ensure that the para-content of the final gas samples is very nearly 100%.

A block diagram of the experimental arrangement is shown in Figure A 1.1 while a cross sectional view of the conversion chamber is shown in Figure A 1.2. The gas reservoir was a pre-outgassed stainless steel tank of 15 litres capacity fitted with a Granville-Phillips high pressure U. H. V. valve. The tanks were filled with high purity hydrogen using the palladium osmosis tubes described earlier. The conversion chamber was thoroughly outgassed and leak tested. The vacuum cavity of the conversion chamber was approximately 18" long and 2" in diameter. A backing pump was used to draw liquid helium through the 24' coil of 1/16" I. D. copper tubing. The hydrogen and helium systems were completely separate.

Hydrogen gas from the reservoir condensed on the coil and dripped to the bottom of the chamber where a small amount of the activated catalyst was placed. Cooling was continued until the triple point of hydrogen

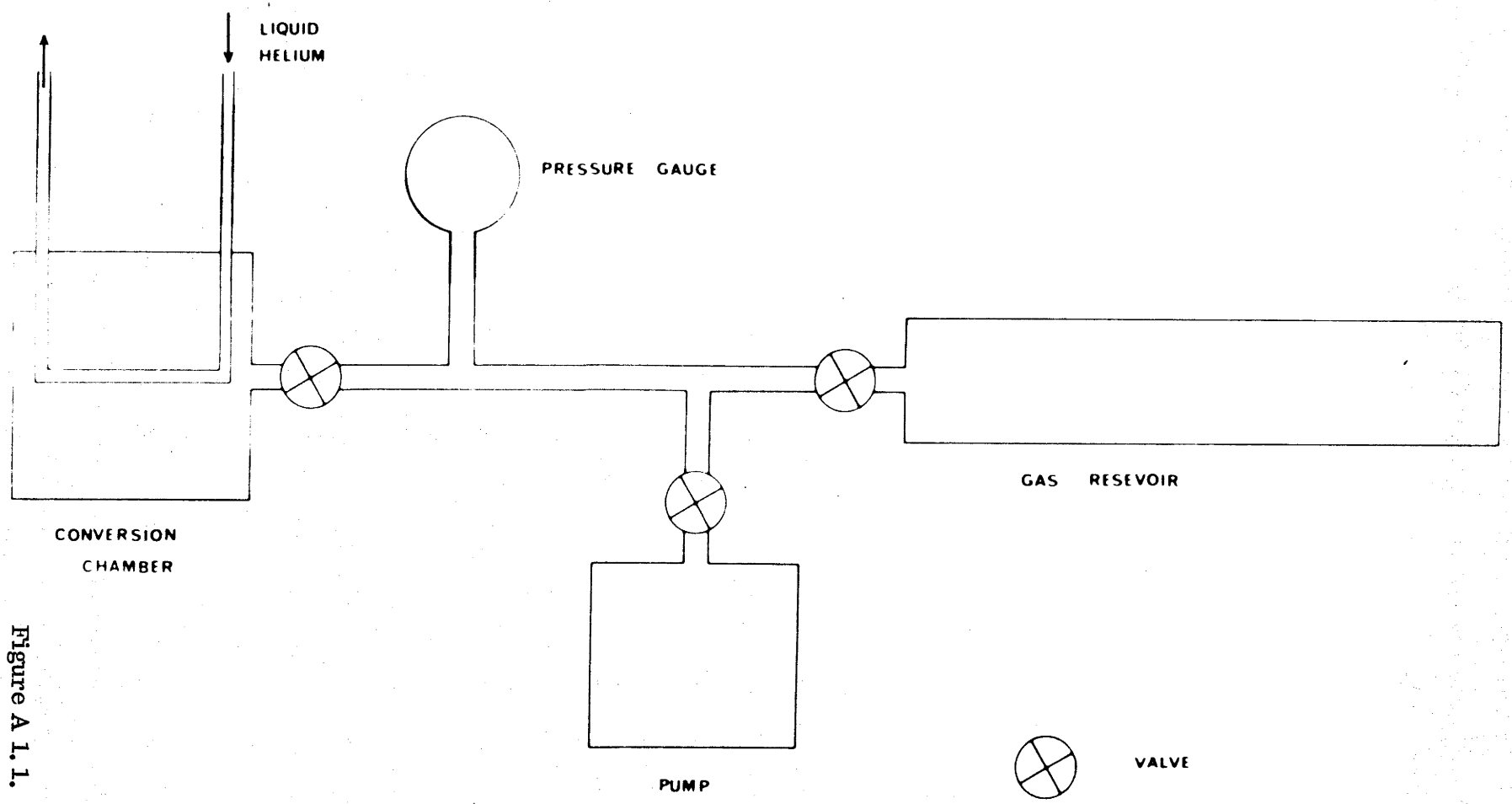
LIQUID
HELIUM
PRESSURE GAUGE
GAS RESEVOIR
CONVERSION
CHAMBER
PUMP
VALVE

Figure A 1.1.

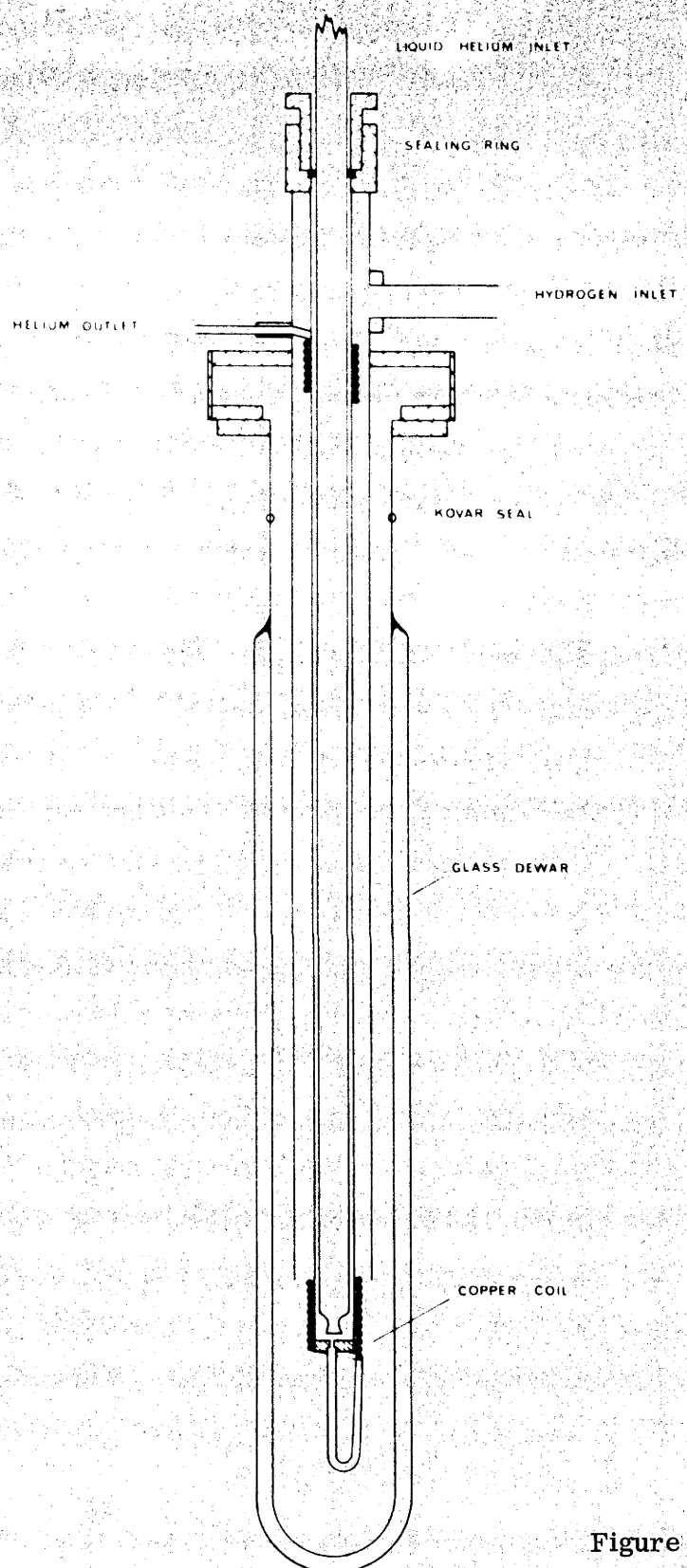
LIQUID HELIUM INLET
SEALING RING
HYDROGEN INLET
HELIUM OUTLET
KOVAR SEAL
GLASS DEWAR
COPPER COIL

Figure A 1.2

was passed, i. e. all the hydrogen which had condensed on the catalyst had turned to solid and the residual pressure throughout the system was about 50 torr. The conversion chamber was then isolated and the reservoir evacuated to better than 10^{-5} torr. Most of the gas in the conversion chamber was then pumped away and the solid hydrogen allowed to partially evaporate. The hydrogen was then condensed again and cycling in this manner repeated several times to ensure that all the hydrogen in the chamber had been in contact with the cold catalyst. The solid or liquid para-hydrogen was then allowed to slowly evaporate and fill the reservoir to atmospheric pressure.

Because the para-hydrogen is made in a closed system the catalyst remains in the conversion chamber during the warm-up cycle. It is therefore necessary to ensure that during evaporation of the liquid para-hydrogen the temperature of the catalyst does not rise sufficiently to reduce the para-concentration of the gas significantly. A number of precautions were taken to ensure that the catalyst was kept cold during the warm-up cycle. The amounts of catalyst and gas were carefully regulated to ensure that when the reservoir reached atmospheric pressure there was still a substantial amount of liquid hydrogen left in contact with the catalyst. A radiation shield over the surface of the catalyst was attached to a heavy copper rod which ran through the catalyst and into the residual liquid hydrogen. The combination of heavy copper rod and heat shield improved the thermal contact between the catalyst and the residual liquid hydrogen and also ensured that the upper surface of the catalyst was not radiantly heated from above. Finally, a small flow of liquid helium was maintained through the heat exchanging coil during the warm-up cycle; the effect of this flow was to reduce radiant heating of the catalyst by keeping the temperature throughout the conversion chamber near 20^{o}K.

As well as the main reservoir, two small glass sample bottles were filled with para-hydrogen, one at the beginning and the other at the end of the warm-up cycle. The bottles then contained samples of gas obtained under the most favourable and least favourable experimental conditions for preparing 100% para-hydrogen.

A 1.4 The Analysis of the para-Hydrogen.

Analysis of the ortho- and para- concentrations relies on the difference in the thermal conductivity of the two forms (Farkas, 1935). A simple analyser based on the design of Grilly (1953) was used. A pair of Sylvania Pirani tubes matched in resistance to within 0.01Ω formed two arms of a Wheatstone bridge network. The tubes were immersed in a liquid nitrogen bath to obtain greater sensitivity (Pirani and Yarwood, 1961). The remaining arms of the bridge circuit were a pair of resistance boxes graduated to 0.001 Ω. Hydrogen at a pressure of 40 torr was admitted to both the Pirani tubes and balance of the bridge obtained by adjusting the resistance boxes. One of the Pirani tubes was then isolated while the other was evacuated and then filled to a pressure of 40 torr with the gas to be analysed. The out-of-balance current in the Wheatstone bridge circuit was then a measure of the para-hydrogen content of the gas sample. The current to the bridge was supplied by a stabilized d.c. supply and was adjusted so that 100% para-hydrogen produced full scale deflection on the meter which measured the out-of-balance current.

The device was calibrated with a sample of para-hydrogen collected under the most favourable experimental conditions. The sensitivity was found by preparing a 90% para-hydrogen sample from a mixture of 100% para-hydrogen and normal hydrogen. The resolution was such that a 0.5% change in the para-hydrogen concentration could be detected.

The gas sample obtained at the end of the warm-up cycle was indistinguishable from the 100% sample. Similarly, gas samples taken from the stainless steel reservoirs and from the drift velocity apparatus at the end of an experimental run were also indistinguishable from the 100% sample. The para-hydrogen content of all the samples used is claimed to be greater than 98%.

A 1.5 Preliminary Experiments to Find a Suitable Electron Source.

Initial tests showed that re-conversion of the para-hydrogen to the 25% - 75% mixture occurred very rapidly in the presence of a heated

platinum filament. For example, total re-conversion of a 1 litre sample of $77^{o}K$ equilibrium hydrogen (approximately 50% ortho -, 50% para-) took place in less than 17 minutes. Tests with a small piece of tritium impregnated titanium (a β source) showed that the re-conversion was due to the platinum filament and not to the presence of the electrons themselves. The Americium source described earlier was used in place of the platinum filament for all the para-hydrogen experiments. No drift in the values of W or D/μ was observed over a period of 48 hours.

APPENDIX 2.

SUPPLEMENTARY DATA.

As explained in the main text all of the data shown below were extracted graphically from tabulated values given elsewhere. The figures quoted below should therefore be treated with caution.

Table A 2.1

Values of D/μ in hydrogen at $293^{o}K$.

E/N	D/μ	E/N	D/μ
2×10^{-19}	0.0259	5×10^{-18}	0.0593
3	0.0265	6	0.0664
4	0.0271	8	0.0811
5	0.0278	1×10^{-17}	0.096
6	0.0285	2	0.196
8	0.0300	3	0.232
1×10^{-18}	0.0315	4	0.286
2	0.0388	5	0.331
3	0.0456	6	0.373
4	0.0525		

Source: Table 4.6 and 4.7.

Table A 2.2

Values of D/μ in deuterium at $293^{o}K$.

E/N	D/μ	E/N	D/μ
2×10^{-19}	0.0258	5×10^{-18}	0.0670
3	0.0263	6	0.0775
4	0.0268	8	0.096
5	0.0274	1×10^{-17}	0.118
6	0.0280	2	0.207
8	0.0294	3	0.275

(Continued on next page)

E/N	D/μ	E/N	D/μ
1×10^{-18}	0.0307	4	0.334
2	0.0388	5	0.387
3	0.0481	6	0.440
4	0.0575		

Source: Table 4. 9.

Table A 2.3

Drift velocity of electrons in hydrogen at 293^{o}K.

E/N	W	E/N	W
2×10^{-19}	3.09×10^{4}	1×10^{-17}	6.23×10^{5}
3	4.61	2	8.35
4	6.00	3	1.00×10^{6}
5	7.36	4	1.15
6	8.73	5	1.29
8	1.13×10^{5}	6	1.42
1×10^{-18}	1.37	8	1.66
2	2.35	1×10^{-16}	1.88
3	3.14	2	2.86
4	3.78	3	3.67
5	4.34	4	4.60
6	4.82	5	5.71
8	5.62		

Source: Lowke, 1963.

Table A 2.4

Drift velocity of electrons in hydrogen at 77.6°K.

E/N	W	E/N	W
3×10^{-20}	1.08×10^{4}	3×10^{-18}	3.64×10^{5}
4	1.41	4	4.30
5	1.73	5	4.88
6	2.07	6	5.39
7	2.37	7	5.81
8	2.66	8	6.16
9	2.94	9	6.47
1×10^{-19}	3.23	1×10^{-17}	6.74
2	5.72	2	8.73
3	7.61	3	1.03×10^{6}
4	9.25	4	1.17
5	1.07×10^{5}	5	1.31
6	1.23	6	1.44
7	1.37	7	1.56
8	1.49	8	1.68
9	1.60	9	1.80
1×10^{-18}	1.72	1×10^{-16}	1.92
2	2.79		

Source: Lowke, 1963.

Table A 2.5

Drift velocity of electrons in deuterium at 293 ^{o}K

E/N	W	E/N	W
2×10^{-19}	3.25×10^{4}	6×10^{-18}	4.30×10^{5}
3	4.62	8	4.87
4	6.00	1×10^{-17}	5.33
5	7.37	2	7.21
6	8.62	3	8.86
8	1.11×10^{5}	4	1.04×10^{6}
1×10^{-18}	1.37	5	1.17
2	2.21	6	1.28
3	2.99	8	1.50
4	3.54	1×10^{-16}	1.69
5	3.98		

Source: Table 6.1

Table A 2.6

Drift velocity of electrons in deuterium at 77.0 ^{o}K.

Note: Below E/N = 5×10^{-18} these data are approximate only because no account has been taken of the pressure dependence of the values of W.

E/N	W	E/N	W
8×10^{-20}	2.70×10^{4}	5×10^{-18}	4.79×10^{5}
9	3.00	6	5.06
1×10^{-19}	3.31	7	5.30
2	6.10	8	5.50
3	8.46	9	5.68
4	1.08×10^{5}	1×10^{-17}	5.86
5	1.28	2	7.51
6	1.47	3	9.06
7	1.65	4	1.04×10^{6}

(Continued on next page)

E/N	W	E/N	W
8	1.82	5	1.17
9	1.97	6	1.28
1×10^{-18}	2.13	7	1.39
2	3.25	8	1.50
3	3.94	9	1.59
4	4.43	1×10^{-16}	1.69

Source: Table 6.2

Table A 2.7

Drift velocity of electrons in para-hydrogen at 77.0°K.

Note: Below E/N = 4×10^{-18} these data are approximate only because no account has been taken of the pressure dependence of the values of W.

E/N	W	E/N	W
2×10^{-19}	5.75×10^{4}	7×10^{-18}	6.30×10^{5}
3	7.78	8	6.65
4	9.60	9	6.95
5	1.13×10^{5}	1×10^{-17}	7.20
6	1.30	2	8.97
7	1.41	3	1.04×10^{6}
8	1.61	4	1.18
9	1.77	5	1.31
1×10^{-18}	1.92	6	1.44
2	3.16	7	1.56
3	4.10	8	1.68
4	4.85	9	1.79
5	5.45	1×10^{-16}	1.90
6	5.91		

Source: Table 6.3.

Table A 2.8

First Townsend ionization coefficient in hydrogen at $293^{o}K$.

E/p_{293}	α_T/p_{293}	E/p_{293}	α_T/p_{293}
15	0.0008	60	0.544
20	0.0071	65	0.639
25	0.0268	70	0.738
30	0.063	75	0.840
35	0.115	80	0.932
40	0.185	85	1.02
45	0.266	90	1.11
50	0.356	95	1.20
55	0.450	100	1.30

Source: Rose, 1956.

APPENDIX 3.

PUBLICATIONS

(i) "The extension of swarm techniques to the measurement of electron energies for conditions near electrical breakdown", R. W. Crompton, B. S. Liley, A. I. McIntosh and C. A. Hurst. Proceedings of the Seventh International Conference on Phenomena in Ionized Gases, Belgrade, 1965.

(ii) "Electron drift and diffusion in deuterium at 293^{o}K", A. I. McIntosh. Aust. J. Phys., 19, 805 (1966)

REFERENCES.

Allis, W.P. - Handbuch der Physik (ed. S. Flugge), volume 21 (Springer-Verlag, Berlin, 1956).

Bandel, H.W. and Golden, D.E. (1965) - Phys. Rev. 138A : 14.

Barrick, P.L., Weitzel, D.H. and Conolly, T.W. (1954) - Advances in Cryogenic Engineering I : 285.

Blewett, J.P. and Jones, E.J. (1936) - Phys. Rev. 50 : 464.

Bowe, J.C. (1960) - Phys. Rev. 117 : 1411.

Bradbury, N.E. and Nielsen, R.A. (1936) - Phys. Rev. 49 : 388.

Bridge, N.J. and Buckingham, A.D. (1964) - J. Chem. Phys. 40 : 2733.

Bruce, F.M. (1947) - J. Inst. Elect. Eng. 94 : 138.

Buyanov, R.A., Zel'dovich, A.G. and Pilipenko, Y.K. (1962) - Cryogenics 2 : 143.

Chapman, S. and Cowling, T.G. (1939) - "Mathematical Theory of Non-Uniform Gases" (C.U.P.).

Cochran, L.W. and Forrester, D.W. (1962) - Phys. Rev. 126 : 1785.

Compton, R.N., Hurst, G.S., Christophorou, L.G. and Reinhardt, P.W. (1966) - Oak Ridge National Laboratory report, ORNL-TM-1409.

Corrigan, S.J.B. and von Engel, A. (1958) - Proc. Roy. Soc. A, 245 : 335.

Crompton, R.W. (1953) - Ph.D. Thesis, University of Adelaide (unpublished).

Crompton, R.W. and Elford, M.T. (1957) - J. Scient. Instrum. 34 : 405.

Crompton, R.W. and Elford, M.T. (1962) - J. Scient. Instrum. 39 : 480.

Crompton, R.W. and Elford, M.T. (1963) - Proc. 6th Int'l Conf. on Ionization Phenomena in Gases, 1337.

Crompton, R.W., Elford, M.T. and Gascoigne, J. (1965) - Aust. J. Phys. 18: 409.

Crompton, R. W., Elford, M. T. and Jory, R. L. (1966) - to be published.

Crompton, R. W., Hall, B. I. H. and Macklin, W. C. (1957) - Aust. J. Phys. 10 : 366.

Crompton, R. W. and Jory, R. L. (1962) - Aust. J. Phys. 15 : 451.

Crompton, R. W. and Jory, R. L. (1965) - IVth Int'l Conf. on Physics of Electronic and Atomic Collisions (Quebec), 118.

Crompton, R. W., Liley, B. S., McIntosh, A. I. and Hurst, C. A. (1965) - Proceedings of Seventh Int'l. Conf. on Phenomena in Ionized Gases (Belgrade).

Crompton, R. W. and Sutton, D. J. (1952) - Proc. Roy. Soc. A, 215: 467.

Druyvesteyn, M. J. (1930) - Physica 10 : 69.

Druyvesteyn, M. J. and Penning, F. M. (1940) - Rev. Mod. Phys. 12 : 87.

Duncan, R. A. (1957) - Aust. J. Phys. 10 : 55.

Elford, M. T. (1957) - Ph. D. Thesis, University of Adelaide, (unpublished).

Elford, M. T. (1965) - Ion Diffusion Unit report (unpublished).

Elford, M. T. (1966) - Aust. J. Phys. 19: 629.

Engelhardt, A. G. (1963) - Westinghouse Research Report 63 - 928 - 113 - RI.

Engelhardt, A. G. and Phelps, A. V. (1963) - Phys. Rev. 131: 2115.

Farkas, A. (1935) - "Ortho-hydrogen, para-Hydrogen and Heavy Hydrogen" (Cambridge Press).

Frost, L. S. and Phelps, A. V. (1962) - Phys. Rev. 127: 1621.

Frost, L. S. and Phelps, A. V. (1964) - Phys. Rev. 136: A 1538.

Gerjuoy, E. and Stein, S. (1955) - Phys. Rev. 97: 1671.

Gerjuoy, E. and Stein, S. (1955) - Phys. Rev. 98: 1848.

Golden, D. E., Nakano, H. and Fisher, L. H. (1965) - Phys. Rev. 138: A 1613.

Grilly, E.R. (1953) - Rev. Scient. Instrum. 24: 72.

Hall, Barbara I.H. (1955) - Aust. J. Phys. 8: 468.

Haydon, S.C. (1964) - "Discharge and Plasma Physics" (University of New England, Australia).

Healey, R.H. and Read, J.W. (1941) - "Behaviour of Slow Electrons in Gases" (A.W.A., Sydney).

Herzberg, G. (1950) - "Spectra of Diatomic Molecules" (D. van Nostrand, Princeton, New Jersey).

Holstein, T. (1946) - Phys. Rev. 70: 367.

Hurst, C.A. (1960) - private communication.

Hurst, C.A. and Liley, B.S. (1965) - Aust. J. Phys. 18: 521.

Huxley, L.G.H. (1940) - Phil. Mag. 30: 396.

Huxley, L.G.H. (1959) - Aust. J. Phys. 12: 171.

Huxley, L.G.H. (1960) - Aust. J. Phys. 13: 718.

Huxley, L.G.H. and Crompton, R.W. (1955) - Proc. Phys. Soc. B68: 381.

Huxley, L.G.H., Crompton, R.W. and Elford, M.T. (1966) - Bulletin Inst. Phys. and Phys. Soc. 17: 251.

Huxley, L.G.H. and Zazou, A.A. (1949) - Proc. Roy. Soc. A 196: 402.

Ishii, H. and Nakayama, K. (1961) - Trans. of 8th Vacuum Symposium (Pergamon Press, Oxford).

Jory, R.L. (1965) - Aust. J. Phys. 18: 237.

Keller, G.E., Martin, D.W. and McDaniel, E.W. (1965) - Technical Report 1, Project A-781, Georgia Institute of Technology.

Kolos, W. and Wolniewicz, L. (1964) - Bull. Amer. Phys. Soc. 9: 103.

Lawson, P.A. and Lucas, J. (1965) - Proc. Phys. Soc. 85: 177.

Llewellyn-Jones, F. (1957) - "Ionization and Breakdown in Gases" (Methuen, London).

Liley, B. S. (1966) - to be published.

Loeb, L. B. (1955) - "Basic Processes of Gaseous Electronics" (Univ. of California Press).

Lowke, J. J. (1962) - Aust. J. Phys. 15: 39.

Lowke, J. J. (1963) - Aust. J. Phys. 16: 115.

McDaniel, E. W. (1964) - "Collision Phenomena in Ionized Gases" (Wiley, New York).

McIntosh, A. I. (1966) - Aust. J. Phys. 19: 805.

Margenau, H. (1946) - Phys. Rev. 69: 508.

Mitchell, A. G. C. and Zemansky, M. W. (1934) - "Resonance Radiation and Excited Atoms" (Cambridge, New York.

Nielsen, R. A. (1936) - Phys. Rev. 50: 950.

Pack, J. L. and Phelps, A. V. (1961) - Phys. Rev. 121: 798.

Pack, J. L., Voshall, R. E. and Phelps, A. V. (1962) - Phys. Rev. 127: 2084.

Parker, J. H. (1963) - Phys. Rev. 132: 2096.

Penning, F. M. (1938) - Physica 5: 286.

Pirani, M. and Yarwood, J. (1961) - "Principles of Vacuum Engineering" (Chapman and Hall, London).

Pursar, K. H. and Richards, J. R. (1959) - J. Scient. Instrum. 36: 142.

Ramsauer, C. and Kollath, R. (1932) - Ann. Physik 12: 529.

Rose, D. J. (1956) - Phys. Rev. 104: 273.

Sampson, D. H. and Mjolness, R. C. (1965) - Phys. Rev. 140A: 1466.

Sherman, B. (1960) - J. Math. Analysis and Application 1: 342.

Skullerud, H. R. (1966) - Technical Report GDL 66-1, Institute of Applied Physics, Norwegian Institute of Technology, Trondheim, Norway.

Tate, J. T. and Smith, P. T. (1932) - Phys. Rev. 39: 270.

Takayanagi, K. and Geltman, S. (1965) - Phys. Rev. 138A: 1003.

Townsend, J. S. (1899) - Phil. Trans. A 193: 129.

Townsend, J. S. (1908) - Proc. Roy. Soc. A 80: 207.

Townsend, J. S. (1908) - Proc. Roy. Soc. A 81: 464.

Townsend, J. S. (1925) - "Motions of Electrons in Gases" (Clarendon Press).

Townsend, J. S. (1948) - "Electrons in Gases" (Hutchinson).

Townsend, J. S. and Bailey, V. A. (1921) - Phil. Mag. 42: 873.

Townsend, J. S. and Tizard, H. T. (1913) - Proc. Roy. Soc. A 88: 336.

Uman, M. A. (1964) - Phys. Rev. 133: A 1266.

Warren, R. W. and Parker, J. H. (1962) - Phys. Rev. 128: 2661.

Weitzel, D. H. and Park, O. E. (1956) - Rev. Scient. Instrum. 27: 57.

Young, J. R. (1963) - Rev. Scient. Instrum. 34: 891.